



Universidade de Brasília
Faculdade de Medicina
Laboratório de Interação Parasito-Hospedeiro

Prolil Oligopeptidases de tripanossomos: aspectos estruturais e funcionais

Flávia da Silva Nader Motta

Orientadora: Prof^a. Dra. Izabela M. D. Bastos
UnB – Universidade de Brasília

Co-orientador: Prof. Dr. Jaime M. de Santana
UnB – Universidade de Brasília

Brasília – DF
2010



Universidade de Brasília
Faculdade de Medicina
Laboratório de Interação Parasito-Hospedeiro

Prolil Oligopeptidases de tripanossomos: aspectos estruturais e funcionais

Flávia da Silva Nader Motta

Orientadora: Prof^a. Dra. Izabela M. D. Bastos
UnB – Universidade de Brasília

Co-orientador: Prof. Dr. Jaime M. de Santana
UnB – Universidade de Brasília

**Tese apresentada ao Programa de Pós-graduação
em Patologia Molecular da Universidade de Brasília
como requisito parcial à obtenção do grau de Doutor
em Patologia Molecular.**

Brasília – DF
2010



Trabalho desenvolvido no Laboratório de Interação Parasito-Hospedeiro – Faculdade de Medicina da Universidade de Brasília e no MNHN – Paris (*Museum National d’Histoire Naturelle*) com apoio financeiro do CNPq, FINEP, CAPES e FAP-DF.



**“Assim como falham as palavras quando querem exprimir
qualquer pensamento, assim falham os pensamentos
quando querem exprimir qualquer realidade...”**

Alberto Caeiro – heterônimo de Fernando Pessoa



**Dedico este trabalho aos meus pais José Carlos e Natália
que sempre me incentivaram**

**Dedico, também, à minha saudosa avó Celeste...
por ser um exemplo de vida!!**

Agradecimentos

Eu agradeço...

Aos **meus pais**, que sempre estiveram ao meu lado, o amor incondicional, compreensão, estímulo, apoio e encorajamento! Vocês fizeram tanto por mim que não sei por onde começar...

Aos **meus maravilhosos irmãos**, o amor, carinho e companheirismo de toda a vida!

Ao **meu amor Paulo Henrique** que esteve durante todo o tempo ao meu lado. Obrigada por sua admiração, por seus conselhos práticos, pela sua paciência, pelo seu amor e carinho... por me fazer tão feliz!

À **Keyla**, mais do que uma colega de laboratório, uma amiga para a vida toda! Muito obrigada pelos conselhos, pelas aflições compartilhadas, pela lealdade e por tornar os dias de trabalho no laboratório mais brandos! Você sempre foi maravilhosa comigo, incrivelmente animada e bondosa!

Aos meus amigos, em especial **Mariana, Lorena, Adelson e Beto**, a vibração, energia e amizade que vocês têm demonstrado por mim ao longo dos anos!

À minha orientadora, **Prof^a. Izabela**, a sua presença constante e dedicação na realização deste trabalho, a sua orientação excepcional e inigualável.

Ao meu co-orientador, **Prof. Jaime**, a oportunidade, o incentivo nos momentos mais críticos e o exemplo de dedicação ao trabalho científico.

À **prof^a Sonia Freitas**, por não somente ter me apresentado a Biofísica, mas por tê-la simplificado!

Ao **Eric Faudry**, por ter me recebido em Grenoble e ter colaborado bastante com esse trabalho.

Aos professores da pós-graduação em Patologia Molecular, em especial **prof^a Anamélia** e **prof^o Antônio Teixeira**, pela contribuição para o meu crescimento profissional.



Ao prof. **Philippe Grellier**, a oportunidade e acolhida em seu laboratório em Paris.

Aos colegas de laboratório: **Thiago, Hugo, Paula, Isabel, Brina, André, Raquel, Vivi, Márcio, Isaque, Ana Camila, André Amaral, Alice, Yanna, Felipe, Clênia e Bruna**, a convivência e momentos compartilhados. Agradeço, em especial, ao **David** e à **Teresa**, agora distantes, a amizade e o bom exemplo!

Aos colegas do laboratório do MNHN – Paris: **Agnès, Elizabeth, Christianne, Barbara, Linda, Isabelle** e **Jimmy** pelo acolhimento. Em especial, **Cissé** e **Marion**, obrigada pela amizade que tornou a estada mais agradável! *Mes collègues du MNHN – Paris : Agnès, Elizabeth, Christianne, Barbara, Linda, Isabelle e Jimmy, je voulais tous vous remercier pour votre accueil chaleureux, j'ai passé de très bons moments parmi vous. Je remercie, en particulier, Cissé et Marion. Vous avez fait mon séjour plus agréable!*

Aos ótimos amigos que fiz em Paris, especialmente na Maison du Brésil – **Alexandra, Vera, Ana Carolina, Priscila, Renata, Isabela, Hugo e família!** Paris ficou ainda mais bela porque tive vocês ao meu lado!

Lista de abreviaturas

AMC	7-amino-4-metilcomarina
Da	Dalton
DNA	ácido desoxirribonucléico
dNTP	desoxirribonucleotídeos fosfatados
DTT	Ditiotreitol
$[E]_0$	concentração de enzima
EDTA	Etileno bis(oxi-etilenonitrilo) do ácido tetraacético
HEPES	ácido (2-hidroxietil)-piperazina etanosulfônico
IC ₅₀	Concentração inibitória 50%
IPTG	isopropil- β -D-tiogalactopiranosídeo
kb	kilobase
k_{cat}	Constante catalítica
k_{cat}/K_m	Eficiência catalítica
K_i	Constante de inibição
K_m	Constante de Michaelis-Menten
N-CBZ	N-carbobenziloxi
N-Suc	N-Succinil
ORF	fase aberta de leitura
pb	pares de bases
PBS	Tampão fosfato 50 mM, NaCl 0,15 M pH 7,2
PMSF	Fenilmetilsulfonil fluoreto
RNA	ácido ribonucléico
$[S]$	concentração do substrato
SDS-PAGE	Eletroforese em gel de poli(acrilamida) contendo Dodecil Sulfato de Sódio
TLCK	n- α -Tosil-L-Lisina clorometil cetona
TPCK	n- α -Tosil-L-Fenilalanina clorometil cetona
UTR	região não traduzida
V_{max}	Velocidade máxima



Sumário

Resumo.....	1
Summary.....	2
INTRODUÇÃO.....	3
O <i>Trypanosoma cruzi</i> e a doença de Chagas.....	4
Ciclo de vida do <i>Trypanosoma cruzi</i>	5
Manifestações clínicas.....	7
Tratamento quimioterápico.....	8
O <i>Trypanosoma brucei</i> e a doença do sono.....	8
Ciclo de vida do <i>Trypanosoma brucei</i>	9
Manifestações clínicas.....	12
Tratamento quimioterápico.....	12
Alvos de drogas nos tripanossomos.....	14
Proteases.....	14
Família Prolil Oligopeptidase ou S9.....	18
Prolil Oligopeptidase (POP).....	20
Prolil oligopeptidase de <i>T. cruzi</i> (POPTc 80).....	24
Oligopeptidase B (OPB).....	26
Oligopeptidase B de <i>T. cruzi</i> (OPBTc).....	27
Dicroísmo circular e sua aplicação no estudo de proteínas.....	29
Fluorescência intrínseca e sua aplicação no estudo de proteínas.....	31
JUSTIFICATIVA.....	33
OBJETIVOS.....	36
I. Propriedades estruturais da OPBTc.....	39
II. Estudo da prolil oligopeptidase de <i>Trypanosoma brucei</i>	72
III. Elucidação do mecanismo catalítico da POP Tc80.....	89
IV. Nocaute do gene <i>poptc80</i> no <i>T. cruzi</i>	108



CONCLUSÕES.....	119
PERSPECTIVAS	122
REFERÊNCIAS BIBLIOGRÁFICAS	124

Resumo

A linha de pesquisa do nosso grupo visa à identificação e caracterização de alvos potenciais para a quimioterapia da doença de Chagas tendo as proteases como principal enfoque, uma vez que estão envolvidas em processos biológicos fundamentais para a viabilidade e virulência de patógenos. Neste contexto, essa tese aborda alguns aspectos estruturais e funcionais de serino-proteases pertencente à família Prolil Oligopeptidase: a oligopeptidase B (OPBTc) e prolil oligopeptidase (POPTc 80) de *Trypanosoma cruzi* e a prolil oligopeptidase (POP Tb) de *Trypanosoma brucei*. A OPBTc participa da invasão celular por meio do recrutamento e fusão de lisossomos da célula hospedeira até o local de ligação do parasito por uma via dependente de Ca^{2+} . Por meio deste trabalho, a OPBTc tornou-se a primeira oligopeptidase B a ter sua estrutura dimérica confirmada por ultracentrifugação analítica. Experimentos de dicroísmo circular mostraram que em altas temperaturas, a enzima conserva sua estrutura secundária, mas não a terciária. A perda da estrutura terciária por tratamento térmico acompanha a diminuição da atividade da enzima e a perda da dimerização, que ocorrem a partir de 50 °C. No entanto, a associação do dímero é resistente a altas concentrações de sal e a tratamento com reagentes redutores, indicando que esta interação não ocorre devido a pontes dissulfeto intermoleculares. Este trabalho também mostra a caracterização funcional da POP de *T. brucei*, protozoário causador da doença do sono. Esta protease foi capaz de hidrolisar colágeno tipo I semi-purificado *in vitro* e colágeno nativo em mesentério de rato, além de peptídeos hormonais. Foi observado ainda, que POP Tb é liberada na corrente sanguínea de camundongos infectados pelo *T. brucei*, onde permanece ativa, sugerindo sua contribuição para a patogênese da doença do sono. Como já proposto em estudos prévios, a POP Tc80 está envolvida na entrada do *T. cruzi* em células hospedeiras não fagocíticas e alguns de seus substratos naturais foram caracterizados mostrando que a mesma hidrolisa colágenos do tipo I e IV e fibronectina. O mecanismo desta catálise não é completamente entendido, porém cálculos de interação entre o modelo estrutural teórico da POP Tc80 com o colágeno mostraram que ocorre uma abertura dos domínios da enzima para entrada do substrato. Para verificar essa hipótese, mutações sítios dirigidas na POP Tc80 acarretaram na perda da sua atividade devido à rigidez da enzima, impedindo o acesso do substrato à fenda catalítica. Finalmente, ainda na tentativa de esclarecer o papel da POP Tc80 na infecção do *T. cruzi*, foi montada uma estratégia para silenciar seu gene. Os resultados preliminares indicam que um alelo do gene *poptc80* sofreu recombinação homóloga sendo trocado pelo marcador de seleção, o gene de resistência a neomicina.

Summary

The research activities of our group aim the identification and characterization of potential targets for chemotherapy of Chagas's disease, and proteases are the main focus since they are involved in biological processes essential for the viability and virulence of pathogens. In this context, this thesis addresses some structural and functional features of serine-proteases that belong to the Prolil Oligopeptidase family: the oligopeptidase B (OPBTc) and prolyl oligopeptidase (POP Tc80) of *Trypanosoma cruzi* and the prolyl oligopeptidase (POPTb) of *Trypanosoma brucei*. The OPBTc participates in cell invasion through the recruitment and fusion of the host cell lysosomes to the binding site of the parasite by a Ca^{2+} dependent pathway. In this work, the OPBTc had a structural approach, being the first oligopeptidase B to have its dimeric structure confirmed by analytical ultracentrifugation. Circular dichroism experiments showed that at high temperatures, the enzyme retains its secondary structure but not the tertiary. The loss of tertiary structure by heat treatment follows the decline of enzyme catalytic ability, which occurs from 50 °C. However, the association of the dimer is resistant to salt high concentration and treatment with reducing reagents, indicating that this interaction is not due to intermolecular disulfide bonds. This work also shows the functional characterization of the enzyme POP of *T. brucei* (protozoan that causes sleeping sickness), the POPTb. This protease was able to hydrolyze native and semi-purified collagen type I and peptide hormones. In addition, POPTb is released into the bloodstream of *T. brucei* infected mice, where it remains active, suggesting their contribution to the pathogenesis of sleeping sickness. As shown in previous studies, the POP Tc80 is involved in the entry of the parasite in the non-phagocytic host cell and some of its natural substrates were characterized showing that the enzyme hydrolyzes collagen type I and IV and fibronectin. The mechanism of this catalysis is not completely understood, but docking analysis of the theoretical structural model of POP Tc80 with collagen, showed that the enzyme domains open to substrate entry. To investigate this hypothesis, site directed mutations in POP Tc80 resulted in loss of its activity due to the rigidity of the enzyme, preventing the substrate access to the catalytic pocket. In an attempt to clarify the role of POP Tc80 in *T. cruzi* infection, it was set up a strategy to silence its gene. Preliminary results indicate that one allele of the *poptc80* gene has been replaced by the selection marquee, the gene for resistance to neomycin, through homologous recombination.



INTRODUÇÃO

Introdução

O Trypanosoma cruzi e a doença de Chagas

A doença de Chagas, ou tripanossomíase americana, foi descrita pelo Dr. Carlos Ribeiro Justiniano das Chagas em 1909, que relatou suas características clínicas, anatomopatológicas, epidemiológicas, seu agente etiológico – o *Trypanosoma cruzi* e o vetor inseto da ordem Hemiptera (Molina *et alli*, 2001). A doença de Chagas é encontrada principalmente no Continente Americano com uma ampla distribuição geográfica, desde o México até o sul da Argentina. Durante o século XX, a doença de Chagas foi considerada, em todos os países da América Latina, a enfermidade parasitária mais importante em termos de impacto sobre as economias nacionais e sistemas públicos de saúde (WHO, 2002). No entanto, desde o começo da década de 90, deu-se início, na maioria dos países latino-americanos, aos programas regionais de controle contra vetores domésticos. Esses programas levaram a uma redução de 16-18 milhões de pessoas infectadas para um número estimado em 9 milhões (Schofield *et alli*, 2006). Porém ainda existem muitos obstáculos para o controle efetivo da doença e milhões de pacientes chagásicos necessitam de ajuda médica específica. A doença de Chagas é considerada uma doença negligenciada porque acomete comumente populações pobres e marginalizadas, faltam incentivos para a pesquisa e para o desenvolvimento de drogas terapêuticas (Ault, 2007).

A transmissão do parasito acontece principalmente por vetores hematófagos da família Reduviidae e subfamília Triatominae, conhecidos popularmente como barbeiros. Apesar de todas as espécies de triatomíneos serem vetores potenciais do protozoário, apenas aquelas mais presentes no ambiente domiciliar ou na região próxima ao domicílio apresentam uma maior probabilidade de transmitir o parasito. Contudo, a transmissão vetorial da doença vem sofrendo algumas alterações: Triatomíneos silvestres com tendências sinantrópicas estão, cada vez mais, entrando em contato com seres humanos (Noireau *et alli*, 2009). Além disso, micro epidemias recentemente registradas no Brasil, causadas pela ingestão de alimentos contaminados com o protozoário, preocupam as autoridades de saúde, uma vez que a sua transmissão por via oral é caracterizada por sua severidade que culmina, em

muitos casos, na morte rápida do paciente. Alguns desses casos que vieram a conhecimento público ocorreram, em 2005, no Estado de Santa Catarina devido à ingestão de caldo de cana e, em 2006, no norte do país devido à ingestão de sucos feito de açaí e bacaba (Yoshida, 2008).

Desde a descoberta do *T. cruzi*, como o agente etiológico da tripanossomíase americana, o conhecimento sobre sua variabilidade genética e as relações filogenéticas entre as diferentes linhagens do parasito tem crescido exponencialmente. Atualmente, o *T. cruzi*, eucarioto flagelado da ordem Kinetoplastidae, é classificado como uma única espécie, que possui diferentes linhagens e sublinhagens (Zingalle *et alli*, 2009).

Este protozoário apresenta 4 formas de desenvolvimento durante o seu ciclo de vida que foram classificadas em função da sua morfologia, da maneira como o flagelo emerge do corpo celular e da posição relativa do cinetoplasto, uma única mitocôndria presente no parasito (Molina *et alli*, 2001). Essas formas alteram-se entre vertebrados e insetos vetores, com estágios específicos de desenvolvimento em cada hospedeiro: epimastigota proliferativo, presente no intestino médio do vetor e tripomastigota metacíclico, forma não proliferativa, presente na porção final do intestino do inseto. No hospedeiro vertebrado, o parasito se apresenta de duas formas: tripomastigota e amastigota; a primeira é a forma infectiva presente no sangue e a última, a forma intracelular proliferativa que, ao contrário das outras formas, é arredondada ou oval com um flagelo curto que não se exterioriza (Brenner *et alli*, 2000).

Ciclo de vida do *Trypanosoma cruzi*

O ciclo de vida evolutivo do *T. cruzi* (Figura 1) no hospedeiro vertebrado inicia-se quando tripomastigotas metacíclicos são liberados nos excrementos do inseto vetor após seu repasto. Essas formas invadem o hospedeiro mamífero através da pele ou mucosa, infectando diferentes tipos celulares. A penetração do *T. cruzi* nas células do hospedeiro é um processo multifatorial que começa com a adesão do tripomastigota à célula alvo mediada por receptores presentes em ambas as superfícies celulares (Schenkman *et alli*, 1991). Logo após a adesão, conjuntos

distintos de moléculas de superfície do parasito, como gp82, gp35/50 e gp90 (Yoshida and Cortez, 2008), e da célula hospedeira interagem entre si promovendo modificações importantes na superfície destas duas células. Essas modificações culminam tanto na mobilização intracelular de Ca^{+2} em ambas as células, o que permite a formação da vesícula parasitófora com recrutamento de lisossomos. (Burleigh and Andrews, 1998; Docampo and Moreno, 1996; Tardieux *et alli*, 1992; Yoshida, 2006).

Após a fusão de lisossomos com a vesícula parasitófora (fagolisossomo), os tripomastigotas começam a transformar-se em formas amastigotas e, gradualmente saem para o citoplasma. Essa transição é dependente de pH ácido e de atividade proteassômica (Hall *et alli*, 1992). Amastigotas citossólicos se multiplicam por divisão binária e, após sucessivas divisões, eles se diferenciam em tripomastigotas, rompem a célula hospedeira e entram na circulação sanguínea do hospedeiro mamífero, disseminando a infecção (Brener *et alli*, 2000).

Formas tripomastigotas presentes no sangue do hospedeiro vertebrado são sugadas por vetores hematófagos no momento da sua alimentação. No trato digestivo do inseto, os protozoários se diferenciam em epimastigotas, se multiplicam e sofrem outra diferenciação, agora para a forma tripomastigota metacíclica, que será eliminada nas fezes do barbeiro no próximo repasto, dando prosseguimento ao ciclo de vida do *T. cruzi*.

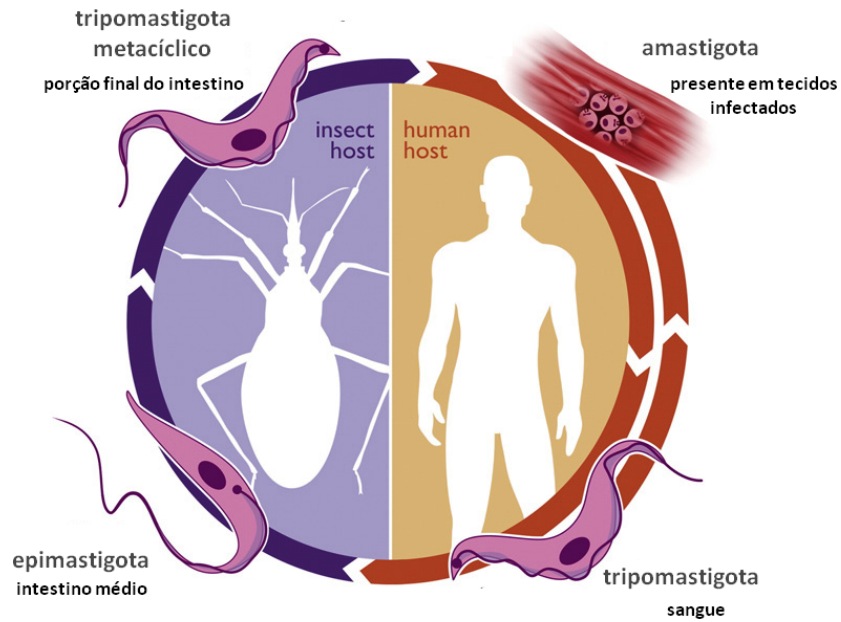


Figura 1. Ciclo de vida do *Trypanosoma cruzi*. Representação esquemática adaptada de Cuervo *et alli*, 2010

Manifestações clínicas

A doença de Chagas pode apresentar três fases: aguda, indeterminada e crônica, diferindo em seus sintomas. A fase aguda é caracterizada pela alta parasitemia dos tecidos e do sangue sendo, na maioria das vezes, assintomática. Os sintomas desta fase, quando ocorrem, são comuns a outras doenças o que pode dificultar o diagnóstico precoce da infecção. Uma característica desta fase é o chagoma de inoculação ou sinal de Romaña, um inchaço no sítio de entrada do parasito. Se o indivíduo não receber tratamento adequado, a doença pode entrar em uma fase latente ou indeterminada, na qual as pessoas infectadas não apresentam as alterações patológicas comuns da cronicidade da doença. Estima-se que metade dos indivíduos infectados pelo *T. cruzi* entra na fase indeterminada (Macedo, 1980).

Em geral, após 10 a 20 anos de latência, 27% dos indivíduos infectados desenvolvem a fase crônica. Essa fase é caracterizada principalmente por cardiopatias, arritmias, infarto do miocárdio, síndrome dos megas: megaesôfago e

megacolon (Oliveira *et alli*, 2009; Prata, 2001; Teixeira *et alli*, 2006) e, em alguns casos, lesões de nervos periféricos. A principal causa de morbidade da doença de Chagas é a cardiopatia crônica proveniente de lesões irreversíveis inflamatórias no músculo cardíaco que vai se tornando fibroso com a evolução da doença, resultando em hipertrofia e disritmia do coração. Contudo, muitas pessoas podem permanecer assintomáticas durante toda a vida e nunca desenvolverem os sintomas relacionados à doença de Chagas (Sanchez-Sancho *et alli*, 2009).

Tratamento quimioterápico

Atualmente, os únicos medicamentos disponíveis para o tratamento clínico da doença são o nifurtimox e o benzonidazol. Os efeitos colaterais mais frequentes dessas drogas incluem anorexia, perda de peso, alterações psíquicas, insônia, náusea, vômitos, cólicas, diarreias, perda de memória, polineurite e hepatite tóxica, entre outros (Urbina and Docampo, 2003). Esses dois medicamentos apresentam atividade antiparasitária contra todas as formas do parasito, principalmente na fase aguda da doença, com até 80% de cura parasitária em pacientes tratados (Sanchez-Sancho *et alli*, 2009). No entanto, a eficácia desses compostos varia entre as cepas de *T. cruzi* devido, principalmente, as diferenças de susceptibilidade à droga. Além disso, essas drogas possuem grandes limitações no tratamento da fase crônica da doença.

Outros medicamentos derivados desses dois compostos acima citados foram testados, mas apesar da aparente capacidade de provocar a morte do parasito *in vitro*, demonstram dados farmacocinéticos desfavoráveis e não são capazes de controlar a infecção na sua fase crônica.

O Trypanosoma brucei e a doença do sono

Tripanossomíase africana humana (HAT), ou doença do sono, é prevalente em 36 países da África subsaariana. A doença resulta da infecção das subespécies *Trypanosoma brucei gambiense* ou *Trypanosoma brucei rhodiense* transmitidas pela picada da mosca vetor tsé-tsé (*Glossina* sp). As duas subespécies possuem a

mesma morfologia. A primeira é encontrada na África Ocidental e Oriental responsável por uma forma mais crônica da doença que pode passar vários anos sem quaisquer sinais ou sintomas importantes. A segunda é encontrada na África Oriental e Austral, neste caso a doença é aguda com duração de uma semana até vários meses. Essa forma representa menos de 10% dos casos reportados (Rodgers, 2009; Simarro *et alli*, 2008). Sem tratamento, a doença é fatal. A outra subespécie, *Trypanosoma brucei brucei*, não é capaz de infectar o homem e causa a doença Nagana em animais selvagens e domésticos.

Desde 1995, em muitas ocasiões, a Organização Mundial da Saúde (OMS) manifestou a sua preocupação com o aumento dos casos de HAT. Em resolução publicada em 1997, a OMS defendeu fortemente a necessidade da população ter acesso ao diagnóstico e tratamento da doença, reforçando a atividade de vigilância e controle (WHO, 1997). No entanto, os levantes sociais e guerras, combinado com a falta de consciência dificultam o controle da doença, podendo aumentar a probabilidade de surto e taxa de mortalidade. Outros fatores como a aparente resistência química do parasito e do vetor, migrações e susceptibilidade de populações fortalecem a necessidade de novas medidas e ferramentas na investigação desta tripanossomíase a fim de reduzir seu impacto sobre o bem-estar das populações africanas (Garcia *et alli*, 2006).

Ciclo de vida do *Trypanosoma brucei*

Assim como o *T. cruzi*, *T. brucei* é um parasito que apresenta um ciclo de vida digenético alternado entre um inseto hematófago e hospedeiro mamífero. No curso do seu ciclo de vida, o tripanossomo africano encontra diferentes ambientes e responde a isso com alterações morfológicas dramáticas e padrões de expressão gênicos distintos (Matthews, 1999). Em cada caso, estas mudanças são programadas com precisão (Barry and McCulloch, 2001). Nos últimos anos, tem ocorrido um grande esforço para identificar marcadores que ajudem a acompanhar a progressão das diferentes formas do parasito, tanto em nível celular como molecular (Matthews *et alli*, 2004).

Durante os diferentes estágios de seu ciclo de vida, o *T. brucei* permanece circulante nos fluidos tissulares: saliva e hemolinfa da mosca tsé-tsé; no sangue, linfa

e líquido encéfalo-raquidiano do hospedeiro mamífero. Na corrente sanguínea de mamíferos, o tripanossomo se apresenta em duas formas: uma forma proliferativa, longa e delgada (*slender*) e outra forma não proliferativa, curta e achatada (*stumpy*) [Figura 2; adaptada de (Matthews, 1999)]. Essa diferenciação permite ao parasito cumprir seu duplo objetivo no hospedeiro humano: (1) proliferar e (2) assegurar a transmissão para o vetor, a mosca tsé-tsé.

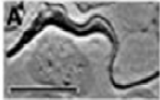

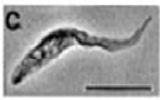
Tipo Celular	Localização	Antígeno de superfície	Status de divisão
Longo e delgado 	Corrente sanguínea	VSG	Se divide
Curto e achatado 	Corrente sanguínea	VSG	Não se divide
Prociclico 	Intestino médio da mosca tsé-tsé	Prociclina	Se divide

Figura 2. Algumas formas do *Trypanosoma brucei*. As características biológicas básicas de cada tipo celular do tripanossomo africano são mostradas do lado direito de cada imagem. VSG, glicoproteínas de variação antigênica. Barra de escala = 10 µm. Figura adaptada de Matthews, 1999

O ciclo de vida (Figura 3) se inicia no momento em que o hospedeiro mamífero é picado pela mosca tsé-tsé e as formas tripomastigotas metacíclicas, presentes nas glândulas salivares do vetor, são inoculadas. No sangue, o parasito se transforma na forma longa e delgada e se prolifera. Essa forma é extremamente adaptada ao ambiente rico em glicose do sangue (Bakker *et alli*, 1995). A absorção de açúcares, aminoácidos e nucleosídeos é mediada por translocadores escondidos sob um espesso glicocálice constituído basicamente de glicoproteínas de variação antigênica (VSG) (Coppens and Courtoy, 2000). Estas proteínas desempenham um papel fundamental na evasão do sistema imune (Donelson *et alli*, 1998). A forma longa e delgada se prolifera rapidamente, o que lhe permite estabelecer a parasitemia no mamífero. Em contraste, as formas curtas e achatadas do tripanossomo africano se

acumulam no pico da parasitemia; elas não se dividem e possuem uma mitocôndria altamente ampliada com os componentes da cadeia respiratória ativos. Isso permite que, quando ingerida no repasto da mosca tsé-tsé, a forma curta e achatada possa rapidamente se adaptar ao novo ambiente, o intestino do vetor. No intestino médio da mosca tsé-tsé, a forma curta completa sua mudança bioquímica e morfológica o que culmina com a geração de uma população proliferativa, a forma procíclica. As células longas e delgadas também podem concluir esta transformação, mas é a célula curta e achatada que a faz com mais eficiência (Matthews, 1999).

A transformação da forma sanguínea em forma procíclica é dependente de temperatura e de intermediários do ciclo de Krebs. Além disso, neste estágio, o parasito perde as VSGs e começa a expressar uma nova glicoproteína de superfície, a prociclina (Clayton and Hotz, 1996). O glicocálce de prociclina tem o papel crucial em proteger o parasito contra a ação de proteases gástricas do inseto, promover a maturação e tropismo do parasito em direção às glândulas salivares. Neste compartimento, as formas procíclicas se diferenciam em epimastigotas que ainda possuem a camada de prociclinas que finalmente dão lugar às formas infectivas tripomastigotas metacíclicas, completando assim o ciclo do *T. brucei*.

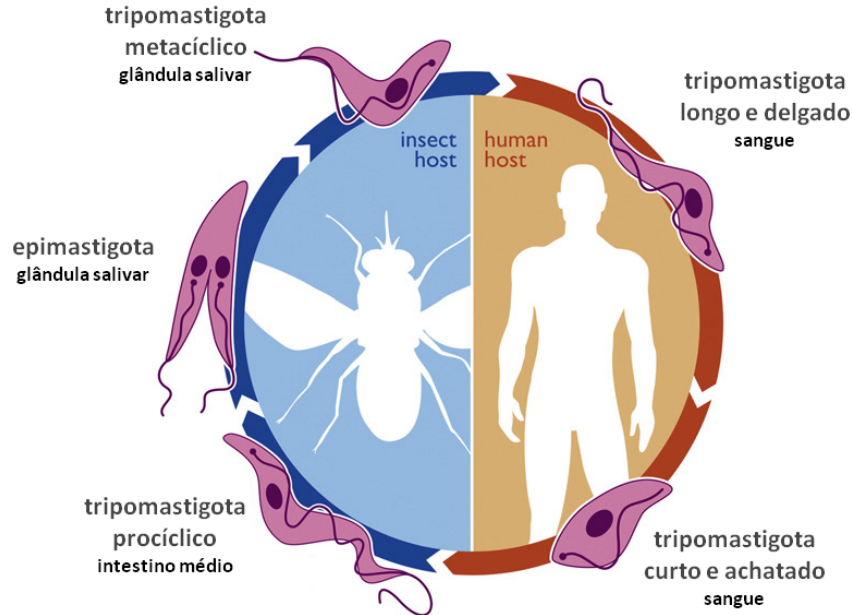


Figura 3. Ciclo de vida do *Trypanosoma brucei*. Representação esquemática adaptada de Cuervo *et alli*, 2010.

Manifestações clínicas

A doença se apresenta em duas fases: fase inicial ou hemolinfática e fase tardia ou encefálica. A fase inicial começa, geralmente, 1-3 semanas após a picada da mosca tsé-tsé causando uma variedade de sintomas não específicos tais como febre, cefaléia, mal-estar e fraqueza. Enquanto a doença progride, ocorrem disfunções em órgãos específicos, tais como: taquicardia e insuficiência cardíaca devido ao comprometimento cardiovascular, lesões de pele, distúrbios endócrinos, comprometimento do fígado, baço e envolvimento ocular. O estágio tardio envolve o sistema nervoso central (SNC) sendo, geralmente, mais longo na doença causada por *T. b. gambiense*, em comparação com doença causada por *T. b. rhodesiense*. Enquanto a primeira pode durar meses ou anos, a última é mais rápida, durando de 3-4 semanas. Neste estágio, o parasito é capaz de atravessar a barreira hematoencefálica e invadir o SNC o que resulta em uma reação inflamatória no cérebro (Mott, 1907). Existe um amplo espectro de possíveis envolvimento neurológicos na doença do sono, mas nem todos irão ocorrer no mesmo paciente. Sinais de envolvimento neurológicos incluem distúrbios mentais como irritabilidade, falta de concentração e mudança de personalidade. O envolvimento do sistema motor é detectado pelo desenvolvimento de convulsões, fasciculações musculares e, em alguns casos, paralisia. Os sinais do envolvimento da parte sensitiva podem ser hiperestesia, anestesia ou prurido intenso. Distúrbios característicos do sono são: o desenvolvimento de sonolência diurna seguido por insônia noturna; alterações no padrão e estrutura do sono além de crises de narcolepsia. Com a progressão da doença, o paciente se torna indiferente ao seu entorno e fica mais difícil de acordá-lo. Sem tratamento, o paciente progredirá para coma e morte em ambas as formas de HAT (Rodgers, 2009).

Tratamento quimioterápico

Até abril de 2009, somente quatro drogas eram registradas e liberadas para o tratamento da doença: pentamidina, suramina, melarsoprol e eflornitina (Barrett *et alli*, 2007). A eficácia das drogas depende do estágio (inicial ou tardio) em que a doença é diagnosticada. No entanto, nenhuma delas é anódina assim como todas têm certo

nível de toxicidade. Em abril de 2009, a OMS incluiu a combinação de eflornitina e nifurtimox (atualmente usado para tratar a doença de Chagas) em sua lista de medicamentos essenciais para melhorar a gestão de casos de tripanossomíase africana humana (WHO, 2010).

A suramina, droga utilizada no tratamento da doença em sua fase inicial, pode apresentar efeitos secundários que variam de lesões cutâneas, choque anafilático, insuficiência renal à neurotoxicidade. Outra opção para o tratamento da fase inicial é o composto pentamidina que apesar de bem tolerado, o tratamento pode resultar tanto em hipo- como em hiperglicemia além de diminuir a pressão sanguínea. Nenhuma das duas drogas é capaz de atravessar a barreira hematoencefálica de forma eficiente e, portanto, não podem ser administradas no estágio encefálico da doença (Rodgers, 2009).

Uma vez que a fase tardia é caracterizada pela presença de tripanossomo no líquido encéfalo-raquidiano e no cérebro, o tratamento indicado inclui os compostos eflornitina e melarsoprol. A eflornitina só é eficaz contra a infecção causada por *T. b. gambiense*, pois *T. b. rhodesiense* mostrou ter resistência inata à droga. Os efeitos adversos da eflornitina incluem pancitopenia, distúrbio gastrointestinal, convulsões ou hemiparesia, que são reversíveis espontaneamente sobre a retirada da droga (Legros *et alli*, 2002; Pepin and Milord, 1994). Já o melarsoprol, única droga que pode ser usada para tratar a infecção tardia das duas subespécies, é um medicamento altamente tóxico (Rodgers, 2009). Efeitos colaterais mais sérios incluem taquicardia, hemorragia subconjuntival e dor retroesternal. No entanto, de longe, o efeito colateral mais grave decorrente da administração dessa droga é o desenvolvimento de uma encefalopatia reativa grave pós-tratamento. Isso ocorre em aproximadamente 10% dos pacientes tratados e pode ser fatal em metade dos indivíduos afetados. Assim, a administração de melarsoprol resulta na morte de até 5% de todos os pacientes que recebem o tratamento (Pepin and Milord, 1994). Por fim, as perspectivas de vacinação são dificultadas pelo processo de variação de superfície celular, onde os parasitos alteraram repetidamente o revestimento da superfície que interage com o sistema imunológico (McCulloch, 2004).

Alvos de drogas nos tripanossomos

Como exposto anteriormente, as drogas utilizadas no tratamento das tripanossomíases são antigas, causam efeitos colaterais abusivos e, muitas vezes, não são eficazes. Devido a estes fatores, a pesquisa científica tem se esforçado para identificar e caracterizar alvos específicos para o desenvolvimento de potenciais fármacos para tratar essas doenças (Teixeira, 2007).

Com referência a alvos potenciais, proteínas e enzimas do parasito têm sido estudadas por participarem na interação parasito-hospedeiro, no metabolismo de açúcares e lipídeos, na digestão de proteínas internalizadas do hospedeiro ou em outros processos vitais do parasito (Chang and McGwire, 2002).

Dentre os potenciais alvos quimioterápicos estão incluídas as proteases. Essa classe especializada de enzima é utilizada por protozoários em diversas funções, incluindo a invasão de células hospedeiras e tecidos, a degradação de mediadores da resposta imune e na hidrólise de proteínas do hospedeiro para fins nutricionais (Klemba and Goldberg, 2002; McKerrow *et alli*, 1993; Rosenthal, 1999).

Não é somente em protozoários que as proteases são importantes, elas encontram-se distribuídas em todos os sistemas biológicos, desde vírus a eucariotos. Eventos proteolíticos são essenciais na ovulação, fertilização, desenvolvimento embrionário, formação óssea, apresentação de antígenos, regulação do ciclo celular, cicatrização de feridas, angiogênese, apoptose e muitos outros. Alterações na estrutura e padrões de expressão de proteases acarretam muitos processos patológicos em humanos, incluindo câncer, artrite, osteoporose, moléstias neurodegenerativas e doenças cardiovasculares (Puente *et alli*, 2003).

Proteases

Proteases ou peptidases são enzimas que hidrolisam ligações peptídicas de proteínas ou de fragmentos protéicos. Ao fazê-lo, podem causar alterações irreversíveis ou destruição dos seus substratos com consequências biológicas importantes (Barrett *et alli*, 2001). As que clivam ligações peptídicas internas são conhecidas como endopeptidases ou proteinases, enquanto as que removem

resíduos de aminoácidos das extremidades dos substratos são chamadas de exopeptidases (carboxi ou aminopeptidases) (Barrett and McDonald, 1986). Em termos de especificidade, algumas proteases mostram alta fidelidade em relação a um único substrato, enquanto outras são claramente promíscuas, com uma atividade indiscriminada contra a degradação de seus alvos (Puentes *et alli*, 2003).

Em 1986, Barrett e McDonald apresentaram um sistema de classificação para as enzimas proteolíticas de acordo com o mecanismo catalítico da proteína e sua susceptibilidade a determinados inibidores. As classes propostas por Barrett foram quatro: aspártico-, cisteíno-, metalo- e serino-protease. E, mais recentemente, duas classes foram incluídas: treonino- e glutâmico-protease (Figura 4). Essas diferentes classes podem ainda ser divididas em famílias com base na comparação de sequência de aminoácidos, e estas famílias podem ser montadas em clãs, baseada em suas estruturas tridimensionais (Rawlings *et alli*, 2008).



Figura 4. Classes de proteases. O diagrama representa as seis classes de proteases descritas até o momento.

Metallo-proteases - amplamente distribuídas em procariontos e eucariotos, possuem um cátion bivalente, geralmente zinco ou cálcio, no sítio ativo que pode direcionar a ligação peptídica a ser clivada e estabilizar a própria proteína. Essas proteases são inibidas por agentes quelantes de íons bivalentes tais com 1,10 fenatrolina e fosforamidon. As collagenases fazem parte dessa classe, mas a

representante mais importante é a termolisina de *Bacillus thermoproteolyticus* (Inouye *et alli*, 2007). Um exemplo de metalo-protease em tripanossomos é a glicoproteína de superfície gp63. Em *T. cruzi*, essa protease mostrou ter uma variação considerável de sua expressão nos diferentes estágios do parasito e em diferentes cepas (Lowndes *et alli*, 1996), porém seu papel na doença ainda não foi elucidado.

Aspártico-proteases - o sítio ativo é, normalmente, formado por um par de resíduos de ácido aspártico e são enzimas mais ativas em pHs ácidos. Possuem uma preferência por clivar ligações peptídicas entre resíduos de aminoácidos hidrofóbicos e são inibidas por pepstatina A ou compostos de diazoacetil (Davies, 1990; Rawlings and Barrett, 1995). Geralmente as aspártico-proteases são sintetizadas como precursores maiores inativos (zimogênio), que são posteriormente convertidos em enzimas ativas por remoção de um peptídeo no N-terminal que obstrui a fenda do sítio catalítico (Khan and James, 1998). Em *Plasmodium falciparum*, enzimas dessa classe (plasmepsina) digerem a hemoglobina do hospedeiro e já foram reconhecidas como alvo de drogas no tratamento da malária. A inibição dessas proteases cessa o crescimento do parasito levando-o à morte dentro da hemácia (Humphreys *et alli*, 1999; Rosenthal, 2002).

Cisteíno-proteases - existem mais de 400 tipos conhecidos atualmente e muitos estão envolvidos em funções vitais ou em processos infecciosos (Lecaille *et alli*, 2002). Elas requerem um resíduo de cisteína no sítio ativo e sua tríade catalítica é formada por Cys-His-Asn (a ordem pode variar de acordo com o clã). O grupo tiol é nucleofílico devido à proximidade a histidina do sítio ativo, que atua como próton. A interação entre esses dois aminoácidos é estabilizada por um resíduo de asparagina, altamente conservado nessa classe. Muitas cisteíno-proteases são sintetizadas como precursores que contêm um pró-domínio e um domínio maduro (com função catalítica). Essa pró-região possui funções independentes incluindo: chaperona intramolecular, inibidor endógeno da atividade proteolítica da enzima e, em alguns casos, um sinal que endereça a protease ao seu destino intracelular (Sajid and McKerrow, 2002). Os representantes mais importantes desta classe são as catepsinas, as calpains e as capases.

A cruzipaina, uma cisteíno-protease da família de catepsina L, é considerada a protease mais abundante em *T. cruzi* sendo expressa em todos os estágios do parasito e apresenta ampla especificidade catalítica. A cruzipaina libera agonistas de

cinina a partir do cininogênio que se liga a receptores do tipo bradicinina promovendo a liberação de Ca^{2+} no interior da célula hospedeira, o que facilita a entrada do parasito (Scharfstein *et alli*, 2000; Todorov *et alli*, 2003). Inibidores irreversíveis de cisteíno-protease derivados da classe vinil sulfonas inativaram a cruzipaina e cessaram a replicação celular do parasito (Engel *et alli*, 1998a). Em modelo experimental murino da doença de Chagas aguda, um desses inibidores – o K777 - administrado via oral, produziu aproximadamente 50% de cura parasitológica (Engel *et alli*, 1998b). Outra cisteíno-protease, a catepsina B, identificada por nosso grupo, é expressa nas três formas do parasito sendo localizada no lisossomo. Sua relevância na nutrição do parasito pode ser sugerida pela hidrólise de substratos não relacionados como BSA, colágeno do tipo I, gelatina, fibrinogênio e IgG desnaturada (Garcia *et alli*, 1998). Além disso, a superexpressão do seu gene em epimastigostas promoveu um incremento na taxa de replicação e metaciclogênese do parasito (Nóbrega, 2001). Por serem próximas filogeneticamente, estas duas catepsinas L e B apresentam a estrutura das suas bolsas catalíticas muito similares, compartilhando sensibilidade a inibidores. Por isso, estas e outras cisteíno proteases do parasito são consideradas, coletivamente, alvos promissores para quimioterapia da doença de Chagas (McKerrow *et alli*, 1999).

Em *T. brucei*, podemos destacar a bruceína ou rodesaina (catepsinas L) e uma catepsina B. A primeira é capaz de degradar IgG, gelatina e BSA, o que leva a sugerir sua função na nutrição do parasito também. (Troberg *et alli*, 1996). A função da catepsina B (TbcatB) foi inferida por meio de experimentos com RNA de interferência. Os resultados mostraram que a baixa expressão da enzima levou a um aumento do endossomo, falhas na mitose e morte dos parasitos. Parece que TbcatB é essencial para sobrevivência do parasito em cultura e não a rodesaina, como já sugerido (Mackey *et alli*, 2004). Cisteíno-proteases de *T. brucei* também parecem estar envolvidas no cruzamento da barreira hematoencefálica por um processo de sinalização dependente de cálcio (Grab *et alli*, 2009; Nikolskaia *et alli*, 2006).

Glutâmico- e Treonino-proteases - As glutâmico-proteases foram descritas recentemente e apresentam uma única família, cuja atividade catalítica parece iniciar-se com a ativação do resíduo de ácido aspártico. O composto 1,2-epoxi-3-(p-nitrofenoxi) propano (EPNP) é potente inibidor desta classe de proteases (Fujinaga *et alli*, 2004).

Já as treonino-proteases foram primeiramente descritas como parte do proteassoma de *Thermoplasma acidophilum* (Seemuller *et alli*, 1995). Atualmente existem somente seis famílias classificadas nessa classe e parece existir uma participação nucleofílica do resíduo de treonina na porção N-terminal da enzima. Até o momento não se conhece nenhum inibidor natural da enzima. O proteassoma é composto por várias subunidades com atividade de treonino-proteases fundamental na degradação ubiquitina-dependente de proteínas (Goldberg and Rock, 1992) e é encontrado desde arqueobactérias até eucariotos superiores. A atividade do proteassoma de *T. cruzi* foi inibida especificamente por lactacistina, o que impediu a diferenciação intracelular de amastigotas em tripomastigotas (Gonzalez *et alli*, 1996). Isso indica que essa protease multicatalítica está envolvida na remodelação celular essencial para a diferenciação do parasito (Cazzulo, 2002). Já em *T. brucei*, experimentos utilizando RNA de interferência para bloquear a expressão de subunidades do complexo resultaram em significativo acúmulo de proteínas ubiquitinadas, seguido da interrupção de ciclo celular dos parasitos.

Serino-proteases - classe de peptidases caracterizadas pela presença de um resíduo de serina no sítio ativo da enzima. Esse resíduo possui uma hidroxila que participa da reação de catálise e ligação ao substrato. Essa classe de proteases é encontrada em eucarioto, procariotos, arqueias e vírus. Participam de muitos processos fisiológicos importantes como digestão (tripsina, quimotripsina), repostas imunológicas (fatores do complemento), coagulação sanguínea (fatores VIIa, IXa, Xa e XIIa) e reprodução (acrosina) (Polgar, 2005). Geralmente essas proteases não requerem cofatores. A determinação da estrutura tridimensional da quimotripsina, a primeira estrutura resolvida de uma peptidase, permitiu um conhecimento melhor do mecanismo catalítico dessa classe (Matthews *et alli*, 1977). Uma das famílias dessa classe, a família Prolil Oligopeptidase, é o alvo de estudo dessa tese e a sua descrição será apresentada a seguir.

Família Prolil Oligopeptidase ou S9

A família POP é amplamente distribuída nos organismos, abrangendo desde espécies de bactérias e arqueias até os seres humanos (Myohanen *et alli*, 2009; Venalainen *et alli*, 2004). Os principais representantes desta família são: prolil

oligopeptidase propriamente dita (POP, EC 3.4.21.26), a oligopeptidase B (OPB, EC 3.4.21.83), a dipeptidil peptidase IV (DPP IV, EC 3.4.14.5) e a acilaminocil peptidase (ACPH, EC 3.4.19.1) (Rawlings *et alli*, 1991). Juntamente com outros representantes, essas enzimas são agrupadas no clã de serino-carboxipeptidase (SC) (Rawlings and Barrett, 1994) (Figura 5).

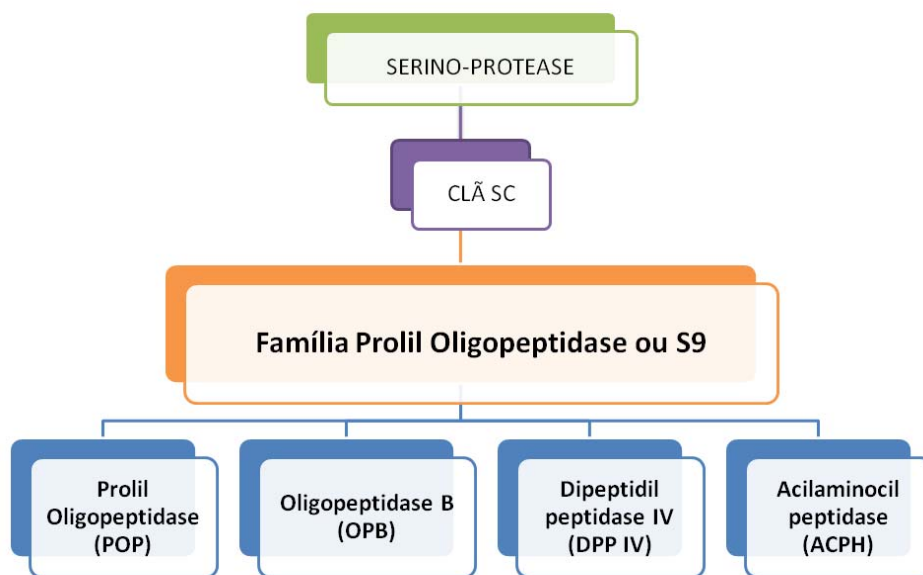


Figura 5. Representantes da família Prolil Oligopeptidase. O diagrama mostra a hierarquia na classe serino-protease, enfatizando a família estudada nesta tese.

Os membros que compõem esta família possuem uma estrutura tridimensional bastante conservada, com a presença de um domínio catalítico com arranjo α/β hidrolase (Goossens *et alli*, 1995), apesar de suas sequências primárias serem divergentes. A tríade catalítica Ser-Asp-His na porção C-terminal também é preservada, outra característica própria da família. Porém existem diferenças na especificidade por substrato, a POP hidrolisa peptídeos do lado carboxílico de resíduos de prolina, a DPPIV libera dipeptídeos nos quais o último aminoácido é também uma prolina, OPB cliva peptídeos após lisina e arginina e ACPH remove aminoácidos N-acetilados de peptídeos bloqueados (Venalainen *et alli*, 2006). Uma das propriedades mais notável dos membros da família POP é a sua seletividade a substratos, que é limitada a oligopeptídeos compreendendo não mais do que

aproximadamente 30 resíduos de aminoácidos (Polgar, 2002). No entanto, nosso grupo já mostrou que a POP de *Trypanosoma cruzi* (POPTC 80) é capaz de clivar colágeno humano do tipo I e IV (Santana *et alli*, 1997).

Prolil Oligopeptidase (POP)

Prolil Oligopeptidase foi primeiramente descrita no útero humano como uma enzima degradadora de oxitocina. Originalmente, recebeu o nome de “enzima que cliva pós prolina” por hidrolisar preferencialmente do lado carboxílico de resíduos de prolina (Koida and Walter, 1976; Walter *et alli*, 1971). Sua suposta seletividade por oligopeptídeos, também descrita na década de 70 (Camargo *et alli*, 1979), foi responsável por sua nomenclatura atual – prolil oligopeptidase (Barrett and Rawlings, 1992).

A POP está envolvida no metabolismo de peptídeos hormonais e neuropeptídeos, o que a correlaciona com distúrbios neurológicos como depressão, mania, esquizofrenia, ansiedade nervosa, anorexia e bulimia (Maes *et alli*, 1995; Maes *et alli*, 2001; Maes *et alli*, 1998). Além disso, sua participação na doença de Alzheimer já foi sugerida, em particular na perda de memória (Kato *et alli*, 1997), mas ainda é controversa, uma vez que inibidores específicos de POP não afetaram a degradação de peptídeos envolvidos na doença (Petit *et alli*, 2000). POP também parece estar relacionada à regulação de vias que envolvem inositol (1,4,5)-trifosfato (Williams *et alli*, 1999; Williams and Harwood, 2000). Baixos níveis de atividade de POP parecem causar efeitos neurotróficos pelo aumento de inositol (1,4,5)-trifosfato na célula (Maes *et alli*, 2001).

Com referência à especificidade para substratos, POPs clivam ligações peptídicas do lado C-terminal de resíduos prolina do tipo Pro-X, onde X é qualquer grupo amino (Yoshimoto *et alli*, 1978), com exceção de prolina. Esta enzima é incapaz de clivar Pro-X se prolina ocupar a posição N-terminal na cadeia peptídica, mesmo se este estiver bloqueado. Desta forma, tais proteases têm requerimento absoluto por ligações Y-Pro-X, (Lin and Brandts, 1983). POPs também hidrolisam substratos contendo alanina no lugar de prolina sob as mesmas condições descritas acima. No entanto, esta atividade enzimática é consideravelmente menor (Yoshimoto *et alli*, 1978).

Inibidores clássicos de serino-protease como PMSF (fenilmetilsulfonil fluoreto) podem provocar pouco ou nenhum efeito em sua atividade (Santana *et alli*, 1997; Yoshimoto *et alli*, 1987). No entanto, são completamente inibidas por diisopropilfluorossulfato (DFP). Compostos contendo clorometil cetona como N- α -Tosil-L-lisina clorometil cetona (TLCK) e N- α -Tosil-L-fenilalanina clorometil cetona (TPCK) alquilam resíduos de histidinas do sítio ativo constituindo-se inibidores eficazes dessas proteases. Em adição, peptídeos aldeídicos análogos à porção acila de substratos são potentes inibidores de serino-proteases (Westerik and Wolfenden, 1972). Com base neste dado, foi desenvolvido o inibidor não competitivo Z-Pro-Prolinal que é capaz de inibir POP de forma altamente específica com $K_i = 14$ nM (Friedman *et alli*, 1984).

A estrutura da POP suína foi resolvida a partir de um cristal com 1,4 Å de resolução, na presença ou não do inibidor Z-Pro-Prolinal [(Fulop *et alli*, 1998); Figura 6A e B]. A enzima tem uma forma cilíndrica e possui dois domínios: o catalítico e o β -propeller. O domínio catalítico tem o arranjo clássico de α/β hidrolase, formado pela porção N- e C-terminal da enzima. Em geral, domínios β -propellers são constituídos por folhas β antiparalelas que se dispõem em forma de pás de hélice (em média de 4 a 8) estabilizadas por um “Velcro” (Figura 6C), rede de pontes de hidrogênio, entre a primeira e última pá (Fulop *et alli*, 2000). No caso da POP, as folhas β antiparalelas do domínio β -propeller estão dobradas e arranjadas radialmente em volta de um túnel central. No entanto, este túnel é estabilizado por ligações hidrofóbicas entre a primeira e última pá e não pelo “Velcro”, como esperado (Figura 6. D). Este domínio não tem papel catalítico, mas, inicialmente, especulou-se que sua função, em POPs, fosse a regulação do tamanho do substrato, uma vez que o diâmetro do túnel central restringiria a passagem de peptídeos maiores que 3 kDa (Fulop *et alli*, 1998).

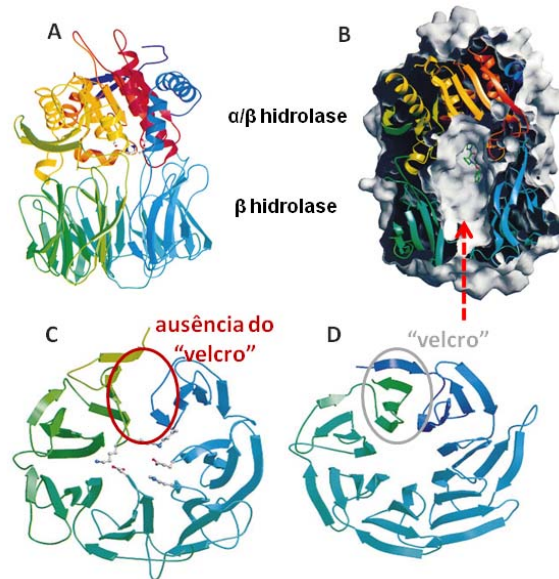


Figura 6. Representação da estrutura da Prolil oligopeptidase suína. (A) Diagrama em fita da estrutura da POP suína, a cor vai da escala de azul para vermelho desde o N- para o C-terminal (PDB 1qfm). (B) Representação de superfície da POP suína – seta vermelha representa o local por onde o substrato acessa a fenda catalítica. O sítio catalítico é representado em *bola e bastão*. (C) e (D) mostram uma comparação do dobramento do domínio β -propeller da POP suína e de proteína G (PDB 1tbg), respectivamente. A visão perpendicular (em relação à fig. 6A) do domínio não-catalítico mostra a ausência do “Velcro” na estrutura da POP suína (círculo vermelho). O “Velcro”, na proteína G (círculo cinza) é fechado por pontes de hidrogênio entre o N-terminal (azul) e 3 folhas β antiparalelas do C-terminal (verde) da proteína. Figura final adaptada de Fülöp *et alli*, 1998.

Todavia, a estrutura da POP suína revelou que a entrada do domínio β -propeller, oposta a tríade catalítica, é pequena para permitir a passagem de peptídeos de até 3 kDa. No intuito de responder como o substrato teria acesso ao sítio catalítico, Fulop *et al.* (2000), propuseram que as pás 1 e 7, que não fazem o “Velcro”, podiam separar-se, aumentando o espaço para a entrada do substrato. Tal possibilidade daria tanto acesso ao sítio ativo quanto protegeria proteínas maiores de hidrólises acidentais. Esse mecanismo foi verificado por meio de mutações sítio-específicas para a formação de pontes dissulfeto entre as pás 1 e 7 do domínio β -propeller. Tais modificações inativaram a enzima, o que confirmaria a necessidade do movimento do domínio β -propeller para o passagem do substrato, (Fulop *et alli*, 2000). Em 2003, cálculos de interação entre a POP de *T. cruzi* e o colágeno indicaram que este substrato teria acesso pela interface entre os dois domínios (Bastos *et alli*, 2005; Bastos, 2003). Este mesmo mecanismo foi sugerido para POP

suína, após a inserção de pontes dissulfeto (por mutações sítio-específicas) entre o domínio β -propeller e o domínio catalítico, tornando a estrutura da enzima mais rígida, o que resultou em sua inativação. Após a análise das mutações inseridas na enzima, o grupo concluiu que uma movimentação do domínio β -propeller aliviaria essa interação, permitindo a entrada do substrato na cavidade do sítio ativo e, conseqüentemente, a clivagem do substrato (Szeltner *et alli*, 2004). Contudo, um ano depois, em 2005, esse mesmo grupo publicou outro trabalho em que excluía o envolvimento do domínio β -propeller na entrada do substrato (Juhasz *et alli*, 2005). Dessa vez, eles fizeram estudos termodinâmicos que mostraram que o domínio β -propeller sozinho é mais estável do que quando acoplado ao domínio α/β hidrolase. Parece, então, que este último desestabiliza o domínio β -propeller, o que poderia facilitar os movimentos da enzima para a catálise. Como o domínio β -propeller é rígido, isso afasta a hipótese de que o mesmo se abriria (na região de interação entre as pás 1 e 7) para a entrada do substrato. Em vez disso, um pequeno túnel na região intra-domínios seria o único caminho possível por onde o substrato acessaria o sítio catalítico (Fuxreiter *et alli*, 2005) (Figura 7).

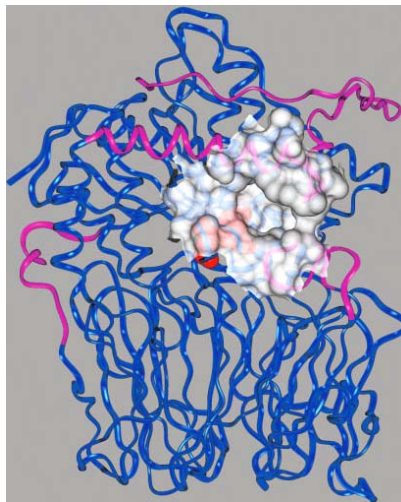


Figura 7. Representação do pequeno túnel formado entre os domínios da POP. Em cinza está representado o túnel por onde o substrato acessaria o sítio catalítico; em rosa estão destacadas as partes funcionais deste evento; o sítio catalítico está representado em “space filling”. Figura adaptada de Fuxreiter *et alli*, 2005.

Prolil oligopeptidase de *T. cruzi* (POPTc 80)

O sucesso da infecção pelo *T. cruzi* vai depender da sua capacidade em migrar através da intricada matriz extracelular (ME) para ter acesso à célula hospedeira. Para isso, o parasito precisa se ligar e desligar a ME e ainda degradá-la. De fato, o parasito apresenta na sua superfície moléculas capazes de se ligarem a fibronectina/laminina, como membros da família Tc-85 que são expressos somente na forma tripomastigota do parasito e possuem afinidade por elementos da ME (Giordano *et alli*, 1994; Giordano *et alli*, 1999). Em termos da degradação da ME, a POPTc 80 tem grande potencial para fazê-la, pois é secretada por formas tripomastigotas e hidrolisa colágenos dos tipos I e IV e fibronectina em vários sítios pós prolina (Grellier *et alli*, 2001; Santana *et alli*, 1997). Esta atividade colagenolítica foi demonstrada *in situ* sobre o mesentério de rato (tecido rico em colágeno do tipo I) sendo comparável a colagenase de *Clostridium*, bactéria altamente invasiva (Santana *et alli*, 1997). Além disso, o envolvimento da POPTc 80 no processo de infecção foi sugerido pelo uso de inibidores específicos e seletivos. Essas moléculas inibem, *in vitro*, a entrada de tripomastigotas em diferentes tipos de células não fagocíticas, de forma dose dependente, com IC₅₀ variando entre 10 a 20 µM (Bastos *et alli*, 2005). O bloqueio da entrada de tripomastigotas na célula não foi pela inibição da ancoragem do parasito à membrana celular e sim da entrada propriamente dita, um processo ativo mediado por transdução de sinal (Bastos *et alli*, 2005).

Mas, como a POPTc 80 é capaz de hidrolisar substratos tão grandes como os componentes da matriz extracelular? A alta massa molecular dessas proteínas a impediria de acessar o sítio ativo pelo pequeno túnel formado entre os domínios da POP, como foi proposto por (Fuxreiter *et alli*, 2005; Juhasz *et alli*, 2005) e explicado anteriormente.

No intuito de compreender um pouco mais dessa característica da POPTc 80, seu modelo tridimensional foi construído com base na estrutura cristalizada da POP suína (Bastos *et alli*, 2005). A POPTc 80 apresenta, assim como as demais POPs, um domínio catalítico do tipo α/β hidrolase e um domínio β -*propeller* composto de sete pás (Figura 8A e B). Apesar da grande sobreposição estrutural entre o modelo da POP Tc80 e a estrutura da POP suína, foi observado que as cadeias laterais dos resíduos que formam a tríade catalítica são posicionadas em diferentes ângulos.

Estas diferenças podem explicar a estéreo-especificidade em relação aos substratos e inibidores, uma vez que inibidores da POP Tc80 são até sessenta vezes menos eficientes em bloquear a atividade da POP de mamíferos (Bal *et alli*, 2003).

Além disso, foi construído um modelo baseado em cálculos de interação entre a POP Tc80 e o colágeno tripla-hélice (Bastos *et alli*, 2005) (Figura 8C). Este modelo propõe que os dois domínios da enzima se movimentem através de uma alça que os une, permitindo assim que o colágeno se posicione na interface entre eles e próximo à bolsa catalítica. Em 2005, a estrutura da POP de *Sphingomonas capsulata* foi resolvida em configuração aberta, o que reforça ainda mais a nossa hipótese (Shan *et alli*, 2005) (Figura 8D).

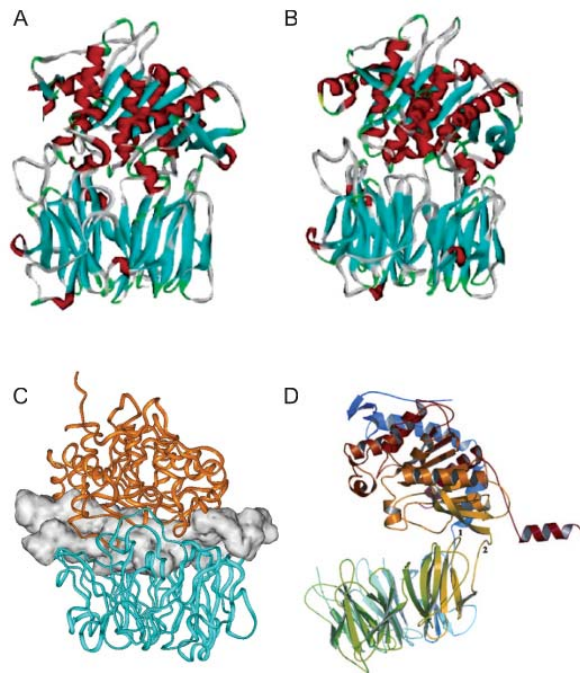


Figura 8. Modelos estruturais de Prolil Oligopeptidase. Modelo estrutural da POPTc 80 (A) baseado na estrutura da POP suína (B), a POPTc 80 possui um domínio catalítico composto por α -hélices (vermelho) e folhas β (azul) formando uma estrutura de α/β hidrolase. O domínio não catalítico β propeller é localizado logo abaixo e é composto somente por folhas β antiparalelas. (C) O colágeno (cinza) interage com a interface do domínio catalítico (laranja) e do domínio β propeller (azul). (D) Estrutura da POP de *Sphingomonas capsulata*. Os números 1 e 2 mostram as alças que conectam os domínios. Figura final adaptada de Bastos *et alli*, 2005; Fülöp *et alli*, 1998; Shan *et alli*, 2005.

Oligopeptidase B (OPB)

Oligopeptidase B foi primeiramente isolada de *E. coli* com especificidade para substrato parecida com a da enzima tripsina, clivando peptídeos após lisina e arginina (Pacaud and Richaud, 1975). Interessantemente, OPB não é capaz de clivar após resíduos de prolina embora seja classificada como um membro da família POP. Porém estas duas proteínas compartilham algumas semelhanças em nível de estrutura primária, como a conservação de resíduos importantes para atividade enzimática. Neste sentido, a OPB de *E. coli* compartilha 25% de identidade com a POP suína (Kanatani *et alli*, 1991). A oligopeptidase B de *Trypanosoma brucei* (OPBTb) já foi cristalizada (2,7 Å de resolução) mas, até o momento, sua estrutura não foi resolvida uma vez que a homologia que compartilha com a POP suína parece não ser suficiente para a montagem de sua estrutura final. Contudo, modelos estruturais 3D da oligopeptidase de *E. coli* e *L. amazonensis* mostraram que, como a POP, a enzima tem dois domínios, o domínio catalítico com arranjo α/β hidrolase e o domínio β -propeller sem o “Velcro” (de Matos Guedes *et alli*, 2007; Gerczei *et alli*, 2000) (Figura 9).



Figura 9. Modelo teórico da Oligopeptidase B de *L. amazonensis* (La_OpB). Representação em fita da La_OpB – vermelho, α -hélice e amarelo, folhas β . Figura adaptada de De Matos Guedes *et alli*, 2007.

Sua distribuição é restrita a bactérias Gram-negativas e positivas, eucariotos inferiores e plantas (Coetzer *et alli*, 2008; Usuki *et alli*, 2009). A presença da OPB em eucariotos foi mostrada, pela primeira vez, em *T. cruzi* (Cazzulo, 2002) e suas implicações na doença de Chagas serão descritas posteriormente. Em *T. brucei*, essa enzima é liberada na circulação de animais infectados e permanece ativa, podendo ter uma participação na patogênese da doença do sono (Morty *et alli*, 2001). O mesmo foi demonstrado para OPB de *Trypanosoma evansi*. Essa peptidase inativa o fator natriurético atrial de camundongos infectados tendo um papel na desregulação hormonal, característica da *surra*, tripanossomíase que afeta animais domésticos e selvagens (Morty *et alli*, 2005).

Apesar de não haver muitos relatos referentes à atividade dessa enzima sobre substratos naturais, é sugerido que sua atividade é restrita a peptídeos com menos de 30 resíduos de aminoácidos, assim como em POPs. Entretanto, a OPB de *Salmonella enterica* tem a habilidade de degradar histonas H2A e H4 que são proteínas altamente básicas com massa moleculares de 14 e 11 kDa, respectivamente (Morty *et alli*, 2002). A atividade da OPB é rapidamente inibida por inibidores clássicos de serino-protease como diisopropilfluorofosfato (DFP) e N- α -Tosil-L-lisina clorometil cetona (TLCK), no entanto, o PMSF (fenilmetilsulfonil fluoreto) tem uma taxa de inibição quase nula (Coetzer *et alli*, 2008).

Oligopeptidase B de *T. cruzi* (OPBTc)

A invasão de células hospedeiras pelo *T. cruzi* é, sem dúvida, um processo altamente eficiente que envolve a participação de vias de sinalizações bilaterais resultando na entrada ativa do parasito (Moreno *et alli*, 1994; Ruiz *et alli*, 1998; Tardieux *et alli*, 1992). Além do envolvimento de proteínas de superfície e moléculas sinalizadoras clássicas, como o emaranhado sistema de quinases/fosfatase (Rodriguez *et alli*, 1999; Ruta *et alli*, 1996; Wilkowsky *et alli*, 2001; Zhong *et alli*, 1998), proteases do parasito estão intimamente relacionadas com a invasão (Burleigh *et alli*, 1997; Grellier *et alli*, 2001; Scharfstein *et alli*, 2000). Em adição a cruzipaina e a POP Tc80, o parasito dispõe de outra protease-chave para garantir sua entrada na célula mamífera, a oligopeptidase B (OPBTc), originalmente descrita por Santana *et alli*, 1992, como Tc120 (Burleigh and Andrews, 1995; Santana *et alli*, 1992). Sua

participação na invasão celular ocorre por meio da geração de um agonista que ativa fosfolipase C da célula hospedeira resultando na formação de inositol trifosfato (IP₃) e, conseqüentemente, na liberação de Ca²⁺ intracelular (Burleigh and Andrews, 1995; Rodriguez *et alli*, 1995). Ainda não é possível afirmar se a produção do agonista ocorre no citoplasma do parasito ou no meio extracelular pela OPBTc secretada (Fernandes *et alli*, 2005). No entanto, a liberação de Ca²⁺ resulta em modificações do citoesqueleto, que promovem recrutamento e fusão de lisossomos da célula hospedeira no local de ligação do parasito, facilitando sua entrada. Ao contrário de muito patógenos intracelulares que evitam a fusão com os lisossomos, o *T. cruzi* depende da presença dessa organela para sobreviver, uma vez que seu ambiente ácido ativa processos fisiológicos essenciais que resultam na diferenciação de tripomastigotas em amastigotas e escape do sistema imunológico. (Andrews and Whitlow, 1989; Ley *et alli*, 1990; Tomlinson *et alli*, 1995; Vendeville *et alli*, 1999).

A relevância da OPBTc na doença de Chagas tem sido corroborada por meio de vários experimentos. A utilização de anticorpos específicos contra essa enzima foi capaz de neutralizar sua ação inibindo a sinalização de Ca²⁺ em células hospedeiras (Burleigh *et alli*, 1997). O parasito mutante *opb*^{-/-}, incapaz de produzir a enzima, apresentou significativa redução na capacidade infectante *in vitro* e de estabelecer a infecção em camundongos (Caler *et alli*, 1998). Em adição, a OPBTc recombinante purificada foi capaz de restaurar a sinalização de Ca²⁺ no mutante (Caler *et alli*, 1998).

Além de ser um fator de virulência do parasito, a vantagem de se utilizar a OPBTc como alvo potencial de droga reside na ausência de ortólogos em mamíferos (Venalainen *et alli*, 2004). Em teoria, isso facilitaria o desenvolvimento de drogas seletivas, isto é, com menor possibilidade de efeitos colaterais ao homem. Já existem relatos de inibidores de oligopeptidase B de outras espécies que podem fornecer informações úteis para o aprimoramento de inibidores sintéticos mais efetivos contra o *T. cruzi* (Caler *et alli*, 2000; Morty *et alli*, 2005; Tsuji *et alli*, 2006; Venalainen *et alli*, 2004).

Neste contexto, o conhecimento das características estruturais de uma enzima é de grande valia para o desenho racional de inibidores com finalidade terapêutica. Assim, nós estudamos o comportamento estrutural e a estabilidade da OPBTc por

meio de técnicas de ultracentrifugação analítica, espectroscopia de fluorescência e dicroísmo circular (Barrett and McDonald) near e far-UV.

A seguir será apresentada uma breve descrição dos princípios e aplicações destas técnicas.

Dicroísmo circular e sua aplicação no estudo de proteínas

O dicroísmo circular (CD) se fundamenta na absorção diferencial da luz circularmente polarizada no sentido horário ou anti-horário. Se após passarem pela amostra, esses dois componentes forem absorvidos diferentemente, a radiação resultante deixa de ser circular e passa a ter uma polarização elíptica; a diferença na absorção da luz pela amostra é que definirá o sinal dicróico. Esse efeito somente ocorrerá quando o cromóforo for quiral (opticamente ativo). Essa é uma técnica excepcionalmente sensível à conformação das moléculas, e assim tem sido muito utilizada no estudo de biomoléculas (Sreerama and Woody, 2004).

Os espectros de CD na região do UV-próximo (255-310 nm) derivam da cadeia lateral dos aminoácidos aromáticos (tirosina, triptofano e fenilalanina), refletindo a estrutura terciária e, ocasionalmente, quaternária da molécula (Figura 10A). Eles podem ser positivos ou negativos e variam em intensidade de acordo com as interações dos resíduos aromáticos. Já os espectros do CD na região do UV-distante (abaixo de 250 nm) derivam das ligações peptídicas e refletem a estrutura secundária da proteína (Figura 10 B) (Kelly *et alli*, 2005).

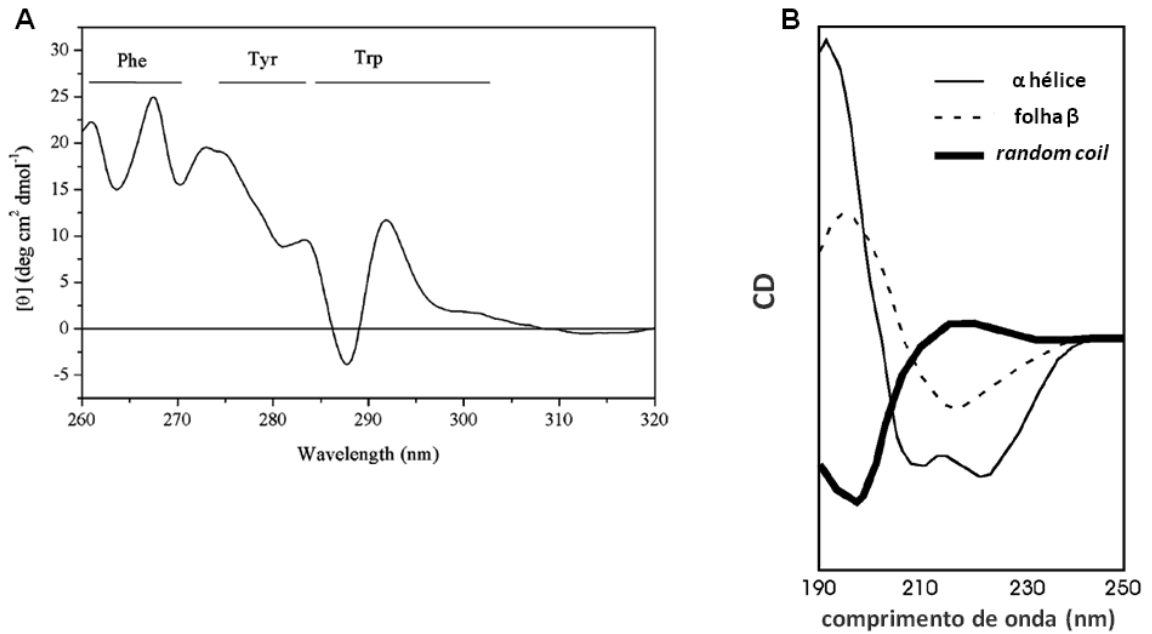


Figura 10. (A) O espectro do CD na região do UV-próximo da dehidroquinase de *Streptomyces coelicolor*. A gama de comprimentos de onda correspondente aos sinais oriundos das cadeias laterais de Phe Tyr e Trp está indicada. (B) Espectros na região UV-distante das diversas formas de estruturas secundária de uma proteína. Figura adaptada de Kelly *et alli*, 2005

Apesar da técnica de dicroísmo circular oferecer poucas informações acerca da estrutura da proteína em níveis atômicos, ela tem duas grandes vantagens: a sua sensibilidade a quaisquer mudanças conformacionais da molécula; e a plasticidade de condições experimentais acessíveis com o uso de pouca amostra (Martin and Schilstra, 2008).

As principais aplicações desta espectroscopia no estudo de biomoléculas são:

- Os espectros de CD na região do UV-distante permitem, com ajuda de softwares, a predição do conteúdo de estrutura secundária da amostra;
- A detecção de mudanças estruturais e conformacionais causadas por modificações de pH, concentração de sal, solventes diversos e etc.;
- Análise estrutural e comparativa de proteínas nativas e seus respectivos mutantes;

- d. Monitoramento das mudanças estruturais a partir de tratamento térmico e adição de desnaturantes químicos (uréia e guanidina, por exemplo);
- e. Monitoramento de interações proteína-proteína; proteína-ligante, proteína-DNA e outros;

Os experimentos de desnaturação térmica, tanto para o UV-próximo como o distante, analisam a influência da temperatura no desdobramento/redobramento da proteína, determinando a transição entre seu estado nativo e desnaturado. De uma forma geral, o aumento da temperatura afeta, primeiramente, as interações necessárias para manutenção da estrutura terciária. Quando essas interações são rompidas, a molécula adquire uma estrutura mais flexível, expondo certas partes que antes estavam em ambientes mais hidrofóbicos e agora interagem mais com o solvente. Aumentando ainda mais a temperatura, as ligações que estabilizam as estruturas secundárias da molécula podem se romper, culminando com a perda total da estrutura nativa da proteína. As análises matemáticas das curvas de desdobramento permitem calcular parâmetros termodinâmicos de estabilidade estrutural e cinéticas de dobramento.

Fluorescência intrínseca e sua aplicação no estudo de proteínas

Assim como o CD, a espectroscopia de fluorescência tem sido largamente explorada em estudos estruturais e funcionais de proteínas (Ammor, 2007). O fenômeno de fluorescência ocorre quando o fluoróforo absorve radiação UV e visível, passando para o estado de excitação eletrônica. Ele permanece excitado por alguns nano segundos, e depois libera a energia remanescente por meio da emissão de radiação eletromagnética, a fluorescência. A intensidade da fluorescência de uma amostra depende da eficiência de absorção da luz emitida e da eficiência de emissão do fluoróforo excitado (Johnson, 2005). O sinal de fluorescência pode ser analisado de várias formas: intensidade, tempo de vida, energia (comprimento de onda) e liberdade rotacional (polarização e anisotropia) de forma a revelar diferentes aspectos estruturais da proteína de interesse.

A fluorescência intrínseca de proteínas é dependente da cadeia lateral de três resíduos de aminoácidos: fenilalanina, triptofano e tirosina. O triptofano é o fluoróforo

mais abundante em proteínas e sua sensibilidade à polaridade e mobilidade do ambiente faz de sua fluorescência uma importante ferramenta em estudos de dinâmica e estrutura de proteína.

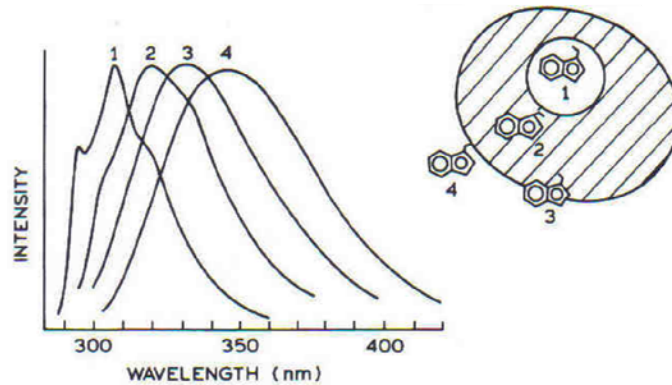


Figura 11. Exemplos dos espectros de fluorescência do triptofano. A figura ilustra os diferentes espectros de emissão do triptofano de acordo com sua localização na molécula; Lakowicz, 2004.

A emissão máxima da proteína reflete a exposição dos seus triptofanos ao ambiente aquoso. Na molécula, quando o ambiente do triptofano é completamente apolar, o espectro de emissão esperado é mais próximo da faixa do azul (aproximadamente 320 nm). Com a mudança do triptofano para ambientes mais expostos ao solvente, a emissão muda para comprimentos de ondas maiores. A observação da fluorescência é usada para acompanhar mudanças estruturais, desnaturação ou renaturação de proteínas sob influências de temperaturas, pH ou na presença de solutos como guanidina e uréia. Dependendo das modificações que essas condições causem na estrutura da proteína, o espectro do triptofano sofrerá deslocamentos, permitindo inferências sobre a conformação da proteína (Lakowicz, 2004).



JUSTIFICATIVA

Justificativa

Doenças negligenciadas são aquelas cujo tratamento é inadequado, ou mesmo inexistente, e não apresentam atrativos econômicos para o desenvolvimento de fármacos por atingir principalmente a população de países tropicais pobres. A escassez de tratamentos eficazes para tais doenças é devido à falta de interesse das indústrias farmacêuticas em investir na pesquisa e desenvolvimento de drogas voltadas a pacientes de baixa renda financeira. Entre 1975 e 1999, menos de 1,1 % de novas drogas produzidas foram desenvolvidas para o tratamento de doenças tropicais e tuberculose (Trouiller *et alli*, 2002). Deste número irrisório (13 de 1.393 produzidas), nenhuma droga foi direcionada para a doença de Chagas. Sua quimioterapia continua praticamente a mesma preconizada desde os anos 70 do século passado, apresentando sérios efeitos colaterais e baixa eficácia para a fase crônica da doença. Devido a este panorama, diversos grupos de pesquisadores têm se esforçado para identificar e validar alvos no *T. cruzi* com potencial terapêutico para doença de Chagas. Dentre os alvos candidatos, várias enzimas do metabolismo e proteases do parasito têm destaque.

O envolvimento da OPBTc e POP Tc80 nos mecanismos moleculares associados ao processo infectivo do parasito coloca estes dois membros da família de POPs no rol dos alvos potenciais para tratamento da doença de Chagas (Bastos *et alli*, 2005; Burleigh *et alli*, 1997; Caler *et alli*, 1998; Grellier *et alli*, 2001; Santana *et alli*, 1997). Vários inibidores específicos foram desenvolvidos para a POP Tc80 com K_s da ordem de nano e picomolar, somados a uma considerável seletividade comparada a POPs de mamíferos (Bal *et alli*, 2003; Joyeau *et alli*, 2000; Vendeville *et alli*, 1999; Vendeville *et alli*, 2002). No entanto, estes inibidores (e/ou outros) precisam ser aprimorados ainda mais, a fim de apresentarem biodisponibilidade ideal para testes *in vivo* em modelos animais da doença de Chagas. A obtenção de inibidores com tais características seria, sem dúvida, otimizada por meio do desenho racional dessas moléculas. Para isso, o conhecimento das características estruturais tanto da POP Tc80 quanto da OPBTc é fundamental.

Tendo em mente a importância de conhecer a estrutura das proteases que trabalhamos de *T. cruzi* e também de *T. brucei*, nosso grupo tem empregado muito das técnicas disponíveis para tal finalidade. Nesse trabalho abordaremos a

modelagem molecular por homologia como uma opção útil para o conhecimento da estrutura terciária da enzima e elucidação do mecanismo catalítico da POP Tc80. Embora a obtenção de um modelo da OPBTc seja dificultado pela indisponibilidade de uma estrutura tridimensional resolvida, é possível ter informações estruturais relevantes por meio de dicroísmo circular na região do UV próximo e distante. Mesmo que o CD não forneça informações em nível de resolução atômica, essa técnica pode explorar estruturas de proteínas em inúmeras condições experimentais, inclusive as que sejam mais relevantes fisiologicamente, o que é mais difícil em cristalografia e ressonância nuclear magnética (NMR). Usamos também espectroscopia de fluorescência, outra técnica importante no estudo do dobramento protéico.

O uso de inibidores específicos de uma enzima auxilia na sua validação como alvo terapêutico. No entanto, é quase impossível, nos dias de hoje, controlar a especificidade dos inibidores administrados *in vivo*. Assim a validação de um alvo por meio de nocaute dos alelos do seu gene é praticamente incontestável. Neste sentido, mostraremos nesta tese um estudo preliminar do nocaute do gene da POP Tc80 o que permitira, futuramente, elucidar seu papel na patogenia da doença de Chagas.

Contudo, a manipulação de genes no *T. cruzi* é ainda bastante complexa, uma vez que seu genoma apresenta peculiaridades e grande plasticidade, dando ao parasito uma enorme capacidade de adaptação. Uma característica é a ausência do efeito de RNA de interferência (RNAi) no parasito, fenômeno tão empregado para estudo de função gênica nos mais diversos organismos. Em contraste, o RNAi é largamente explorado em *T. brucei*, parasito com proximidade filogenética com o *T. cruzi* e, graças a isto, é possível inferir funções comuns a genes ortólogos desses dois parasitos. A partir desta idéia, nós começamos o estudo da POP de *T. brucei* - que será apresentado nesta tese - onde propomos um possível papel na patogenia da doença do sono.

Enfim, as informações estruturais de uma enzima aliadas a sua função biológica podem nortear o desenho racional de pequenas moléculas específicas que bloqueiem sua atividade ou mesmo que desestabilizem a sua estrutura. Assim, isso daria início ao desenvolvimento de estratégias terapêuticas para o combate de doenças.



OBJETIVOS

Objetivos

Esse trabalho de tese está inserido numa linha geral de pesquisa que tem por base o entendimento de mecanismos moleculares da interação patógeno-hospedeiro com a finalidade de identificar potenciais alvos de drogas para o tratamento de doenças infecciosas. Neste sentido, esta tese aborda alguns aspectos estruturais e funcionais de três proteases de tripanosomatídeos, pertencentes à família de prolil oligopeptidases. Estas enzimas são oligopeptidase B (OPBTc) e prolil oligopeptidase (POPTc 80) de *T. cruzi* e a prolil oligopeptidase (POP Tb) de *T. brucei*. Neste contexto propomos estudar:

I. Aspectos estruturais da OPBTc- este estudo visa o conhecimento acerca da estabilidade estrutural e da oligomerização da enzima. Para alcançar este objetivo, desenvolvemos as seguintes atividades:

- Análise da dimerização da enzima por gel filtração e ultracentrifugação analítica;
- Teste do efeito de aditivos (DTT e NaCl), temperaturas e pHs na oligomerização e atividade da enzima;
- Caracterização estrutural da OPBTc por meio de fluorescência intrínseca e dicróismo circular.

II. Estudo da prolil oligopeptidase de *T. brucei*- tem o objetivo de caracterizar suas propriedades enzimáticas, investigar seu papel na viabilidade do parasito e na patogenia da doença do sono. Para isso, as seguintes etapas foram traçadas:

- Teste da atividade da POPTb sobre peptídeos hormonais humanos, colágeno humano purificado e sobre o colágeno nativo presente em mesentério de rato;
- Mapeamento da expressão da POPTb nas diferentes formas do parasito;
- Detecção da POPTb ativa no plasma de animais infectados por *T. brucei*

III. Elucidação do mecanismo catalítico da POP Tc80- o objetivo deste trabalho é de validar experimentalmente o modelo tridimensional teórico da POP Tc80 e do seu mecanismo catalítico, previamente construídos por nosso grupo. Este modelo supõe

que é necessário um movimento dos dois domínios da enzima para expor sua interface e conseqüentemente permitir a entrada do substrato. Para impedir este movimento de abertura, nosso objetivo foi de inserir uma ponte dissulfeto entre os dois domínios, tornando a estrutura da proteína inflexível. Para isso foi necessário:

- Realização da dinâmica molecular do modelo sob diferentes condições;
- Mutação de forma sítio-específica os resíduos A, S ou N para Cys, localizados no domínio α/β hidrolase da POP Tc80 e assim, formar uma ponte dissulfeto com a Cys 255 do domínio β -propeller;
- Comparação dos parâmetros enzimáticos e catalíticos dos mutantes da POP Tc80 com a enzima não mutada.

IV. Nocaute do gene *poptc80* no *T. cruzi*- tem a finalidade de elucidar o papel da POP Tc80 na patogenicidade da doença de Chagas e assim, talvez, legitimá-la como fator de virulência. As etapas foram:

- Construção de um cassete contendo as regiões 5' e 3' não traduzidas do gene *popt80* intercalado por um marcador de seleção, o gene de resistência a neomicina (*neo*);
- Seleção de clones resistentes à G418;
- Mapeamento físico da presença de *neo* nos clones selecionados.



I. Propriedades estruturais da OPBTc

Apresentado na forma de manuscrito para publicação



An insight into the structural properties of Oligopeptidase B from *Trypanosoma cruzi*.

Authors listed in alphabetical order:

Christine Ebel¹

Eric Faudry¹

Flávia Nader Motta²

Izabela M. D. Bastos²

Jaime Martins de Santana²

João Alexandre Barbosa³

Sônia Maria de Freitas³

¹ Laboratório da Interação Parasito-Hospedeiro, Universidade de Brasília, Brazil

² Commissariat à l'Énergie Atomique (CEA), France

³ Laboratório de Biofísica, Universidade de Brasília, Brazil

ABSTRACT

Oligopeptidase B (OpdB, EC3.4.21.83) belongs to the prolyl oligopeptidase family of serine protease (clan SC, family S9). It is increasingly being implicated as an important virulence factor in trypanosomiasis. The drugs most commonly used in sleeping sickness treatment reduce the activity of *T. brucei* oligopeptidase B. *T. cruzi* oligopeptidase B (OPBTc), the focus of this work, is involved in cell invasion by generating a Ca^{2+} agonist necessary for recruitment and fusion of host lysosomes at the site of parasite attachment. This scenario indicates that further structural and functional characterization of OPBTc should help clarifying its physiological function and lead to the development of therapeutic targets for Chagas' disease. In the present work, we report that OPBTc has a dimeric structure confirmed by different methods: gel permeation chromatography and analytical ultracentrifugation (AU) assays. The dimer association is not due to intermolecular disulfide bonds and it is salt-resistant. The enzyme retains its dimeric structure and it is fully active until 42 °C. The structural stability of the fully active recombinant OPBTc was investigated through thermal unfolding processes monitored by circular dichroism. Far UV CD experiments showed that OPBTc has a highly stable secondary structure at different pHs and less stable at moderate ionic strength condition. On the other hand, near UV CD spectra demonstrated that the tertiary structure of OPBTc is completely lost when the enzyme is heated at temperatures above 45°C, which correlates well with temperatures-dependent activity assays.

INTRODUCTION

Chagas disease (American Trypanosomiasis) is a multisystemic illness resulting from infection with the intracellular protozoan parasite *Trypanosoma cruzi*, which is able to invade a wide variety of mammalian cells. It affects millions of people in Latin America, representing a major public health problem because of its high rates of morbidity and mortality due to clinical complications at the chronic phase [1; 2]. This scenario requires functional and molecular characterization of *T. cruzi* virulence factors that could be used as targets for the development of vaccine and chemotherapy of this disease. The pathogenesis of *T. cruzi* is due to its ability to colonize, grow and persist in human tissue for years and to elicit immunopathological and parasitological reactions [3].

The corresponding biological processes that account for these pathogenic mechanisms include those associated with the entry of *T. cruzi* into mammalian host cells, which involve specific interactions among host cell and many parasite molecules such as GP82, cruzipain, prolyl oligopeptidase (POP Tc80) and oligopeptidase B (OPBTc) [4]. To infect nonphagocytic mammalian cells, *T. cruzi* trypomastigotes trigger Ca^{+2} -signalling in the host cells that results in the recruitment and fusion of lysosomes at the parasite binding site. Inhibition of the OPBTc activity precludes entry of trypomastigote forms of the parasite into host cells. Furthermore, specific silencing of OPBTc gene greatly inhibited the infective capacity of trypomastigotes both *in vitro* and *in vivo*, revealing OPBTc as a *T. cruzi* virulence factor and, thus, a good target for developing new drugs to treat *T. cruzi* infection [5; 6]

Oligopeptidase B (OPB, EC3.4.21.83) belongs to the prolyl oligopeptidase (POP) family of serine protease (clan SC, family S9) [7] and different from other POP members it does not cleave after proline residues. However, OPB shares similarities

of catalytic domain amino acids and of secondary structure prediction with POP family members, what include it in this family [8; 9]. OPB is a potential processing enzyme of prokaryotes, being very specific for the basic amino acid pairs of peptides [10].

OPB has a restrict distribution and it has been described in Gram-negative and positive bacteria, spirochetes, protozoaries and it is not found in higher eukaryotes with the exception to plants [11; 12; 13]. Although significant efforts have been made towards understanding the structural and functional properties of OPB [9; 12; 13; 14], the physiological role of the enzyme is unknown and its natural substrate has not been identified. Oligopeptidase B from *T. brucei* had been crystallized, but its structure determination is not reported [12]. In addition of *T. cruzi*, OPB is increasingly being implicated as an important virulence factor in other trypanosomes [15]. The oligopeptidase B of *Trypanosoma evansi* inactivated atrial natriuretic factor in the bloodstream of the infected host [16]. The drugs most commonly used in sleeping sickness treatment reduce the activity of *T. brucei* oligopeptidase B [17].

The OPBTc has a predicted molecular mass of nearly 80 kDa, however it was observed that it migrates as 120-kDa in semi-native SDS-PAGE, what would not correspond to a monomer or to a dimer [18]. Afterward, the dimerization of *T. cruzi* oligopeptidase B was suggested through gel filtration assays but it has been never confirmed [5]. The knowledge of protein folding and interaction is of immense biological significance. A protein must fold correctly in order to achieve its functional native state. For example, the association or dissociation of monomers can create or destroy a functional binding site that occurs at the subunit interfaces. Structural data of a protein can also provide comprehension of the molecular mechanism related to protein stability, biological implications and biotechnological applicability [19]. This scenario indicates that further structural and functional characterization of OPBTc

should assist in the development of specific inhibitors that will be useful for probing OPBTc physiological roles and that may have potential therapeutic applications.

In this work, we carried out a variety of biophysical tests, such as circular dichroism, intrinsic fluorescence and analytical ultracentrifugation in order to elucidate the dimerization of OPBTc and its structural stability.

MATERIALS AND METHODS

Parasites

T. cruzi epimastigote forms from CL Brener stock were grown in liver infusion tryptose medium (LIT) supplemented with 100 µg/mL of Gentamicin and 5% (v/v) fetal calf serum at 28 °C [20].

Cloning, expression and purification of T. cruzi Oligopeptidase B

Specific primers OPB1 (forward, 5' – attctaCTCGAGATGAAGTGTGGTCCCATTGC – 3'; lowercase, random bases; underlined, *XhoI* site; bold, initiation codon) and OPB2 (reverse, 5' – attctaGGATCCTCACCTCCGAAGAAGTGTCC – 3'; lower case, random bases; underlined, *BamHI* site; bold, stop codon) were designed from Oligopeptidase B gene (*opbtc*) sequence (Tc00.1047053511557.10; www.genedb.org). The *opbtc* ORF was amplified by PCR using OPB1 and OPB2 primers from genomic *T. cruzi* DNA (CL Brener). The PCR product was subsequently cloned into pGEM-T easy vector (Promega) and completely sequenced on both directions. The ORF was excised from the vector using *XhoI* and *BamHI* enzymes and subcloned into a previously *XhoI* and *BamHI*-digested pET19b plasmid (Novagen), generating pET19b/*opbtc*.

The active OPBTc was produced in *Escherichia coli* BL21(DE3) [21] and purified by affinity chromatography [22]. Briefly, the N-terminal His-tagged OPBTc was expressed in *E. coli* BL21(DE3) by induction of a log phase culture with 0.5 mM isopropylthio- β -D-galactoside (IPTG) at 28 °C over 16 h. Cells were harvested, lysed with Bugbuster™ (Novagen) and submitted to centrifugation at 16,000 g for 20 min at 4 °C. The recombinant protein was purified using His-Band Kit (Novagen). To verify the purity and yield, purified OPBTc was subjected to 10% SDS-PAGE under reducing conditions followed by Coomassie Blue staining. Concentration of the protein was determined using the molar absorption coefficient ϵ value of 118,775 ($M^{-1}cm^{-1}$) at 280 nm measured in water.

Assay of enzyme activity

Recombinant OPBTc activity was determined by measuring the fluorescence of 7-amido-4-methylcoumarin (AMC) released by hydrolysis of the enzyme substrate *N*-Suc-Gly-Gly-Arg-AMC [23]. Purified OPBTc was assayed in reaction buffer, 25 mM Tris-HCl pH 8.0, containing 20 μ M substrate in 100 μ L final volume at different concentrations of DTT and NaCl. AMC release was recorded up to 20 min at 460 nm excitation and 355 nm emission in a 96-well microplate fluorescence reader. The temperature assay was carried out differently: the enzyme was incubated at each temperature for 15 min and afterwards, 20 μ M of substrate was added to a final volume reaction of 50 μ L. After 15 min, 150 μ L of ethanol were added to stop the reaction. In this case, AMC release was recorded as endpoint, a value of accumulated fluorescence.

In-gel proteolytic activity

Visualization of the proteolytic activity in SDS-PAGE was carried out as described [23]. Briefly, 1 μg of OPBTc was solubilized in the electrophoresis sample with or without SDS or 2- β -mercaptoethanol at room temperature. For proteolytic visualization, the gel was washed twice in 2.5% Triton X-100 for 30 min, four times in 25 mM Tris-HCl pH 8.0 at 4 °C and incubated for 2 min with 20 μM of substrate at room temperature. The enzymatic activity was visualized in an ultraviolet light box.

Analytical ultracentrifugation

Sedimentation velocity experiments were performed using a Beckman XL-I analytical ultracentrifuge and an AN-60 TI rotor (Beckman Coulter). The experiments were carried out at 10 °C for *T. cruzi* oligopeptidase B at 28.1, 8.4 and 1.8 μM in 25 mM Tris pH 8.0, 100 mM NaCl. A volume of 100 μL for the most concentrated sample or 400 μL was loaded into 0.3 or 1.2 cm path cells and centrifuged at 42,000 rpm. Scans were recorded every 6 min, overnight, at 280 nm and by interference. We used the Sednterp software (free available at <http://www.jphilo.mailway.com/>) to estimate the partial specific volume of the polypeptide chain, $\bar{v}=0.727$ mL/g, the solvent density, $\rho=1.00458$ g/mL, and the solvent viscosity, $\eta=1.3072$ mPa.s, at 10 °C. The sedimentation profiles were analyzed by the size-distribution analysis of Sedfit (free available at <http://www.analyticalultracentrifugation.com>). In Sedfit, finite element solutions of the Lamm equation for a large number of discrete, independent species, for which a relationship between mass, sedimentation and diffusion coefficients, s and D , is assumed, are combined with a maximum entropy regularisation to represent a continuous size-distribution (Schuck, 2000). We used typically 200 generated sets of data on a grid of 300 radial points, calculated using fitted frictional ratio for

sedimentation coefficients comprised between 1 and 15 S. For the regularization procedure a confidence level of 0.68 was used.

Gel permeation chromatography

An Akta Purifier system equipped with a Superdex 200 10/300 analytical column (GE healthcare) was used to estimate the protein apparent molecular mass in solution. Before each run, the column was equilibrated with 25 mM acetate pH 4.0; 5.0; 6.0 or Tris-HCl pH 7.0 or 8.0 containing 200 mM NaCl. Samples were diluted with the buffer used for column equilibration and 100 μ L were injected and resolved at a flow rate of 0.5 mL/min at room temperature. For the temperature assays, the enzyme was incubated at 28, 37, 42, 55 or 60 °C for 20 min before each run. The column was previously equilibrated with 25 mM Tris-HCl pH 8.0 or in the presence of 0.2, 0.5 or 1M NaCl. The Absorption at 280 nm was monitored and 500 μ L fractions were collected and analyzed by standard SDS-PAGE. Proteins of known Stokes radii (Ferritin, Aldolase, Albumin, Ovalbumin, Ribonuclease) were used for column calibration.

Circular dichroism spectroscopy

Far UV Circular dichroism (CD) measurements were carried out on a JASCO J-810 spectropolarimeter equipped with a Peltier temperature controller and a thermostated cell holder interfaced with a thermostatic bath. Far-UV spectra were recorded in 0.1-cm path length quartz cells at a protein concentration of 0.15 mg/mL (1.72 μ M) in 2.5 mM of the buffers: citric acid pH 3.0, sodium-acetate pH 4.0, sodium-acetate pH 5.0, sodium-acetate pH 6.0, N-2-Hydroxyethylpiperazine-N'-2-ethanesulfonic acid (HEPES) pH 7.0, HEPES pH 8.0, 2-(N-Cyclohexylamino)ethane

Sulfonic Acid (CHES) pH 9.2 and CABS pH 10.0. All buffers contained 200 mM NaCl. The spectra presented in this work represent the average of four accumulated consecutives scans. Thermal denaturation assays were carried out by increasing the temperature from 20 to 75 °C, allowing the temperature to stabilize for 5 min before recording each spectrum. Spectra scans were recorded every increased of 5 °C. Thermal denaturation was monitored at 218 nm.

Near UV CD spectra were acquired on a Jasco J-810 spectrophotometer with a scan speed of 50 nm.min⁻¹. Spectra are the average of 15 scans and were corrected with buffer spectra. Data were collected from 320 to 250 nm, using 1-cm cells and a protein concentration of 0.4 mg/mL under stirring. Buffers are the same mentioned above. For thermal denaturation experiments, temperature was controlled by a Peltier and water bath device. Thermal denaturation was monitored at 283 and 290 nm.

The ellipticity values ($[\theta]_{\text{obs}}$) were baseline corrected by subtracting each buffer's spectra and converted to the mean residue ellipticity $[\theta]_{\text{MRW}}$ in deg.cm²dmol⁻¹, according to the equation:

$$[\theta]_{\text{MRW}} = [\theta]_{\text{obs}} \text{MRW}/C/l \quad (1)$$

where C is the protein concentration (mg/mL), *l* is the path length (cm) and MRW is the average residue weight of OPBTc.

Fluorescence spectroscopy

Fluorescence measurements were carried out using an ISS K-2 (Champaign, IL) spectrofluorimeter at 25 °C. Spectra were recorded from 305 to 450 nm using an excitation wavelength of 295 nm and 2 nm bandwidth for both excitation and emission. Solutions of 0.87 μM of OPBTc were prepared in the buffers: 2.5 mM sodium-acetate

pH 5.0, sodium-acetate pH 6.0, HEPES pH 7.0, Tris-HCl pH 8.0, CHES pH 9.2 and CABS pH 10.0. Measurements were carried out in a 1.0 x 1.0-cm cuvette. The final spectra were baseline corrected by subtracting each buffer.

RESULTS

The OPBTc is a dimeric enzyme

The active recombinant *T. cruzi* oligopeptidase B was expressed in *E. coli* sharing similar properties to its native form purified from *T. cruzi* [5; 18; 24]. One of these features is the peculiar pattern of migration in SDS-PAGE, at apparent molecular mass of 80 kDa when fully denatured and at 120 kDa when submitted to electrophoresis in sample buffer without SDS and DTT. To investigate whether the two bands corresponded to different structure states of the OPBTc and whether SDS and DTT could interfere with that pattern, the purified enzyme was incubated with sample buffer in the presence of different concentrations of these reagents before SDS-PAGE (Fig. 1A and B). Upon staining of the gel, the pattern revealed indicated that DTT did not modify OPBTc migration. In contrast, the appearance of the 80-kDa band depends on the concentration of SDS in the sample buffer. Only the 80-kDa band was seen in the gel when the sample had been heated before electrophoresis (data not shown).

The activity of OPBTc was assayed by an *in-gel* procedure that allowed us to identify the molecular mass of the active enzyme. For this, a replica of the gel in Figure 1B was washed for SDS removal and incubated with N-CBZ-Gly-Gly-Arg-AMC at pH 8.0. Under these conditions, a single 120-kDa fluorescent band corresponding to substrate hydrolysis was revealed (Fig. 1C). These results suggest that the conformation of OPBTc at 120-kDa is required for *in-gel* activity.

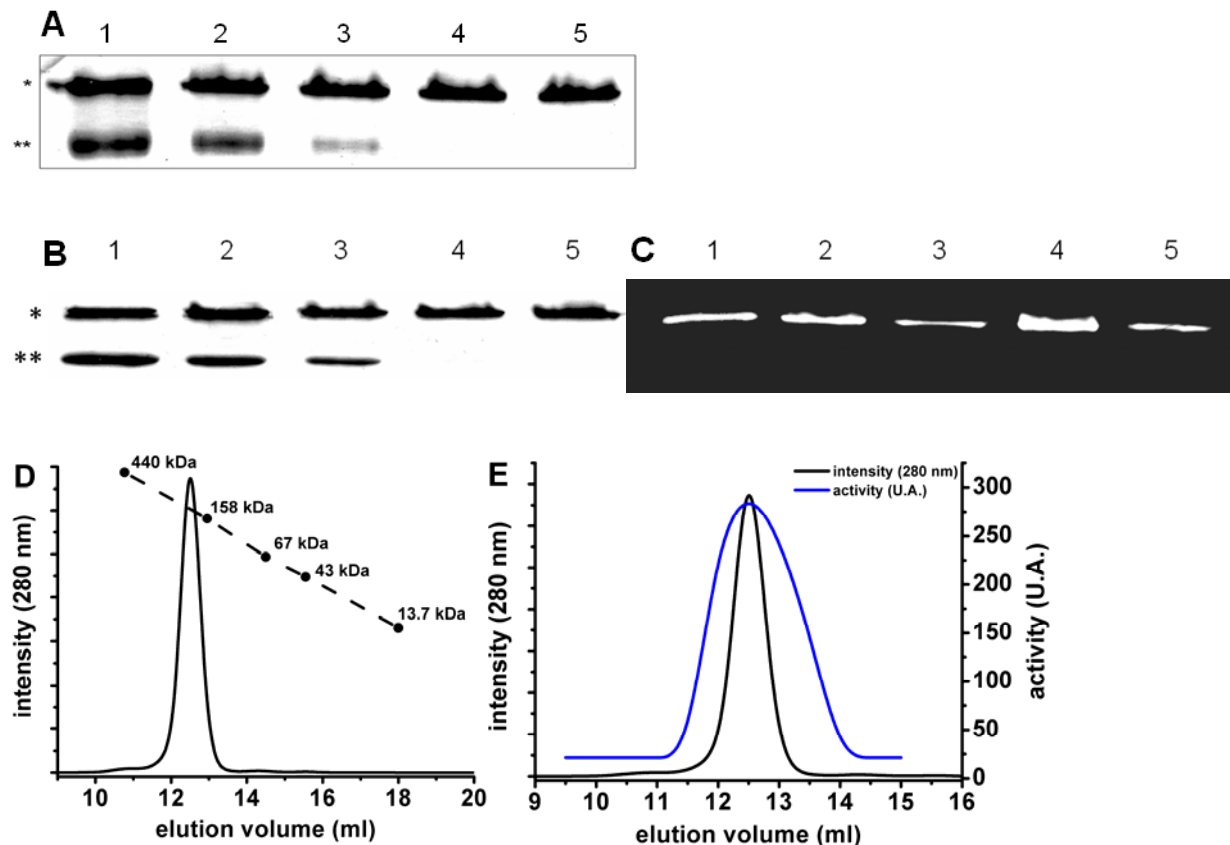


Figure 1. Analysis of OPBTc under SDS-PAGE and Gel permeation chromatography. (A) 2 µg of OPBTc was subjected to 10% SDS-PAGE with buffer loader 5x with 2% SDS (1); 1% SDS (2); 0.5% SDS (3); 0.1% SDS (4) and 0.05% SDS (5) without DTT; * - 120 kDa; ** - 80 kDa. (B) 2 µg of OPBTc was subjected to 10% SDS-PAGE with buffer loader 5x with 2% SDS (1); 1% SDS (2); 0.5% SDS (3); 0.1% SDS (4) and 0.05% SDS (5) and 10 mM DTT; * - 120 kDa; ** - 80 kDa. (C) The OPBTc (500 ng) activity was detected by incubating a replica of the gel in Fig 1B with its fluorogenic substrate as described in Material and Methods. (D) Gel permeation chromatography followed by activity assay (E) at pH 8.0 suggests that OPBTc is a 160-kDa enzyme.

Since the deduced molecular mass of the OPBTc is 80 kDa and the 120-kDa band corresponds neither to a monomeric nor to a dimeric state, the molecular mass of the active OPBTc was assessed by gel permeation chromatography (Fig. 1D). Enzymatic activity of each collected fraction was assayed on N-CBZ-Gly-Gly-Arg-AMC (Fig 1E). Under the conditions of this experiment, a single peak was observed corresponding to a 160-kDa-active enzyme what matches with a dimer. Since both electrophoresis and gel permeation chromatography are not accurated methods to determine molecular masses of many proteins, including oligomers, the dimeric state of the OPBTc was confirmed by analytical ultracentrifugation (AU), a versatile and powerfull tool for the identification of oligomeric states and determination of molecular masses of proteins [25].

Figure 2 shows the experimental and fitted sedimentation velocity profiles obtained at 28.1 μM and the superposition of the distributions $c(s)$ of sedimentation coefficients, s , obtained with OPBTc at 1.8, 8.4 and 28.1 μM . The three samples show essentially the same behavior, taking into account the different signal over noise in the experimental profiles and limited non-ideal effects -leading to smaller s -values at larger protein concentration. A main species sediments at 6.2S ($s_{20,w} = 8.2$ S). The s -value depends on the molar mass, M , and Stokes radius, R_S , of the particle, according to the Svedberg equation:

$$s = M(1 - \bar{v}) / (N_A 6 \pi \eta R_S).$$

The combination of the s -values with $R_S = 5.0$ nm estimated from calibrated size exclusion chromatography gives an estimate for the complex of $M = 171$ kDa close to the expected molecular mass for a dimer (168.4 kDa). Considering a dimer, the R_S - value corresponds to a frictional ratio of 1.35, a value slightly above the usual one of 1.25 for compact globular proteins. It suggests that OPBTc dimer has an

elongated or extended shape. About 10% of larger species are also detected, at about 9 S ($s_{20,w}=12S$), with a proportion increasing with dilution. Most probably aggregates of dimers are formed in an aging process (the fact that a larger concentration protects from aging is a generally observed feature). These data clearly indicates that active OPBTc is an oligomeric protein formed by two monomers.

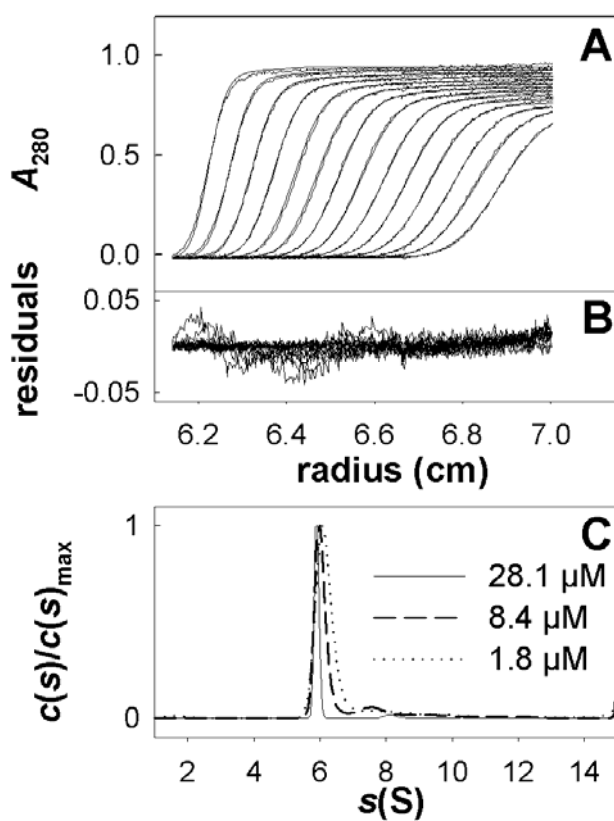


Figure 2. Sedimentation velocity experiments of purified *T. cruzi* oligopeptidase B. (A): Superimposition for oligopeptidase B at 28.1 μM in 25 mM Tris pH 8,0, 100 mM NaCl, of selected experimental sedimentation profiles obtained at 280 nm during 3 h at 42000 rpm, at 10 °C, in 3 mm cell and of their modelled profiles with the $c(s)$ analysis. (B): Corresponding residuals. (C): Result of the $c(s)$ analysis for oligopeptidase B at 28.1, 8.4 and 1.8 μM .

Effects of NaCl, DTT and pH on OPBTc catalysis

Two well-known features of oligopeptidase B is the improvement of its activity by thiol-reacting reagents and its sensitivity to salts [13]. Based on that, we tested the effects of these two additives on OPBTc enzymatic activity. The presence of up to 40 mM DTT in the reaction buffer did not interfere with the hydrolytic activity of OPBTc on N-CBZ-Gly-Gly-Arg-AMC (Fig. 3A). This result correlates well with the observation that the migration pattern of OPBTc is not affected by the presence of DTT both in SDS-PAGE (Fig. 1A) and in gel permeation chromatography (not shown), so it can be concluded that interchain disulfide bonds do not take part in the stabilization of the active OPBTc dimer. To evaluate the effect of salt on the activity of the enzyme, we assayed the hydrolysis of N-CBZ-Gly-Gly-Arg-AMC by purified OPBTc in the presence of increasing concentrations of NaCl (Fig. 3B). Under these conditions, the activity of the enzyme showed to be very sensitive to the presence of NaCl. The enzyme lost almost 50 and 70% of its activity in the presence of 0.2 and 1.0 M NaCl, respectively. To investigate whether the inhibition of the activity by NaCl was due to induction of OPBTc monomerization, the active enzyme was subjected to gel permeation chromatography in the presence of 1.0 M NaCl (Fig. 3C). Under this condition, the enzyme was eluted from the column as a single 160-kDa protein, demonstrating that NaCl did not disrupt the dimeric structure of the OPBTc.

We also determined the pH optimum profile for OPBTc using constant ionic strength buffers (Acetate-Mes-Tris). As presented in Figure 3D, the enzyme was almost inactive over the acidic pH range. At neutral pH range, the enzyme had approximately 80% of its maximal activity observed at pH 8.0, which correlates well with the native OPBTc [18]. As for DTT and NaCl, we also examined the effect of pH on OPBTc dimerization by gel permeation chromatography. The column was



equilibrated with buffers at each pH (4.0 – 8.0) before loading the enzyme. At pH 6.0, 7.0 and 8.0, the enzyme was eluted at the expected 160-kDa position (not shown). At pH 4.0 and 5.0, the elution of the enzyme had a slight retention but it was not detected in or near the 80 kDa fraction. This retention may be due to conformational changes caused by the pH on the OPBTc structure, which are not enough to induce monomerization of the dimeric structure. Consequently, we attempted to investigate the effects of pH on the conformational change of OPBTc employing spectroscopic methods.

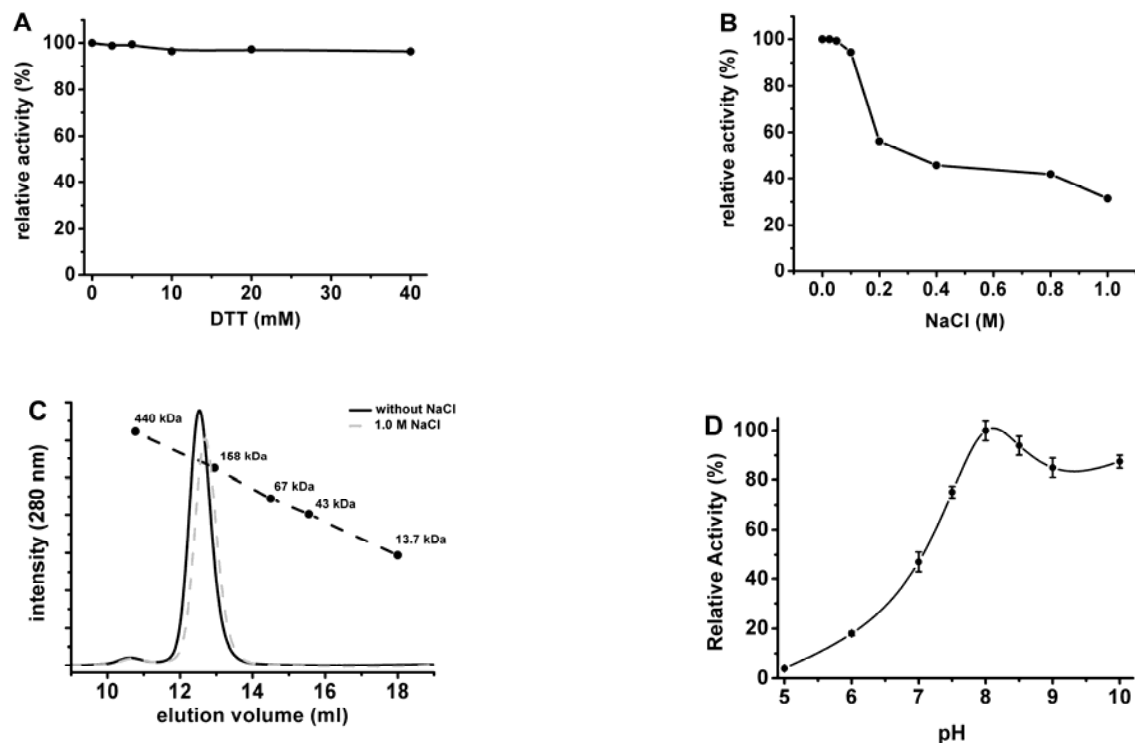


Figure 3. Effects of additives and pH on OPBTc catalysis. Substrate Gly-Gly-Arg-AMC was hydrolyzed by OPBTc in the presence of 0-40 mM DTT (A) and 0-1.0 M NaCl (B). (C) Gel filtration permeation chromatograms of OPBTc in the absence (black line) or in the presence of 1.0 M NaCl (gray dashed-line). (D) pH optimum activity of OPBTc. The tests here were carried out as described in Material and Methods. Results are expressed as the percent activity relative of the maximum value obtained at each condition.

Effects of pH on OPBTc intrinsic fluorescence and conformation

A valuable feature of intrinsic protein fluorescence is the high sensitivity of tryptophan to its local environment. Thus, it is possible to observe changes in emission spectra of tryptophan in response to protein conformational transitions, subunit association, substrate binding or denaturation, all of which can affect the local environment surrounding the tryptophan indole ring [26]. Each *T. cruzi* oligopeptidase B monomer contains 12 tryptophan residues and, as shown in Figure 4A, the emission maximum (λ_{max}) of OPBTc was at 330 nm, indicating that most tryptophans are partially buried in the protein. The intrinsic fluorescence of OPBTc does not change between pH 5.0 to 7.0 and pH 8.0 - 9.0, suggesting that the environment around the tryptophan residues is preserved over those pH ranges. It seems that at higher pHs, the local environments of some of OPBTc tryptophans are apolar, leading to an increase of the fluorescence intensity. It is interesting to notice that the increase in fluorescence intensity accompanies the increase in the enzyme activity. Fluorescence intensity at pH 8.0, the optimal pH for its activity (Fig. 3D) [23], is one with the highest intensity. This result may suggest the proximity of, at least, one tryptophan residue to the enzyme active site and/or substrate binding site.

The near UV CD of proteins also arises from the environments of each aromatic amino acid side chain as well as others contributions, which might absorb in this spectral region. The near UV CD spectra of OPBTc under different pHs are presented in Figure 4B. The CD spectra displayed two peaks, one at 283 nm and the other at 290 nm, at neutral to alkaline pH range (pH 7-9). As the pH becomes acid (pH 4-6), a decay of signal at 283 nm could be observed though the signal at 290 nm did not change. Once again the changes in the enzyme tertiary structure can be well-associated with the enzyme activity, as in the case for the fluorescence assays (Fig.

3A). The loss of signal at 283 nm, when the enzyme was incubated at acid pHs (4-6), indicates a conformational variation that could be responsible for OPBTc inactivation. At pH 3, an extremely acid pH, the enzyme completely lost its tertiary structure (Fig. 3B) and it is not active (not shown). We also investigated the influence of NaCl, 0.2 M, on the OPBTc near UV spectrum at different pHs. The data showed that there is no significant difference from the spectra without NaCl (not shown). Thus far, we demonstrated that the dimer stabilization is not due to intermolecular disulfide bonds, it is salt-resistant and OPBTc tertiary structure is sensitive to acid pHs.

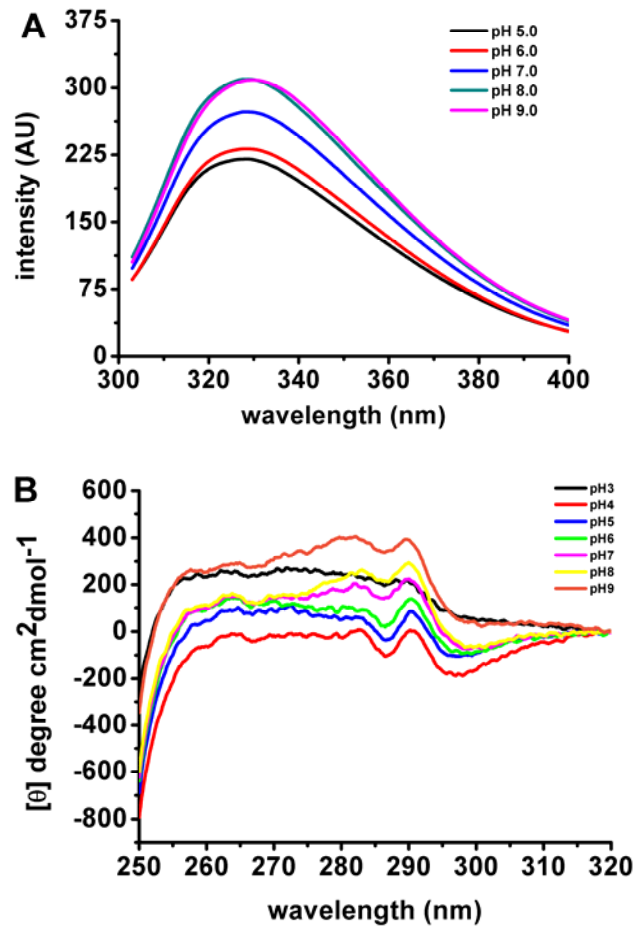


Figure 4. pH influence on OPBTc tertiary structure. (A) The intrinsic spectra were recorded at 25 °C from 305 to 400 nm using excitation wavelength of 295 nm at

different pHs. (B) Near – UV CD spectra of OPBTc at different pHs. All near – UV CD spectra were recorded at 25 °C from 250 to 320 nm.

Effects of heat treatment on OPBTc dimerization and activity

Thermostability studies give precious information about activity behavior and structure properties of proteins. With this purpose, we first assayed the activity of the enzyme at different temperatures (20 - 100 °C). At 20 °C the enzymatic activity corresponded to 80% of the optimal temperature activity measured when the assay was performed at 37-42 °C, while at 50 °C the enzyme activity decreased drastically to nearly 25% (Fig. 5A). When the enzyme previously incubated at different temperature was submitted to a SDS-PAGE analysis, it was observed that the dimer disruption coincided with the OPBTc enzymatic inactivation (Fig. 5B). Up to 42 °C, the OPBTc maintained its eletrophoretic migration pattern at 120 kDa. In contrast, after 50 °C, a transition from the 120 kDa to the 80 kDa state was clearly observed which correlated with the temperature activity profile. Moreover, in the SDS PAGE migration, we could also observe that the enzyme tended to aggregate after 50 °C. At 60 and 70 °C, it could be detected the 80 kDa form and a band with high molecular mass that did not migrate through the SDS PAGE (data not shown). This aggregation could explain why the enzyme suffers an abrupt decrease of activity upon incubation at temperatures higher than 42 °C.

We also submitted the enzyme previously heated at the same temperatures as above to a gel filtration column (Fig. 5C). The purpose was to elute the OPBTc monomer and dimer, especially after 50 °C when the 80 kDa form appeared in SDS PAGE (Fig. 5B). Up to 42 °C, the OPBTc was eluted as a dimer. At 50 and 60 °C, we observed 2 peaks; the first was eluted as a high molecular mass, what may be the aggregated enzyme and, surprisingly, the second peak was eluted as a 160-kDa

protein. Once more, under these conditions, the 80-kDa form of the enzyme was not detected. However, when the high molecular mass peak was analyzed in SDS PAGE, a single 80-kDa band was detected, indicating denaturation of the enzyme.

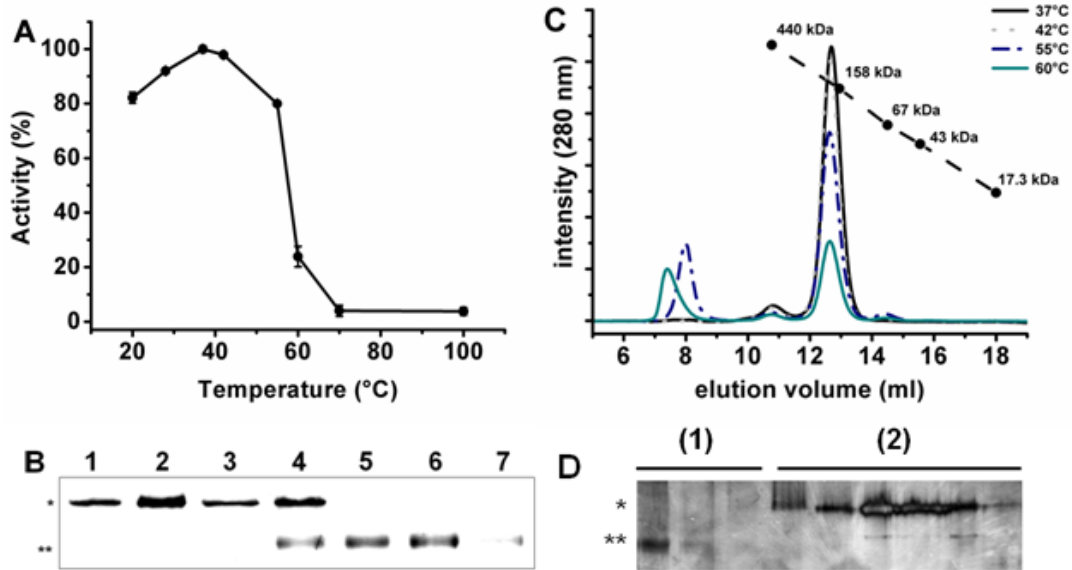


Figure 5. Influence of temperature on OPBTc activity and dimerization. (A) OPBTc was incubated with substrate at different temperatures for 20 min and the enzymatically released of AMC was quantified as described in Material and Methods. (B) OPBTc was incubated at 20 °C (1), 28 °C (2), 37 °C (3), 42 °C (4), 50 °C (5), 60 °C (6), 70 °C (7) and 100 °C (8) for 20 min in 25 mM Tris-HCl pH 8.0 followed by SDS-PAGE analysis at 4 °C without previous heating; * 120 kDa; ** 80 kDa (C) OPBTc was previously incubated at different temperatures for 20 min and, then, subjected to gel permeation chromatography. (D) Eluted samples of OPBTc from the column, previously heated at 50 °C, were submitted to SDS PAGE analysis without boiling of the enzyme followed by silver staining: (1) samples corresponding to the higher molecular mass and (2) samples corresponding to the OPBTc dimer eluted from the column; * 120 kDa; ** 80 kDa.

OPBTc structural thermostability

The singular behavior of OPBTc after heat treatment prompted us to deepen our OPBTc study by using circular dichroism (near and far UV CD), which has been extensively used to give useful information about protein structure, the extent and rate of structural changes [27]. We started our analysis by monitoring the thermal unfolding of OPBTc by far UV CD. OPBTc spectrum at pH 8.0 and 25 °C presented a characteristic band at 218 nm corresponding to β -structure (Fig. 6A). This correlates well with OPBTc secondary structure prediction, since β -strands are the major components of the β -propeller domain of POP family [28]. For the thermal unfolding, OPBTc was monitored at 218 nm. Surprisingly, at pH 8.0, the protein spectra patterns were kept similar from 20 to 95 °C (Fig. 6A). According to all the adjusted spectra, temperature until 95 °C has no effect over the secondary structure. Similar results were obtained at pH 5.0, 6.0, and 7.5 (not shown). Indeed, there are no changes on OPBTc secondary structure contents up to 95 °C, although the enzyme tended to aggregates at temperatures higher than 50 °C.

Considering the high thermal secondary stability of OPBTc at different pHs, as described above, we investigated the unfolding curves at ionic strength (0.2 M NaCl), in order to minimize the inter/intramolecular interactions allowing the unfolding process. Figure 6B shows protein spectra pattern from 20 to 75 °C at pH 8.0 in the presence of 0.2 M NaCl. The dichroic bands decreased as function of temperature which indicates the complete unfolding of the protein. Spectra pattern at pH 4.0, 5.0, 6.0, 7.0, 9.2 and 10.0 displayed the same feature (data not shown). In these assays, the ionic strength promotes a perturbation on molecular environment leading to a loss in protein secondary structure stability. However, OPBTc did not unfold at pH 3.0 with 0.2 M NaCl (Fig. 6C) and it was observed a gain in the dichroic bands while

temperature increases. These results strongly indicated that OPBTc has a secondary structure stable at acidic pH. Nevertheless, near UV CD experiments at pH 3 (Fig. 4C) revealed that OPBTc has a lack of stable tertiary structure. These two features indicate that OPBTc could behavior as a molten globule [29].

In an effort to examine the structural behavior of OPBTc tertiary structure upon heat treatment, we followed its unfolding process by near UV CD. As stated before, the OPBTc near UV CD spectra at pH 8.0 and 25 °C displayed two peaks, one at 283 nm and the other at 290 nm (Fig. 3B). As the temperature increased, especially above 50 °C, the spectra suffered abrupt changes and a loss of the specific signal at 283 nm and 290 nm (Fig. 6D) was observed indicating the OPBTc unfolding process. All samples were centrifuged after the experiment and those at temperatures above 50 °C showed an insoluble state, confirming the tendency of OPBTc to aggregate at higher temperatures. Taken together, the near UV CD studies correlate with the OPBTc activity assays. The enzyme lost its activity sharply after 42 °C as shown above what could be due both to loss of its tertiary structure and its tendency to aggregate.

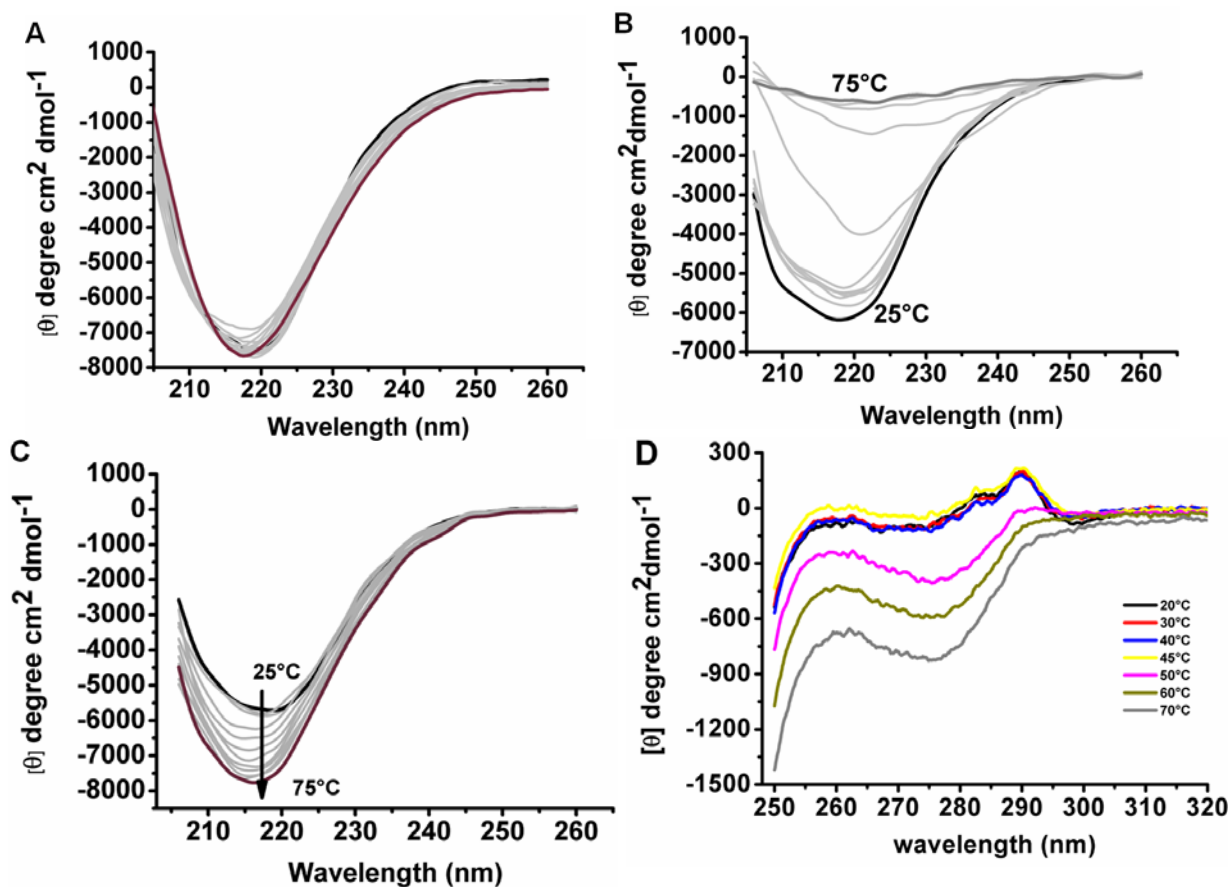


Figure 6. Temperature structure changes of OPBTc monitored by Far- and Near-UV CD. (A) Far – UV CD spectra at pH 8.0 with temperatures ranging from 25 °C (black line) and 95 °C (purple line) in the absence of NaCl. (B) Far –UV CD spectra at pH 8.0 in the presence of 0.2 M NaCl. (C) Far-UV CD spectra at pH 3.0 in the presence of 0.2 M NaCl. (D) Near – UV CD spectra at pH 8.0 in the absence of NaCl.

DISCUSSION

In this study, we examined some structural properties of OPBTc a key protease to triggers Ca^{2+} signaling in both parasite and host cell, crucial to *T. cruzi* infection process. The dimeric state of OPBTc has been suggested but at the present work it was confirmed by a refined technique such as analytical ultracentrifugation. Morty et al. suggested that OPB from *Trypanosoma brucei* did not form dimers, or any other kind of multimers, in the absence or presence of reducing agents, which was evident from its electrophoretic migration and chromatography [30]. However, as for OPBTc, the dimerization of OPB from *Trypanosoma brucei* was also suggested by size exclusion chromatography [14]. Although, chromatography assays is a technique widely employed to estimate the molecular mass of a protein, analytical ultracentrifugation is the method of choice for molar mass determination and the study of self-association and heterogeneous interactions [31]. Therefore, we can state, with no doubt, that OPBTc is a dimer.

None of the OPB characterized until now presented an electrophoresis migration pattern as OPBTc, whose dimer migrates lower than expected. Despite the wide application of SDS-PAGE as a method for estimating protein M_r , considerable uncertainty still exists about the structure of SDS-protein complexes, as well as the mechanism by which they migrate through polyacrylamide gels [32]. The migration pattern of OPBTc is intriguing since the 120 kDa band that appears in SDS PAGE does not correspond to its monomer and neither to its dimer. In practice for most protein, at a single concentration gel, differences in relative mobility become a function of molecular size and shape rather than charge. Anomalously migration of proteins in SDS PAGE, for which M_r would be incorrectly estimated, might be due to an uncommon charge to friction ratio, e.g., as a result of glycosylation or high intrinsic

charge [32]. The intrinsic charge of OPBTc could be one of the responsible for its abnormal migration in SDS PAGE, since the molecular model of OPB from *Leishmania amazonensis* (OPBLa) presented an enzyme with high negative surface [9]. If as for OPBLa, OPBTc also has a high negative charge; it could favor its migration through the SDS PAGE, justifying the 120 kDa band instead of the predicted 160 kDa.

In principle, the folding of dimeric proteins can occur via many different mechanisms, ranging from the simplest mechanism of a two-state transition involving only native dimer (N₂) and unfolded monomers (U), to also forming various numbers of monomeric (M) or dimeric intermediates (I₂). But exactly what intermediates (s) will be observed depends on the relative stabilities of the dimer, dimeric intermediate and monomeric intermediate, as well the protein concentration [19]. The oligomer stability is greatly established by biochemical (interface hydrophobicity, polarity, hydrogen bonds) and geometrical properties (interface size, shape, atomic packing) of their protein-protein interfaces [33]. OPBTc analytical ultracentrifugation did not detect the monomeric intermediate at any of the studied concentration. Gel filtration under several concentrations of DTT or NaCl and different temperatures also did not allow to dissociate the dimer and therefore to elute the monomer. Only in SDS PAGE, at certain conditions, the monomer appeared. Taken all those results together, OPBTc dimer interface seems to be quite stable. Concerning the enzyme activity and its dimerization, it is not possible yet to state whether the dimer is the only responsible for the enzyme activity. Even though *in gel* activity showed that the 80 kDa form did not hydrolyze the substrate, a further characterization of the dimer interface interaction and its dissociation is needed to correlate the enzyme oligomerization to its activity.

The enzyme catalytic activity did not change in the presence of elevated concentrations of DTT; although a common enzymatic characteristic of family S9 is its activity sensitive to thiol-reacting reagents [13]. Among 14 cysteine residues analyzed of OPB from *T. brucei*, the residue Cys²⁵⁶ was identified as one of the key residues that could interact with reducing reagents leading to a conformational change of the enzyme [30]. OPBTc does not have this residue in its primary sequence prediction, what could explain its insensibility to DTT. Yet, the *S. griseus* oligopeptidase B catalysis is activated by reducing reagents independently of its single cysteine residue [13].

Fluorescence intrinsic and near UV CD assays revealed that the OPBTc tertiary structure changes as function of pH. At pH 8.0, the optimum pH, the enzyme intrinsic fluorescence was one of the highest and it decayed as the environment became acid, where the enzyme is almost inactive. Moreover, the near UV CD spectra also correlate with the enzyme activity in different pHs. The loss of the specific signal at 283 nm in pHs acids can be interpreted as a conformational change that caused the enzyme inactivation. Those results could help us understand why the enzyme undergoes a brief retention in gel filtration at acidic pH. As suggested by the AUC, the native dimer is rather elongated but in acidic pH conditions it could become more globular delaying its elution, or else, the enzyme is a little denatured in such conditions leading to an abnormal behavior in gel filtration, for example by interacting nonspecifically with the matrix.

The unfolding process of OPBTc only happened in the presence of NaCl although it has already been described that addition of salts stabilizes OPB against thermal denaturation [14; 34]. At pH 3, the enzyme did not lose its secondary structure even in the presence of NaCl. This result jointly with the very reduced near UV CD

signal of OPBTc at pH 3 suggest a possible molten globule state of the enzyme. This same feature was observed for OPB from *E. coli* [34]. Further studies need to be carried out to confirm this enzyme state. Molten globule states may represent important intermediates in protein folding pathways [35]. It has been suggested that they can be recognized by certain types of molecular chaperones [36] and the flexibility of the molten globule state may have biological roles, such as an important factor in the recognition of DNA by certain proteins [37].

At temperatures above 50°C, OPBTc tended to aggregate, which was not prevent by the presence of NaCl. This phenomenon appears to be very fast since the OPBTc activity decays from almost 100% to 20% above 50 °C. The near UV CD spectra showed that after 50 °C, the tertiary OPBTc structure suffered an enormous change that might be due to its subunits dissociation and/or aggregation leading to its inactive state.

Deciphering the thermodynamics and folding kinetics of OPBTc is important to understand the mechanism of its misfolding and subsequent aggregation. Moreover, determination of the three-dimensional structure of OPBTc is desirable to facilitate the comprehension of its dimer association besides being a crucial step in the rational design of novel inhibitors.

REFERENCES

- [1] WHO, Control of Chagas disease. Techn. Rep. Ser. No. 905 Geneva (2002).
- [2] L. Lauria-Pires, M.S. Braga, A.C. Vexenat, N. Nitz, A. Simoes-Barbosa, D.L. Tinoco, and A.R. Teixeira, Progressive chronic Chagas heart disease ten years

- after treatment with anti-*Trypanosoma cruzi* nitroderivatives. Am J Trop Med Hyg 63 (2000) 111-8.
- [3] M.M. Hecht, N. Nitz, P.F. Araujo, A.O. Sousa, C. Rosa Ade, D.A. Gomes, E. Leonardecz, and A.R. Teixeira, Inheritance of DNA transferred from American trypanosomes to human hosts. PLoS One 5 (2010) e9181.
- [4] N. Yoshida, and M. Cortez, *Trypanosoma cruzi*: parasite and host cell signaling during the invasion process. Subcell Biochem 47 (2008) 82-91.
- [5] B.A. Burleigh, E.V. Caler, P. Webster, and N.W. Andrews, A cytosolic serine endopeptidase from *Trypanosoma cruzi* is required for the generation of Ca²⁺ signaling in mammalian cells. J Cell Biol 136 (1997) 609-20.
- [6] E.V. Caler, S. Vaena de Avalos, P.A. Haynes, N.W. Andrews, and B.A. Burleigh, Oligopeptidase B-dependent signaling mediates host cell invasion by *Trypanosoma cruzi*. Embo J 17 (1998) 4975-86.
- [7] N.D. Rawlings, F.R. Morton, C.Y. Kok, J. Kong, and A.J. Barrett, MEROPS: the peptidase database. Nucleic Acids Res 36 (2008) D320-5.
- [8] T. Gerczei, G.M. Keseru, and G. Naray-Szabo, Construction of a 3D model of oligopeptidase B, a potential processing enzyme in prokaryotes. J Mol Graph Model 18 (2000) 7-17, 57-8.
- [9] H.L. de Matos Guedes, M.P. Duarte Carneiro, D.C. de Oliveira Gomes, B. Rossi-Bergmann, and S. Giovanni De-Simone, Oligopeptidase B from *Leishmania amazonensis*: molecular cloning, gene expression analysis and molecular model. Parasitol Res 101 (2007) 865-75.
- [10] L. Polgar, A potential processing enzyme in prokaryotes: oligopeptidase B, a new type of serine peptidase. Proteins 28 (1997) 375-9.

- [11] A. Tsuji, K. Yuasa, and Y. Matsuda, Identification of oligopeptidase B in higher plants. Purification and characterization of oligopeptidase B from quiescent wheat embryo, *Triticum aestivum*. *J Biochem* 136 (2004) 673-81.
- [12] D. Rea, C. Hazell, N.W. Andrews, R.E. Morty, and V. Fulop, Expression, purification and preliminary crystallographic analysis of oligopeptidase B from *Trypanosoma brucei*. *Acta Crystallogr Sect F Struct Biol Cryst Commun* 62 (2006) 808-10.
- [13] H. Usuki, Y. Uesugi, M. Iwabuchi, and T. Hatanaka, Activation of oligopeptidase B from *Streptomyces griseus* by thiol-reacting reagents is independent of the single reactive cysteine residue. *Biochim Biophys Acta* 1794 (2009) 1673-83.
- [14] N.I. Mohd Ismail, T. Yuasa, K. Yuasa, Y. Nambu, M. Nisimoto, M. Goto, H. Matsuki, M. Inoue, M. Nagahama, and A. Tsuji, A critical role for highly conserved Glu(610) residue of oligopeptidase B from *Trypanosoma brucei* in thermal stability. *J Biochem* 147 (2010) 201-11.
- [15] T.H. Coetzer, J.P. Goldring, and L.E. Huson, Oligopeptidase B: a processing peptidase involved in pathogenesis. *Biochimie* 90 (2008) 336-44.
- [16] R.E. Morty, R. Pelle, I. Vadasz, G.L. Uzcanga, W. Seeger, and J. Bubis, Oligopeptidase B from *Trypanosoma evansi*. A parasite peptidase that inactivates atrial natriuretic factor in the bloodstream of infected hosts. *J Biol Chem* 280 (2005) 10925-37.
- [17] R.E. Morty, L. Troeberg, R.N. Pike, R. Jones, P. Nickel, J.D. Lonsdale-Eccles, and T.H. Coetzer, A trypanosome oligopeptidase as a target for the trypanocidal agents pentamidine, diminazene and suramin. *FEBS Lett* 433 (1998) 251-6.

- [18] J.M. Santana, P. Grellier, M.H. Rodier, J. Schrevel, and A. Teixeira, Purification and characterization of a new 120 kDa alkaline proteinase of *Trypanosoma cruzi*. *Biochem Biophys Res Commun* 187 (1992) 1466-73.
- [19] J.A. Rumfeldt, C. Galvagnion, K.A. Vassall, and E.M. Meiering, Conformational stability and folding mechanisms of dimeric proteins. *Prog Biophys Mol Biol* 98 (2008) 61-84.
- [20] E.P. Camargo, Growth and Differentiation in *Trypanosoma Cruzi*. I. Origin of Metacyclic Trypanosomes in Liquid Media. *Rev Inst Med Trop Sao Paulo* 12 (1964) 93-100.
- [21] B.A. Burleigh, E.V. Caler, P. Webster, and N.W. Andrews, A cytosolic serine endopeptidase from *Trypanosoma cruzi* is required for the generation of Ca²⁺ signaling in mammalian cells. *J Cell Biol.* 136 (1997) 609-620.
- [22] I.M. Bastos, P. Grellier, N.F. Martins, G. Cadavid-Restrepo, M.R. de Souza-Ault, K. Augustyns, A.R. Teixeira, J. Schrével, B. Maigret, J.F. da Silveira, and J.M. Santana, Molecular, functional and structural properties of the prolyl oligopeptidase of *Trypanosoma cruzi* (POP Tc80), which is required for parasite entry into mammalian cells. *Biochem J.* 388 (2005) 29-38.
- [23] J.M. Santana, P. Grellier, M.H. Rodier, J. Schrevel, and A.R. Teixeira, Purification and characterization of a new 120 kDa alkaline proteinase of *Trypanosoma cruzi*. *Biochem Biophys Res Commun* 187 (1992) 1466-1473.
- [24] B.A. Burleigh, and N.W. Andrews, A 120-kDa alkaline peptidase from *Trypanosoma cruzi* is involved in the generation of a novel Ca⁽²⁺⁾-signaling factor for mammalian cells. *J Biol Chem* 270 (1995) 5172-80.
- [25] J. Lebowitz, M.S. Lewis, and P. Schuck, Modern analytical ultracentrifugation in protein science: A tutorial review. *Protein Science* 11 (2002) 2067-2079.

- [26] J.R. Lakowicz, Principles of fluorescence spectroscopy Spring Science+Business Media, Inc., New York, 2004.
- [27] S.M. Kelly, T.J. Jess, and N.C. Price, How to study proteins by circular dichroism. *Biochim Biophys Acta* 1751 (2005) 119-39.
- [28] V. Fulop, Z. Bocskei, and L. Polgar, Prolyl oligopeptidase: an unusual beta-propeller domain regulates proteolysis. *Cell* 94 (1998) 161-70.
- [29] S.H. Qureshi, B. Moza, S. Yadav, and F. Ahmad, Conformational and thermodynamic characterization of the molten globule state occurring during unfolding of cytochromes-c by weak salt denaturants. *Biochemistry* 42 (2003) 1684-95.
- [30] R.E. Morty, A.Y. Shih, V. Fulop, and N.W. Andrews, Identification of the reactive cysteine residues in oligopeptidase B from *Trypanosoma brucei*. *FEBS Lett* 579 (2005) 2191-6.
- [31] J. Lebowitz, M.S. Lewis, and P. Schuck, Modern analytical ultracentrifugation in protein science: a tutorial review. *Protein Sci* 11 (2002) 2067-79.
- [32] W.H. Westerhuis, J.N. Sturgis, and R.A. Niederman, Reevaluation of the electrophoretic migration behavior of soluble globular proteins in the native and detergent-denatured states in polyacrylamide gels. *Anal Biochem* 284 (2000) 143-52.
- [33] H. Ponstingl, T. Kabir, D. Gorse, and J.M. Thornton, Morphological aspects of oligomeric protein structures. *Prog Biophys Mol Biol* 89 (2005) 9-35.
- [34] L. Polgar, and F. Felfoldi, Oligopeptidase B: cloning and probing stability under nonequilibrium conditions. *Proteins* 30 (1998) 424-34.
- [35] O.B. Ptitsyn, Molten globule and protein folding. *Adv Protein Chem* 47 (1995) 83-229.



- [36] J. Martin, T. Langer, R. Boteva, A. Schramel, A.L. Horwich, and F.U. Hartl, Chaperonin-mediated protein folding at the surface of groEL through a 'molten globule'-like intermediate. *Nature* 352 (1991) 36-42.
- [37] D.P. Hornby, A. Whitmarsh, H. Pinarbasi, S.M. Kelly, N.C. Price, P. Shore, G.S. Baldwin, and J. Waltho, The DNA recognition subunit of a DNA methyltransferase is predominantly a molten globule in the absence of DNA. *FEBS Lett* 355 (1994) 57-60.



II. Estudo da prolil oligopeptidase de *Trypanosoma brucei*

Manuscrito aceito para publicação no periódico

Microbes and Infection



ELSEVIER



INSTITUT PASTEUR

Microbes and Infection xx (2010) 1–10



www.elsevier.com/locate/micinf

Original article

Prolyl oligopeptidase of *Trypanosoma brucei* hydrolyzes native collagen, peptide hormones and is active in the plasma of infected mice

Izabela M.D. Bastos^{a,b,*}, Flávia Nader Motta^a, Sébastien Charneau^{c,b}, Jaime M. Santana^a,
Lionel Dubost^d, Koen Augustyns^e, Philippe Grellier^{f,**}

^a Laboratório de Interação Parasito-Hospedeiro, Faculdade de Medicina, Universidade de Brasília, 70910-900-DF, Brazil

^b Faculdade Ceilândia, Universidade de Brasília, 72220-240-DF, Brazil

^c Laboratório de Bioquímica e Química de Proteínas, Universidade de Brasília, 70910-900-DF, Brazil

^d Muséum National d'Histoire Naturelle, FRE 3206 CNRS, USM502, 63, rue Buffon, 75231 Paris cedex 05, France

^e Laboratory of Medicinal Chemistry, University of Antwerp, Universiteitsplein 1, B-2610, Antwerp, Belgium

^f Muséum National d'Histoire Naturelle, FRE 3206 CNRS, USM504, CP52, 61, rue Buffon, 75231 Paris cedex 05, France

Received 22 November 2009; accepted 16 February 2010

Available online xxx

Abstract

Proteases play important roles in many biological processes of parasites, including their host interactions. In sleeping sickness, *Trypanosoma brucei* proteases released into the host bloodstream could hydrolyze host factors, such as hormones, contributing to the development of the disease's symptoms. In this study, we present the identification of the *T. brucei* prolyl oligopeptidase gene (*popb*) and the characterization of its corresponding enzyme, POP Tb. Secondary structure predictions of POP Tb show a structural composition highly similar to other POPs. Recombinant POP Tb produced in *E. coli* was active and highly sensitive to inhibitors of *Trypanosoma cruzi* POP Tc80. These inhibitors, which prevent *T. cruzi* entry into non-phagocytic cells, arrested growth of the *T. brucei* bloodstream form in a dose-dependent manner. POP Tb hydrolyzes peptide hormones containing Pro or Ala at the P1 position at a slightly alkaline pH, and also cleaves type I collagen *in vitro* and native collagen present in rat mesentery. Furthermore, POP Tb is released into the bloodstream of *T. brucei* infected mice where it remains active. These data suggest that POP Tb might contribute to the pathogenesis of sleeping sickness.

© 2010 Published by Elsevier Masson SAS.

Keywords: *Trypanosoma brucei*; Prolyl oligopeptidase; Sleeping sickness; Peptide hormone; Collagen hydrolysis; Prolyl oligopeptidase inhibitors

1. Introduction

Human African trypanosomiasis (HAT), caused by subspecies of the protozoan *Trypanosoma brucei*, is one of the most prominent tropical infections in Africa. This disease progresses a few days after the tsetse (*Glossina* spp.) fly's bite from non-specific signs to typical symptoms such as wake–sleep cycle

alteration and neurological dysfunction, leading to death in untreated patients [1].

Neuroendocrine disturbances in African trypanosome-infected animals and humans often result in hypothyroidism and sexual disorders such as sterility, amenorrhea, abortion and impotence [2–4]. It has been suggested that parasite proteolytic activities are associated with these symptoms. Parasite peptidases released into host plasma by secretion or upon parasite lysis may degrade and inactivate key peptide hormones that regulate the release of central and peripheral hormones [5,6]. Parasite pyroglutamyl peptidase type I, released into the bloodstream of *T. brucei*-infected rats, removes pyroglutamic acid blocking groups from host thyrotropin-releasing hormone (TRH) and gonadotropin-

* Corresponding author. Laboratório de Interação Parasito-Hospedeiro, Faculdade de Medicina, Universidade de Brasília, 70.910-900 Brasília DF, Brazil. Tel.: +55 61 33072256; fax: +55 61 32734069.

** Corresponding author. Tel.: +33 140793510; fax: +33 140793499.

E-mail addresses: dourado@unb.br (I.M.D. Bastos), grellier@mnhn.fr (P. Grellier).

releasing hormone (GnRH), reducing their plasma half-lives [7]. Oligopeptidase B of trypanosomes hydrolyzes and inactivates atrial natriuretic factor in infected rat plasma [8,9] contributing to hypervolemia, characteristic of HAT [10,11].

Due to its unique cyclic and imino structures, proline introduces a fixed bend into a peptide chain promoting conformational changes that protect bioactive peptides against enzymatic degradation [12]. Nevertheless, some specialized peptidases, such as the well described prolyl oligopeptidase (POP; EC 3.4.21.26), are capable of cleaving at the proline bond [13]. POP is a ubiquitous neutral serine protease of the S9 family that hydrolyzes substrates at the carboxyl side of proline and alanine residues. *In vitro*, POPs cleave bioactive peptides such as substance P, oxytocin, vasopressin and angiotensin [14]. The high concentration of POP in the brain suggests that its activity plays a role in regulation of hormonal peptides and neuropeptides in mammals. This hypothesis has been reinforced by previous research showing POP level alterations in neural tissues or plasma in disorders such as amnesia, depression and Alzheimer's Disease and by *in vivo* studies employing POP inhibitors [15,16].

We have previously demonstrated that the *Trypanosoma cruzi* prolyl oligopeptidase (POP Tc80) hydrolyzes fibronectin and native collagens, proline-rich proteins [17], differently to the most described POPs that seem to only cleave peptides [18]. Most interestingly, the specific blockage of POP Tc80 activity by inhibitors arrests the entry of *T. cruzi* trypomastigotes into non-phagocytic host cells, suggesting a role for this enzyme in the parasite life cycle [19,20]. This fact led us to question what would be the role of its counterpart in *T. brucei*, given that, in spite of their phylogenetic proximity, these trypanosomes present both distinct survival strategies and different pathogenic mechanisms in their vertebrate hosts. In this study, we present the biochemical and enzymatic properties of the prolyl oligopeptidase of *T. brucei* (POP Tb) and show that inhibition of its activity precludes *in vitro* growth of the *T. brucei* bloodstream form. We also demonstrate the presence of POP Tb and its activity in the plasma of *T. brucei*-infected mice. Furthermore, POP Tb mediates hydrolysis of both human peptide hormones and native collagen.

2. Materials and methods

2.1. Parasites

Procyclic forms of the *T. brucei brucei* cell line 29-13 derived from the wild-type 427 strain were maintained in SDM-79 containing 10% (v/v) heat-inactivated fetal calf serum (FCS) at 27 °C [21]. Bloodstream forms of the *T. brucei* line 90-13 also from the 427 strain were cultured in HMI-9 supplemented with 10% FCS at 37 °C under 5% CO₂ [21]. Bloodstream forms of *T. brucei* GVR 35 clone 2 were kindly supplied by P. Loiseau (Faculty of Pharmacy, Châtenay-Malabry, France). GVR 35 produces a chronic infection in mice, allowing them to survive for at least 30 days [22].

2.2. Cloning of POP Tb gene and secondary prediction of its product

Primers were designed from predicted POP sequence (GeneDB: Tb10.6k15.2520) in the *T. brucei* database (<http://www.genedb.org/genedb/trypt/>). Forward, 5'-CATATGCGCCTCGCTTACCC-3' (NdeI site, underlined; initiation codon, bold) and reverse, 5'-CTCAGATCAGTCTGTCCACTGGC-3' (XhoI site, underlined; stop codon, bold) primers were used to amplify the *poptb* ORF from genomic DNA of *T. brucei* cell line 29-13. After ligation in pT-Adv (Clontech Laboratories, Palo Alto, CA), the whole insert was sequenced in both directions. The gene sequence of POP Tb is available at <http://www.ebi.ac.uk>, accession number AJ496456 EMBL.

Prediction of POP Tb secondary structures was performed with PSI-PRED methodology that uses profiles generated by the PSI-BLAST program and searches in a non-redundant sequence databank with the target sequence to generate profiles [23]. It was adjusted manually based on POP Tc80 and porcine POP three-dimensional models [20,24].

2.3. Recombinant POP Tb expression in *E. coli*

The 2097 bp *poptb* full-length insert was excised from pT-Adv/*poptb* by NdeI and XhoI and cloned into a pET-15b plasmid (Novagen) that had been previously digested with the same enzymes. The N-terminal His-tagged POP Tb was produced in *E. coli* BL21 (DE3) by 0.5 mM IPTG induction at 16 °C over 5 h. To purify the soluble recombinant proteinase (rPOP Tb), cell lysate supernatants were submitted to affinity chromatography on a nickel-agarose resin (Sigma) at 4 °C. The His-tag was removed from rPOP Tb by hydrolysis with thrombin (Thrombin Cleavage Capture Kit™, Novagen) followed by dialysis against 25 mM HEPES pH 7.5. Purified rPOP Tb was stored in 50% glycerol at -20 °C. Its purity was assessed in 10% SDS-PAGE, under reducing conditions, followed by silver staining.

2.4. Assay of rPOP Tb activity

The rPOP Tb activity was determined by measuring the fluorescence of 7-amido-4-methylcoumarin (AMC) released by hydrolysis of the enzyme substrate N-Suc-Gly-Pro-Leu-Gly-Pro-AMC. The activity of purified rPOP Tb His-tag free (20 ng) was assayed in reaction buffer (25 mM HEPES pH 7.5, including or not 5 mM DTT) containing 20 μM N-Suc-Gly-Pro-Leu-Gly-Pro-AMC in 100 μl final volume. AMC release was recorded up to 30 min at 460 nm upon excitation at 355 nm in a 96-well microplate fluorescence reader (FL600; Bio-Tek Instruments, Inc.) at 25 °C as previously described [19]. The rPOP Tb activity was also assayed on other fluorogenic substrates (N-Suc-Gly-Pro-AMC, N-Boc-Val-Leu-Lys-AMC, N-Boc-Leu-Lys-Arg-AMC, N-Cbz-Val-Lys-Met-AMC, N-Boc-Leu-Gly-Arg-AMC, N-Boc-Ile-Gly-Gly-Arg-AMC, N-Suc-Leu-Tyr-AMC, N-Suc-Ala-Ala-Ala-AMC, N-Boc-Val-Pro-Arg-AMC, N-Cbz-Gly-Gly-Arg-AMC, N-Boc-Gly-Gly-Arg-AMC, N-Suc-Ala-Ala-Pro-Phe-AMC, N-Cbz-Phe-

Arg-AMC, H-Gly-Arg-AMC, H-Gly-Phe-AMC, Ala-Ala-Phe-AMC, L-Arg-AMC, Ala-AMC and Lys-Ala-AMC).

The pH activity optimum of rPOP Tb was determined as described above in AMT buffer (100 mM acetic acid, 100 mM MES and 200 mM Tris–HCl) at pHs ranging from 4 to 11 [25]. Kinetic parameters were determined by incubation of 20 ng of rPOP Tb in reaction buffer with different concentrations of substrates (6.25–150 μ M, N-Suc-Gly-Pro-Leu-Gly-Pro-AMC; 12.5–300 μ M, N-Suc-Gly-Pro-AMC). Active enzyme concentration was determined by titration with a chloromethylketone irreversible inhibitor of POP Tc80 [20]. K_m and V_{max} were determined by hyperbolic regression according to Cornish-Bowden [26]. The k_{cat} was calculated by $k_{cat} = V_{max}/[E]_0$, where $[E]_0$ represents active enzyme concentration.

2.5. Inhibition of rPOP Tb

Classical protease inhibitors or POP Tc80 inhibitors (0.01–100 nM) were assayed by incubating 20 ng of purified rPOP Tb with each inhibitor in reaction buffer for 10 min at 25 °C, before the addition of N-Suc-Gly-Pro-Leu-Gly-Pro-AMC substrate to yield a 20 μ M final concentration. Residual activity was determined as above. The inhibition profile (IC₅₀) using POP Tc80 inhibitors was determined by nonlinear regression analysis from the residual activity versus inhibitor concentrations curve.

2.6. Assay of rPOP Tb activity on human collagen I and on rat mesentery

Collagen hydrolysis was performed by incubating 50 μ g of purified human collagen I or BSA with 200 ng of purified rPOP Tb in 100 μ l of 50 mM Tris pH 8.0, 50 mM NaCl and 5 mM DTT for up to 16 h at 37 °C. Controls consisted of substrate incubated under the same conditions with rPOP Tb inactivated by previous treatment with 1 μ M inhibitor 4. Aliquots (20 μ l) were taken at 1, 3, 5 and 16 h of incubation and the reaction was stopped with 5 μ l of 5 \times SDS-PAGE sample buffer, followed by boiling. Protein hydrolysis was analyzed by 10% SDS-PAGE followed by silver staining. Activity of POP Tb on native collagen was performed as described [17]. Briefly, mesentery from 3-month-old male rats was dissected and dried over a glass slide at room temperature. The buffer (50 μ l) 50 mM Tris pH 8.0, 50 mM NaCl and 5 mM DTT containing 250 ng of purified rPOP Tb was placed on the mesenteric surface and incubated in a moist chamber for up to 16 h at 37 °C. The control consisted of POP Tb inactivated with 1 μ M inhibitor 4. Samples were analyzed on bright field contrast using Leica TCS SP5 microscope.

2.7. In vitro inhibition of *T. brucei* growth by POP Tb inhibitors

T. brucei bloodstream forms (3×10^4 cells/ml) were cultured in a 24-well plate in triplicate either in the absence or in the presence of POP Tc80 inhibitors at different

concentrations. After 24 h of incubation, cells were fixed in 3.7% formaldehyde and the number of cells/ml was determined. IC₅₀s were determined by nonlinear regression analysis from the inhibition growth curve.

2.8. Hydrolysis of peptide hormones by POP Tb

Hydrolysis assays of bradykinin, β -endorphin, neurotensin, TRH (Sigma) or GnRH (Calbiochem) were performed by incubation of 60 nmol of each peptide with 60 pmol of purified rPOP Tb in reaction buffer, for 1, 3 and 16 h at 25 °C. Digested products were isolated by HPLC in a C₁₈ Column, eluted under a linear gradient of 0–60% of acetonitrile in 0.1% trifluoroacetic acid/Milli-Q water, over 30 min at 0.5 mL min⁻¹ flow-rate. Eluted fractions were lyophilized, resuspended in Milli-Q water and peptide masses were determined by electron spray ionization time-of-flight (ESI-TOF) mass spectrometry (Applied Biosystems). The amino acid sequences of peptides were obtained by MS/MS fragmentation.

2.9. POP Tb activity in human plasma

Plasma was obtained by centrifugation (1500g for 10 min at 4 °C) of 10 ml blood drawn from two healthy volunteers into tubes containing 1 ml of 0.109 M sodium citrate. Eighty microliters of each plasma sample were incubated with 70 ng (10 μ l) of purified rPOP Tb at 25 °C. After 15, 30 and 240 min of incubation, POP Tb activity was measured by adding 20 μ M N-Suc-Gly-Pro-Leu-Gly-Pro-AMC. Control reactions were carried out in parallel in the same conditions, except for the replacement of plasma with reaction buffer.

2.10. Detection of POP Tb activity in *T. brucei*-infected mice

Mice were infected intraperitoneally with 2×10^4 bloodstream forms of the VGR 35 strain in two independent experiments with a total of 60 mice. Blood from groups of three infected mice was drawn at different times over 18 days. The first harvest (time zero) was made 2 h post infection. Parasitemia was calculated for each group and plasma was obtained from fresh blood drawn into heparin, centrifuged (8000g, for 5 min, at 4 °C) and immediately filtered through 22 μ m filters before storage at –80 °C. POP Tb and Oligopeptidase B activities were evaluated as above by the incubation of plasmas (90 μ l) from each group with 20 μ M N-Suc-Gly-Pro-Leu-Gly-Pro-AMC or N-Cbz-Gly-Gly-Arg-AMC substrates, respectively.

2.11. Immunoblotting

For anti-rPOP Tb antibody production, BALB/C mice were submitted to one immunization with a 5 μ g aliquot of purified rPOP Tb in Freund's complete adjuvant, followed by three biweekly boosts in Freund's incomplete adjuvant. Resulting sera were employed (diluted 1:300) in immunoblot assays. To detect POP Tb in the plasma of *T. brucei*-infected mice,

a differential protein precipitation was carried out to decrease albumin content from the samples [27]. Briefly, a 100 μ l sample of cell-free serum was added to four volumes of ice-cold acetone containing 10% (w/v) TCA, incubated at -20°C for 90 min and centrifuged (15,000g, at 4°C , for 20 min). The albumin-containing supernatant was discarded and the pellet washed with 4 ml of ice-cold acetone for 15 min on ice, followed by centrifugation as above. The proteins in the pellet were dried, resuspended in water, submitted to 10% SDS PAGE and transferred to a nitrocellulose membrane. Incubation, washing and development were performed as described [20].

3. Results

3.1. POP Tb gene is conserved with its *T. cruzi* counterpart

The *poptb* gene isolated from *T. brucei* contained an open reading frame of 2097 bp encoding a polypeptide of 698 amino acids with a predicted Mr of 77,597. Alignment between amino acid sequences of POPs from *T. brucei* and *T. cruzi* showed that these enzymes share more than 77% identity. POP Tb also exhibited similarity among POPs in general, showing up to 44% identity with mammalian POPs, concentrated mainly in the C-terminal catalytic domain. Although amino acid residues of the POP Tb β -propeller region are not well conserved, structure predictions suggested that POP Tb has a conserved secondary structure arrangement relative to porcine [24] and *T. cruzi* POPs [20] with 28 β -sheets (Fig. S1). The catalytic domain of porcine POP is assembled from an interaction between the extreme N-terminal and C-terminal regions, generating an α/β -hydrolase domain [24]. The catalytic domain of POP Tb is 55% similar to that of mammalian POPs suggesting that the catalytic domains of these proteins share similar three-dimensional structures. Moreover, POP Tb and POP Tc80 share 83% of amino acid identity in the catalytic domain.

Southern blot analysis indicated that *poptb* is present as a single copy per haploid genome of *T. brucei*, as found in the *T. brucei* genome project (<http://www.genedb.org/genedb/tryp/>; data not shown).

3.2. Enzymatic properties of POP Tb

In order to characterize the biochemical and enzymatic features of POP Tb, its recombinant form was produced in *E. coli* by cloning *poptb* into the pET-15b expression plasmid to generate a His-tagged fusion at the NH_2 -end of the protein. Optimal expression conditions were established (0.5 mM IPTG for 5 h at 16°C) allowing the expression of a large amount of soluble and catalytically active rPOP Tb (approx. 16 mg/L of bacterial culture). The expressed enzyme, purified by affinity chromatography on nickel–agarose, migrated at the expected molecular mass of approximately 78 kDa (Fig. 1A). Side-by-side electrophoretic migration showed that rPOP Tb is smaller than its *T. cruzi* counterpart, rPOP Tc80 (Fig. 1A).

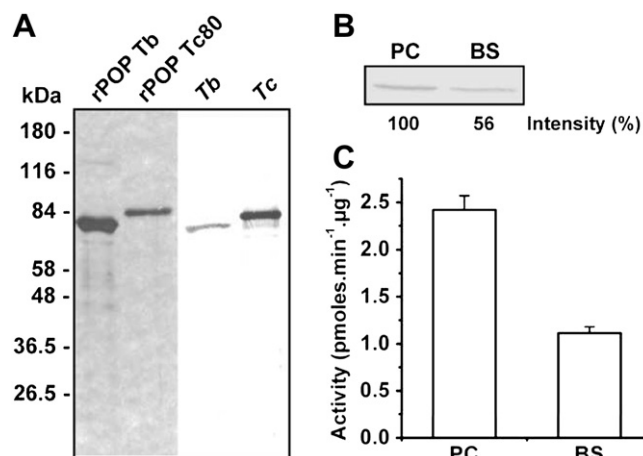


Fig. 1. Analysis of the recombinant and native POP Tb. (A) rPOP Tb was produced in *E. coli*, purified on nickel–agarose resin and evaluated by silver-stained 10% SDS-PAGE. Its electrophoretic profile was compared to that of *T. cruzi*, rPOP Tc80. Native POPs were detected in extracts from *T. brucei* procyclic (Tb) and *T. cruzi* (Tc) epimastigote cells by Western blot using anti-rPOP Tc80. (B) POP Tb in procyclic versus bloodstream forms. Each total extract (50 μ g) was resolved by 10% SDS PAGE and transferred to a nitrocellulose membrane. Blots were probed with anti-*T. brucei* POP. The intensity of the bands was quantified with Image J. PC – procyclic form and BS – bloodstream form. (C) Specific activity of POP Tb in procyclic and bloodstream forms. Three μ g of total extract from each form were incubated with N-Suc-Gly-Pro-Leu-Gly-Pro-AMC and the specific activity was calculated as described [19]. Data are the mean + SD of 3 experiments.

Both sizes correlate well with the calculated molecular masses of 77,597 and 78,230 Da, respectively. A similar difference of mass was also observed between the native POPs from *T. brucei* procyclics and *T. cruzi* epimastigotes forms by Western blotting using an antiserum raised against the rPOP Tc80, which cross-reacted with rPOP Tb (Fig. 1A), showing that POP Tb and POP Tc80 share common epitopes.

Substrate specificity of rPOP Tb was evaluated on different fluorogenic peptides. Except for substrates containing a proline residue at the P_1 position, N-Suc-Gly-Pro-Leu-Gly-Pro-AMC and N-Suc-Gly-Pro-AMC, only N-Suc-Ala-Ala-Ala-AMC was hydrolyzed by rPOP Tb. Enzyme activity on N-Suc-Ala-Ala-Ala-AMC corresponds to 8% of that obtained using N-Suc-Gly-Pro-Leu-Gly-Pro-AMC. These results are supported by previous data showing that other POPs cleave preferentially at the carboxyl side of Pro and, at a weaker rate, Ala [28]. POP Tb was 57% less efficient in cleaving N-Suc-Gly-Pro-AMC, the most commonly employed substrate for POPs, than N-Suc-Gly-Pro-Leu-Gly-Pro-AMC.

The pH optimum profile determined for POP Tb revealed that its activity against N-Suc-Gly-Pro-Leu-Gly-Pro-AMC is strongly dependent on a slightly alkaline pH, between 7.5 and 8.0 (Fig. S2). POP Tb activity was more susceptible to acid than alkaline pH (16% of activity at pH 6.0 versus 62% at pH 9.0).

The kinetic parameters of rPOP Tb were determined using N-Suc-Gly-Pro-Leu-Gly-Pro-AMC, substrate corresponding to a conserved motif of collagen that has been employed in the characterization of native and recombinant POP of *T. cruzi* [17,19,20]. POP Tb activity was strongly

Table 1
Q3 Inhibition of rPOP Tb by protease inhibitors.

Inhibitor	Concentration (μM)	Inhibition (%)
DFP	100	100
pCMB	100	98
TPCK	100	91.1
TLCK	100	73.2
Leupeptin	100	46.1
PMSF	1	18
AEBSF	1	12
Benzamidine	1	7.2
EDTA	1	n.i.
E-64	100	n.i.
Phosphoramidon	100	n.i.
Bestatin	100	n.i.
Pepstatin A	100	n.i.

n.i., No inhibition.

Assays were performed by incubating 20 ng of rPOP Tb with the inhibitor for 10 min, before the addition of 20 μM of substrate. Hydrolysis was recorded up to 30 min.

activated when the assay was performed in the presence of reducing agents. Calculated K_m values were 44.13 μM in the presence and 15.21 μM in the absence of DTT. In spite of the K_m augmentation by DTT, the calculated k_{cat}/K_m of 0.209 $\mu\text{M}^{-1} \text{s}^{-1}$ under this condition revealed that DTT elevated its catalytic efficiency six-fold compared to a k_{cat}/K_m of 0.033 $\mu\text{M}^{-1} \text{s}^{-1}$. This may be due to the reduction of a disulfide bond next to the catalytic site allowing higher substrate turnover even if DTT promotes slight alterations in the interaction between POP Tb and N-Suc-Gly-Pro-Leu-Gly-Pro-AMC reflected in a K_m increase.

Although POP Tb is a serine protease, its activity was weakly inhibited by PMSF or AEBSF (Table 1), as described

for other POPs. However, its activity was readily inhibited by DFP, a serine protease inhibitor, and TPCK, a chymotrypsin-like protease inhibitor. TLCK also inhibited the enzyme activity by more than 70%. POP Tb, as for POPs, it is also susceptible to pCMB, a cysteine protease inhibitor, indicating the presence of a cysteine residue at or near the active site. In contrast, its activity was not sensitive to E-64, pepstatin A and phosphoramidon, which are known to be specific inhibitors of cysteine, aspartic and metalloproteases, respectively.

To evaluate the expression rate of POP Tb in the different life cycle stages of *T. brucei*, we performed an immunoblotting with total extracts from the same number of procyclic or bloodstream forms using an anti-rPOP Tb polyclonal serum produced in mice. Double the amount of POP Tb was detected in procyclic forms compared to bloodstream forms (Fig. 1B). To confirm this, we measured the specific activity against N-Suc-Gly-Pro-Leu-Gly-Pro-AMC in the total extracts from both forms. The measured activity was approximately two times lower in the bloodstream forms (Fig. 1C). This correlates well with the different amounts of POP Tb detected in the parasite forms by Western blotting.

3.3. POP Tb mediates hydrolysis of collagen

Substrate specificities of POPs have been described mainly for peptides of up to 30 amino acids residues in length. However, POP Tc80 hydrolyzes large substrates such as native collagens and fibronectin [17,19]. Since POP Tb shares many molecular and enzymatic properties with POP Tc80, we assayed its ability to cleave collagen. Evident cleavage products were detected, by SDS-PAGE, after 16 h incubation of human purified collagen type I with rPOP Tb (Fig. 2A).

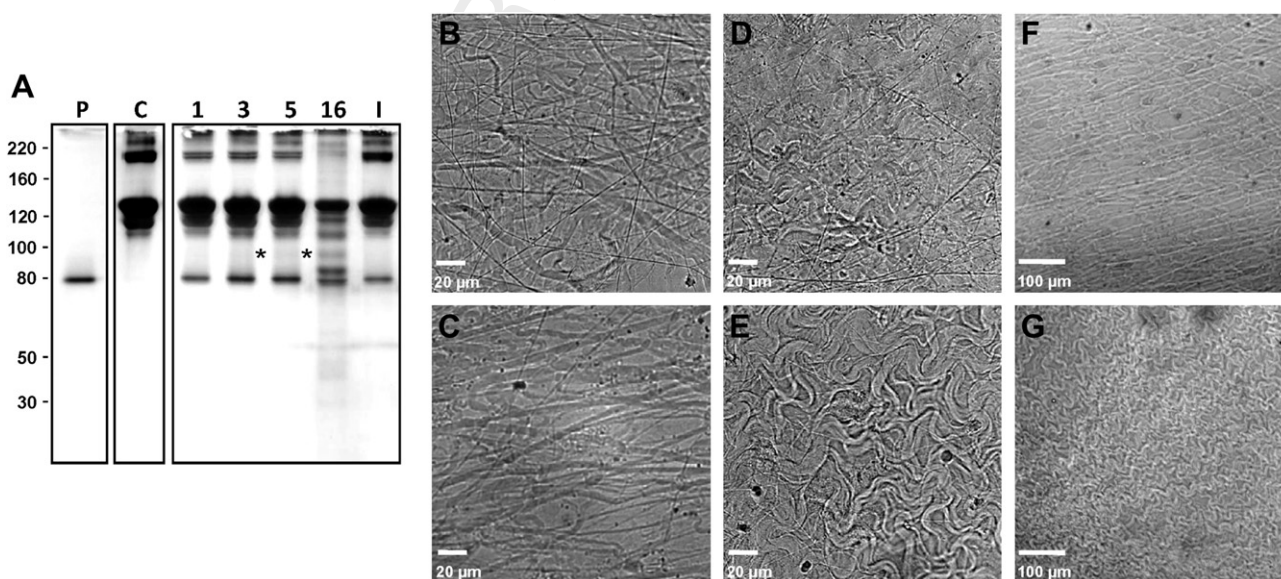
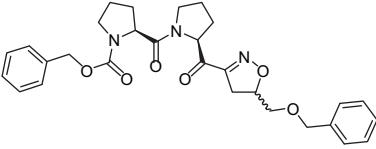
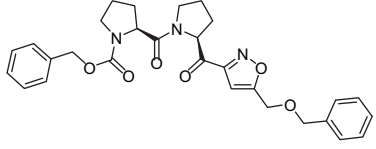
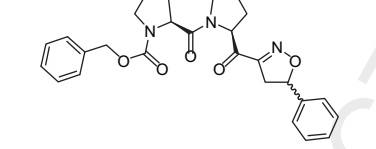
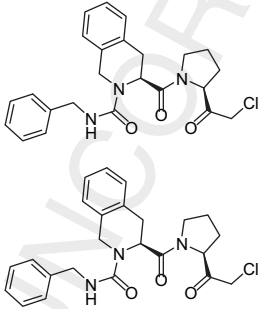


Fig. 2. Collagen degradation by rPOP Tb. (A) Hydrolysis was performed by incubating 50 μg of purified human collagen I with 200 ng of purified rPOP Tb (P) for 1, 3, 5 or 16 h at 37 °C. Controls consisted of incubation of collagen without enzyme (C) or with rPOP Tb inactivated by 1 μM inhibitor 4 (I), a specific inhibitor. Samples were analyzed by silver-stained 10% SDS-PAGE. Cleavage of native collagen fibers on rat mesentery by POP Tb after 3 h (D) or 16 h (E and G) of incubation at 37 °C. Mesentery was incubated without enzyme (B and F) or with rPOP Tb inactivated by 1 μM inhibitor 4 (C). Samples were observed on bright field contrast microscopy.

Table 2
Inhibition of rPOP Tb and *T. brucei* growth by specific inhibitors of trypanosome POP.

Inhibitor	IC ₅₀	
	rPOP Tb ^a (nM)	Bloodstream ^b (μM)
	1.4	16.0 + 3.1
	2.1	8.2 + 3.2
	0.34	12.8 + 3.2
	2	4.8 + 0.7

^a Inhibition assays were performed directly on purified rPOP Tb. Data are the mean of two independent experiments. Less than 10% of variation was observed between both experiments.

^b Inhibition assays on cell cultures of bloodstream *T. brucei* form. Data are the mean + SD of three experiments.

Collagen products were generated from the doublet at apparent molecular weights of 115 and 130 kDa as well as the doublet at 215 and 235 kDa. Slight product of hydrolysis was observed after 3 h of incubation (asterisk, Fig. 2A). In contrast, no hydrolysis was detected when collagen was incubated with rPOP Tb inactivated by the selective inhibitor 4 (see Section

3.4). Furthermore, rPOP Tb did not cleave BSA, showing that its activity seems to be restricted to proline-rich substrates such as collagens (Fig. S3). Since collagen I is abundant in the mesentery, we also incubated rPOP Tb with this tissue to assay its capacity to mediate hydrolysis of native collagen fibers. Disruption of thick fibers was observed after 1 h (data not

Table 3
Hydrolysis of peptide hormones by POP Tb.

Peptides	POP Tb hydrolysis sites
β -endorphin	Tyr-Gly-Gly-Phe-Met-Thr-Ser-Glu-Lys-Ser-Gln-Thr-Pro ↓ Leu-Val-Thr-Leu-Phe-Lys-Asn-Ala ↓ Ile-Ile-Lys-Asn-Ala ↓ Tyr-Lys-Lys-Gly-Glu
Neurotensin	pGlu-Leu-Tyr-Glu-Asn-Lys-Pro ↓ Arg-Arg-Pro ↓ Tyr-Ile-Leu
GnRH	pGlu-His-Trp-Ser-Tyr-Gly-Leu-Arg-Pro ↓ Gly-NH ₂
Bradykinin	Arg-Pro-Pro ↓ Gly-Phe-Ser-Pro ↓ Phe-Arg
TRH	pGlu-His-Pro ↓ NH ₂

shown) and was clearly distinguishable after 3 h incubation (Fig. 2D) compared to the controls (Fig. 2B and C). Cleavage of stretched collagen fibers resulted in their retraction, giving the mesentery a wrinkled aspect which was extensive after 16 h incubation in the presence of rPOP Tb (Fig. 2E).

3.4. POP Tb inhibition arrests *T. brucei* development

Specific inhibitors of POP Tc80 have been described as potent and selective molecules to impair the entry of *T. cruzi* trypomastigotes into mammalian host cells [19]. The irreversible inhibitor **4** was synthesized based on the phenyl-propylcarbonyl-L-tetrahydroisoquinoline (Tic)-pyrrolidine moiety [29], which shares selectivity for POP Tc80. This compound contains a proline mimic (Tic) in the P2 position

and a chloromethylketone as electrophilic reactive group in the pyrrolidine moiety (P1 position) to bind to the serine of the enzyme active site in an irreversible manner [19,30]. High selectivity of inhibitor **4** for POP Tc80 was observed when tested on other *T. cruzi* serine or cysteine proteases, even on the serine oligopeptidase B, which belongs to the same family. Selectivity was also observed when compared to mammalian POPs [19]. Further inhibitors (**1**, **2** and **3**) have been synthesized containing prolylisoxazoles [31]. To evaluate their effect on POP Tb activity, IC₅₀ values were determined by incubating these inhibitors with purified rPOP Tb before adding N-Suc-Gly-Pro-Leu-Gly-Pro-AMC substrate. The inhibition profile ranged from 0.34 nM for inhibitor **3** up to 2.1 nM for inhibitor **2** (Table 2) and were similar to that observed for POP Tc80 [19,31]. We tested their effect on parasite growth by maintaining bloodstream forms of *T. brucei* in the presence of inhibitors for 24 h, sufficient time to produce three parasite generations. The inhibitors induced a decrease in growth rate of the bloodstream form; the best was inhibitor **4**, with an IC₅₀ value of 4.8 μ M (Table 2). This inhibition is not due to non-specific toxicity since the inhibitors are not toxic to mammalian cells at the concentrations used in this test [20]. Despite the effect of these inhibitors, down-regulation performed by RNAi on procyclic and bloodstream *T. brucei* did not provide evidence for phenotype alteration. The remaining activity of POP Tb, about 20% of that of the control, may be sufficient to keep parasites viable (data not shown).

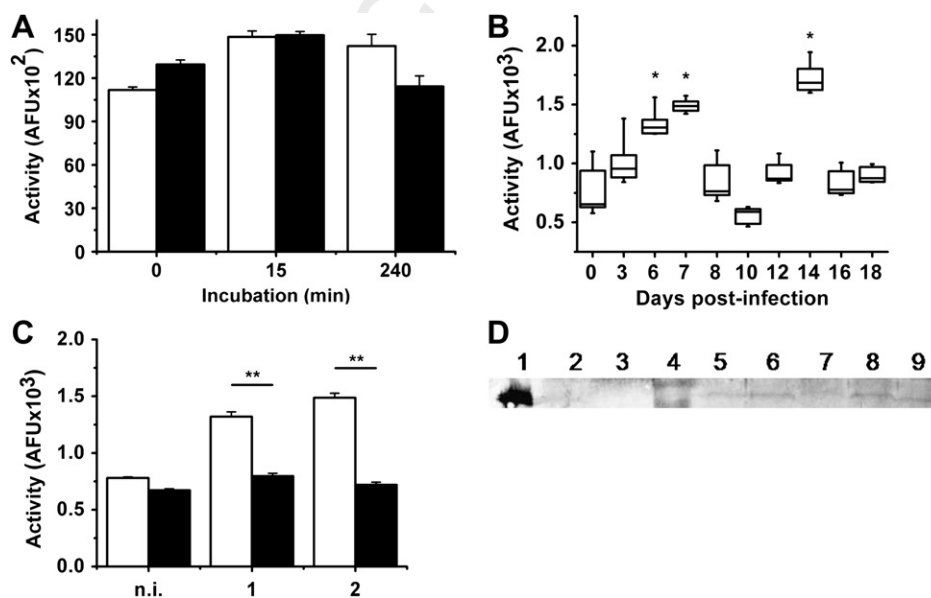


Fig. 3. Detection of POP Tb in the plasma of hosts infected with *T. brucei*. (A) POP Tb is active in human plasma. Purified rPOP Tb was incubated with human plasma (closed bars) or with HEPES 25 mM pH 7.5 (open bars) and aliquots were removed at 0, 15, (30, 60 and 120, not shown) and 240 min. POP Tb activity was measured against N-Suc-Gly-Pro-Leu-Gly-Pro-AMC. Data are the mean + SD of triplicate experiments. $p > 0.05$ for all combinations. (B) POP Tb is released in the plasma of *T. brucei*-infected mice. Activity of POP Tb was determined as described in experimental procedures. The bars represent the data range; the boxes represent lower and upper quartiles. * $p < 0.05$ compared with the beginning of the infection. (C) Plasma of non-infected or *T. brucei*-infected mice was assayed for the activity against N-Suc-Gly-Pro-Leu-Gly-Pro-AMC in the presence (closed bars) or not (open bars) of 100 nM inhibitor **4**. n.i. – non-infected, 1 – infected mouse from day 6, 2 – infected mouse from day 7. Data are the mean + SD of triplicate experiments. ** $p < 0.001$ ($p > 0.05$ for all combinations of non-infected mouse serum without inhibitor and infected mouse serum with inhibitor). (D) POP Tb is present in the plasma of infected mice. rPOP Tb (lane 1), plasma from 2 mice not infected (lane 2–3) or 5 mice infected with *T. brucei* (lane 5–9) were resolved by 10% SDS PAGE, transferred to a nitrocellulose membrane and incubated with anti-rPOP Tb antibody. Lane 4: molecular weight markers.

3.5. POP Tb cleaves bioactive peptides and is released into the plasma of infected mice

The major described feature of POPs is their ability to cleave substrates such as hormones and neuropeptides [18]. Therefore, we assayed POP Tb activity on bioactive peptides, including hormones that are reported to be down-regulated in sleeping sickness. After incubation of peptides with rPOP Tb, the resulting products were separated by HPLC and cleavage positions confirmed by MS/MS fragmentation. TRH hydrolysis released only the amide group that is required for full biological activity [32] (Table 3). GnRH was also cleaved at a single site, losing the Gly–NH₂ group. The cleavage of these two peptides was complete after 1 h of incubation with POP Tb. Neurotensin and bradykinin, which possess 2 proline residues, were partially hydrolyzed after 1 h and fully after 3 h of enzyme reaction. No preferential cleavage of a particular site was evident for these peptides. The hydrolysis of β -endorphin released only IIKNA and YKKGE at 1 h incubation with POP Tb indicating, in this case, a preference of the enzyme for the Ala sites. The other two peptides produced by cleavage after Pro were detected by increasing the enzymatic reaction time, where complete hydrolysis was observed between 3 and 16 h.

The involvement of POP Tb in the hydrolysis of circulating host hormones depends on its activity in plasma that contains natural protease inhibitors such as α_2 -macroglobulin and α_1 -proteinase inhibitor. To determine the POP Tb behavior in host blood, purified enzyme was incubated with human plasma up to 4 h and its activity evaluated on N-Suc-Gly-Pro-Leu-Gly-Pro-AMC. Under these conditions, no significant inhibition of POP Tb activity was detected (Fig. 3A), indicating that inhibitors or other factors present in the plasma do not interfere with the enzyme activity.

Oligopeptidase B has been detected in the plasma of trypanosome-infected rats [8,9], and its activity is associated with an increase of atrial natriuretic factor degradation in *Trypanosoma evansi*-infected animals, suggesting a relevant role of the enzyme in the pathogenesis of sleeping sickness and surra. However, other proteases released from bloodstream trypanosomes may also contribute to host hormone degradation. To verify whether POP Tb plays a similar role, we infected mice, followed their parasitemia and POP Tb activity in plasma over the course of infection. POP Tb activity was detected in plasma as peaks that correlate with the peaks of parasitemia (Fig. 3B). Similar peaks of activity were found for oligopeptidase B, which was used as control (Fig. S3).

Since sera from healthy mice naturally mediate N-Suc-Gly-Pro-Leu-Gly-Pro-AMC hydrolysis, we tested if the POP Tb activity detected during *T. brucei* infection was in fact from the parasite and not from the host POP. To differentiate both enzymes, we incubated the plasma from non-infected or *T. brucei*-infected mice with 100 nM of inhibitor 4, a molecule that shows a selectivity for trypanosome POP of more than 70 times that of mammalian POP [31]. In fact, this inhibitor decreased hydrolysis of the substrate in the plasma of infected mice close to the basal level found in the plasma of non-infected controls (Fig. 3C). In addition, immunoblotting using specific anti-POP Tb antibodies showed the presence of

POP Tb in the cell-free plasma of *T. brucei*-infected mice, but not in the non-infected controls (Fig. 3D). Thus, these results together suggest that POP Tb is released into the plasma of infected mice and remains active.

4. Discussion

Here we present evidence that POP Tb, as was the case for POP Tc80 cleaves collagen at neutral pH contrasting with what has been considered as the most distinguishing property of POP members: their specificity for peptides smaller than 30 amino acid residues [24]. However, this feature is questionable because other members of this protease family can cleave large substrates. One example is the Fibroblast Activation Protein alpha (FAP α), a membrane proteinase implicated in tissue remodeling and invasion of epithelial tumors by degrading collagens [33]. Moreover, a cytosolic prolyl endopeptidase is involved in the degradation of p40-phox variant protein in myeloid cells [34], and *Salmonella enterica* oligopeptidase B, another POP family member, is able to cleave histones H2A and H4 *in vitro* [35].

POP Tb collagenolytic activity could help the parasite to penetrate the capillary endothelium and thus, enable it to multiply outside the blood–vascular system and propagate within its host. One of the most dramatic abilities of *T. brucei* is that it may cross the blood–brain barrier and invade the central nervous system [36]. It has been showed that *T. brucei* cysteine proteases drive parasite transmigration through the blood–brain barrier by calcium dependent signaling events [37,38]. Evidence from both animal models and human studies supports a role for collagenases (matrix metalloprotease, MMP) in the blood–brain barrier disruption in neuro-inflammatory diseases [39]. MMP target substrates include collagens, fibronectin and laminin, all of which are critical vascular matrix components. POP Tb could contribute to the blood–brain barrier disruption by cleaving collagen and/or its degradation products, which are rich in Gly-Pro repetitions, over the course of a trypanosome infection. Nevertheless, extracellular release of active POP Tb would be required to accomplish hydrolysis of collagen. It has been demonstrated that *T. evansi* releases a N-Suc-Gly-Pro-Leu-Gly-Pro-AMC hydrolyzing activity into the culture medium [9]. In addition, we report that specific inhibitors of POP Tc80 arrest the development of the bloodstream parasitic form, indicating that POP Tb might play a fundamental role in parasite growth. In this case, POP Tb could be involved in maturation and/or processing of (poly)peptides necessary for cell proliferation.

The activity of POP Tb assayed in human plasma revealed that this enzyme is insensitive to natural protease inhibitors such as α_2 -macroglobulin and α_1 -proteinase inhibitor. Moreover, POP Tb remained active for many hours in plasma (80% of activity at 8 h, data not shown), indicating that the pH and protein composition (such as albumin and immunoglobulins) are favorable for its activity and/or stability. The same was observed in the plasma of *T. brucei*-infected mice, where POP Tb remains active up to the end of parasitemia peaks, suggesting that POP Tb is not inhibited by specific antibodies

elicited during the infection. Moreover, *in vitro* incubation of purified POP Tb with anti-POP Tb antibodies did not block its activity toward the N-Suc-Gly-Pro-Leu-Gly-Pro-AMC substrate (data not shown). It has also been demonstrated that the oligopeptidase B of *T. cruzi*, another POP family member, is active in human sera containing specific antibodies [40]. These observations suggest that members of this family of peptidases are fully active in mammalian fluids.

POP Tb activity in the plasma of *T. brucei*-infected animals might hydrolyze host circulating factors such as hormones and neurotransmitter peptides contributing to homeostasis breakdown as observed in African trypanosomiasis [41]. Among them, abnormal levels of TRH and GnRH seem to correlate with hypothyroidism and hypogonadism, frequent symptoms seen in sleeping sickness [2]. Since these peptides are pituitary hormones, they are at the top of the regulation cascade of peripheral hormones with physiological action in gonads as sexual hormones controlled by GnRH, and in metabolism-involved organs as thyroid hormones controlled by TRH. We show here that POP Tb cleaves readily after a Pro residue in these peptides, releasing NH₂ from TRH and Gly-NH₂ from GnRH.

As TRH (p-Glu-His-Pro-NH₂) has strict conformational requirements for biological activity, modifications of its native structure result in substantial, if not complete, loss of biological activity [32]. In general, synthetic and natural TRH analogues require the preservation of the cyclised Glu amino-terminal end and the amidated Pro carboxyl-terminal [42] in their sequences for agonist effect. These post-translational modifications compositions confer resistance against exopeptidase degradation. Such a peculiar structure requires specialized proteases for the physiological control of TRH [43]. POP and pyroglutamyl peptidase (PGP; cleaving the p-Glu-His bond) are the major candidates for primary inactivation. In sleeping sickness, the parasite POP and PGP, both active in host plasma [7], might act in synergy to decrease the TRH action during parasitemia peaks or in untreated patients.

Similarly, the release of Gly-NH₂ from GnRH by POP Tb may facilitate its complete inactivation by other parasite proteases. The physiological control of GnRH by POP in a stepwise manner in the hypothalamus and the anterior pituitary gland has been suggested [44]. After C-terminal glycinamide cleavage by POP generating GnRH [1–9], a metalloendopeptidase EC 3.4.24.15 (EP24.15) cleaves at the Tyr⁵-Gly⁶ bond, 11 times more efficiently than GnRH [1–10], generates inactive GnRH [1–5]. Although a metalloendopeptidase orthologue has not been described in *T. brucei*, the incubation of GnRH with the plasma of infected rats did result in several GnRH subproducts such as GnRH [1–5] and GnRH [1–9] [6]. More recently, it has been demonstrated that a decrease in GnRH half-life in trypanosome-infected rats is partially attributed to parasite PGP [7]. These reports and our data may suggest a synergistic involvement of POP Tb and other parasite peptidases to inactivate GnRH.

Our results clearly demonstrate that POP Tb mediates degradation of bradykinin, β-endorphin and neurotensin, which have important regulatory functions [45]. However, the list of bioactive peptides that could be hydrolyzed by POP Tb is much

more extensive, including peptides known to be experimental substrates of mammalian POPs such as oxytocin, vasopressin, substance P, angiotensin, mastoparan and neuropeptide Y, as well as other Pro and/or Ala-containing peptides [14,18]. It is possible that in some cases, the cleavage by POP Tb does not completely inactivate the peptide, generating products with weaker affinity for their receptors resulting in attenuated physiological effects. Moreover, truncated peptides can present an additional inhibitory auto-feedback role such as the possible inhibition of secretion of GnRH by the GnRH [1–5] subproduct, evoked through stimulation of the *N*-methyl-D-aspartate receptors [46]. In conclusion, we characterized POP Tb, a neutral serine protease released into the plasma of *T. brucei*-infected mice that presents enzymatic activities such as collagen degradation and cleavage of proline and alanine-rich peptide hormones. These features suggest that POP Tb might play a role in the ontogeny and/or maintenance of sleeping sickness.

Acknowledgments

We thank D. Campbell, B. Ribeiro and C. Araújo for critical reading of the manuscript, J. Corrêa for microscopy service, A. Haemers for providing inhibitors and the mass spectrometry platform of the MNHN for technical support. This work was supported by CNPq and CAPES, Brazil, and by the French Ministry of Research.

Appendix. Supplementary data

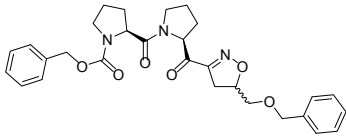
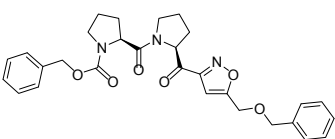
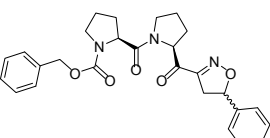
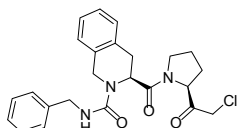
Supplementary data associated with this article can be found, in the online version, at doi:10.1016/j.micinf.2010.02.007.

References

- [1] M. Dumas, B. Bouteille, A. Buguet, Progress in Human African Trypanosomiasis, Sleeping Sickness. Springer, Paris; New York, 1999.
- [2] M. Hublart, L. Lagouche, A. Racadot, A. Boersma, P. Degand, F. Noireau, J.L. Lemesre, A. Toudic. Endocrine function and African trypanosomiasis. Evaluation of 79 cases, Bull. Soc. Pathol. Exot. Filiales. 81 (1988) 468–476.
- [3] E.N. Waindi, S. Gombe, D. Oduor-Okelo, Plasma testosterone in *Trypanosoma congolense*-infected Toggenburg goats. Arch. Androl. 17 (1986) 9–17.
- [4] B.M. Mutayoba, S. Gombe, G.P. Kaaya, E.N. Waindi, Effect of chronic experimental *Trypanosoma congolense* infection on the ovaries, pituitary, thyroid and adrenal glands in female goats. Res. Vet. Sci. 44 (1988) 140–146.
- [5] G. Knowles, S.J. Black, D.D. Whitelaw, Peptidase in the plasma of mice infected with *Trypanosoma brucei brucei*. Parasitology 95 (Pt 2) (1987) 291–300.
- [6] D. Tetaert, B. Soudan, G. Huet-Duvillier, P. Degand, A. Boersma, Unusual cleavage of peptidic hormones generated by trypanosome enzymes released in infested rat serum. Int. J. Pept. Protein Res. 41 (1993) 147–152.
- [7] R.E. Morty, P. Bulau, R. Pelle, S. Wilk, K. Abe, Pyroglutamyl peptidase type I from *Trypanosoma brucei*: a new virulence factor from African trypanosomes that de-blocks regulatory peptides in the plasma of infected hosts. Biochem. J. 394 (2006) 635–645.
- [8] R.E. Morty, J.D. Lonsdale-Eccles, R. Mentele, E.A. Auerswald, T.H. Coetzer, Trypanosome-derived oligopeptidase B is released into the

- plasma of infected rodents, where it persists and retains full catalytic activity. *Infect. Immun.* 69 (2001) 2757–2761.
- [9] R.E. Morty, R. Pelle, I. Vadasz, G.L. Uzcanga, W. Seeger, J. Bubis, Oligopeptidase B from *Trypanosoma evansi*. A parasite peptidase that inactivates atrial natriuretic factor in the bloodstream of infected hosts. *J. Biol. Chem.* 280 (2005) 10925–10937.
- [10] V.O. Anosa, T.T. Isoun, Serum proteins, blood and plasma volumes in experimental *Trypanosoma vivax* infections of sheep and goats. *Trop. Anim. Health. Prod.* 8 (1976) 14–19.
- [11] B. Goossens, S. Osaer, S. Kora, K.J. Chandler, L. Petrie, J.A. Thevasagayam, T. Woolhouse, J. Anderson, Abattoir survey of sheep and goats in the Gambia. *Vet. Rec.* 142 (1998) 277–281.
- [12] R. Mentlein, Proline residues in the maturation and degradation of peptide hormones and neuropeptides. *FEBS Lett.* 234 (1988) 251–256.
- [13] R. Walter, H. Shlank, J.D. Glass, I.L. Schwartz, T.D. Kerenyi, Leucylglycinamide released from oxytocin by human uterine enzyme. *Science* 173 (1971) 827–829.
- [14] M. Koida, R. Walter, Post-proline cleaving enzyme. Purification of this endopeptidase by affinity chromatography. *J. Biol. Chem.* 251 (1976) 7593–7599.
- [15] T. Yoshimoto, K. Kado, F. Matsubara, N. Koriyama, H. Kaneto, D. Tsuru, Specific inhibitors for prolyl endopeptidase and their anti-amnesic effect. *J. Pharmacobiodyn.* 10 (1987) 730–735.
- [16] P. Morain, P. Lestage, G. De Nanteuil, R. Jochemsen, J.L. Robin, D. Guez, P.A. Boyer, S 17092: a prolyl endopeptidase inhibitor as a potential therapeutic drug for memory impairment. Preclinical and clinical studies. *CNS Drug Rev.* 8 (2002) 31–52.
- [17] J.M. Santana, P. Grellier, J. Schrevel, A.R. Teixeira, A *Trypanosoma cruzi*-secreted 80 kDa proteinase with specificity for human collagen types I and IV. *Biochem. J.* 325 (Pt 1) (1997) 129–137.
- [18] A. Moriyama, M. Nakanishi, M. Sasaki, Porcine muscle prolyl endopeptidase and its endogenous substrates. *J. Biochem. (Tokyo)* 104 (1988) 112–117.
- [19] P. Grellier, S. Vendeville, R. Joyeau, I.M. Bastos, H. Drobecq, F. Frappier, A.R. Teixeira, J. Schrevel, E. Davioud-Charvet, C. Sergheraert, J. M. Santana, *Trypanosoma cruzi* prolyl oligopeptidase Tc80 is involved in nonphagocytic mammalian cell invasion by trypomastigotes. *J. Biol. Chem.* 276 (2001) 47078–47086.
- [20] I.M. Bastos, P. Grellier, N.F. Martins, G. Cadavid-Restrepo, M.R. de Souza-Ault, K. Augustyns, A.R. Teixeira, J. Schrevel, B. Maigret, J.F. da Silva, J. M. Santana, Molecular, functional and structural properties of the prolyl oligopeptidase of *Trypanosoma cruzi* (POP Tc80), which is required for parasite entry into mammalian cells. *Biochem. J.* 388 (2005) 29–38.
- [21] R. Brun, Schonenberger, Cultivation and in vitro cloning or procyclic culture forms of *Trypanosoma brucei* in a semi-defined medium. Short communication. *Acta. Trop.* 36 (1979) 289–292.
- [22] P.M. Loiseau, P. Lubert, J.G. Wolf, Contribution of dithiol ligands to in vitro and in vivo trypanocidal activities of dithiaarsanes and investigation of ligand exchange in an aqueous solution. *Antimicrob. Agents Chemother.* 44 (2000) 2954–2961.
- [23] D.T. Jones, Protein secondary structure prediction based on position-specific scoring matrices. *J. Mol. Biol.* 292 (1999) 195–202.
- [24] V. Fulop, Z. Bocskei, L. Polgar, Prolyl oligopeptidase: an unusual beta-propeller domain regulates proteolysis. *Cell* 94 (1998) 161–170.
- [25] K.J. Ellis, J.F. Morrison, Buffers of constant ionic strength for studying pH-dependent processes. *Methods Enzymol.* 87 (1982) 405–426.
- [26] A. Cornish-Bowden, Principles of Enzyme Kinetics. Butterworths, London; Boston, 1976.
- [27] Y.Y. Chen, S.Y. Lin, Y.Y. Yeh, H.H. Hsiao, C.Y. Wu, S.T. Chen, A.H. Wang, A modified protein precipitation procedure for efficient removal of albumin from serum. *Electrophoresis* 26 (2005) 2117–2127.
- [28] T. Yoshimoto, M. Fischl, R.C. Orlowski, R. Walter, Post-proline cleaving enzyme and post-proline dipeptidyl aminopeptidase. Comparison of two peptidases with high specificity for proline residues. *J. Biol. Chem.* 253 (1978) 3708–3716.
- [29] K. Toide, M. Shinoda, A. Miyazaki, A novel prolyl endopeptidase inhibitor, JTP-4819 – its behavioral and neurochemical properties for the treatment of Alzheimer’s disease. *Rev. Neurosci.* 9 (1998) 17–29.
- [30] S. Vendeville, F. Goossens, M.A. Debreu-Fontaine, V. Landry, E. Davioud-Charvet, P. Grellier, S. Scharpe, C. Sergheraert, Comparison of the inhibition of human and *Trypanosoma cruzi* prolyl endopeptidases. *Bioorg. Med. Chem.* 10 (2002) 1719–1729.
- [31] G. Bal, P. Van der Veken, D. Antonov, A.M. Lambeir, P. Grellier, S.L. Croft, K. Augustyns, A. Haemers, Prolylisoaxazoles: potent inhibitors of prolyloligopeptidase with antitrypanosomal activity. *Bioorg. Med. Chem. Lett.* 13 (2003) 2875–2878.
- [32] R. Guillemin, R. Burgus, The hormones of the hypothalamus. *Sci. Am.* 227 (1972) 24–33.
- [33] J.E. Park, M.C. Lenter, R.N. Zimmermann, P. Garin-Chesa, L.J. Old, W. J. Rettig, Fibroblast activation protein, a dual specificity serine protease expressed in reactive human tumor stromal fibroblasts. *J. Biol. Chem.* 274 (1999) 36505–36512.
- [34] T. Hasebe, J. Hua, A. Someya, P. Morain, F. Checler, I. Nagaoka, Involvement of cytosolic prolyl endopeptidase in degradation of p40-phox splice variant protein in myeloid cells. *J. Leukocyte Biol.* 69 (2001) 963–968.
- [35] R.E. Morty, V. Fulop, N.W. Andrews, Substrate recognition properties of oligopeptidase B from *Salmonella enterica* serovar *typhimurium*. *J. Bacteriol.* 184 (2002) 3329–3337.
- [36] L.G. Goodwin, Pathological effects of *Trypanosoma brucei* on small blood vessels in rabbit ear-chambers. *Trans. R Soc. Trop. Med. Hyg.* 65 (1971) 82–88.
- [37] O.V. Nikolskaia, A.L.A.P. de, Y.V. Kim, J.D. Lonsdale-Eccles, T. Fukuma, J. Scharfstein, D.J. Grab, Blood–brain barrier traversal by African trypanosomes requires calcium signaling induced by parasite cysteine protease. *J. Clin. Invest.* 116 (2006) 2739–2747.
- [38] D.J. Grab, J.C. Garcia-Garcia, O.V. Nikolskaia, Y.V. Kim, A. Brown, C. A. Pardo, Y. Zhang, K.G. Becker, B.A. Wilson, A.L.A.P. de, J. Scharfstein, J.S. Dumler, Protease activated receptor signaling is required for African trypanosome traversal of human brain microvascular endothelial cells. *PLoS Negl. Trop. Dis.* 3 (2009) e479.
- [39] V.W. Yong, C. Power, P. Forsyth, D.R. Edwards, Metalloproteinases in biology and pathology of the nervous system. *Nat. Rev. Neurosci.* 2 (2001) 502–511.
- [40] L.C. Fernandes, I.M. Bastos, L. Lauria-Pires, A.C. Rosa, A.R. Teixeira, P. Grellier, J. Schrevel, J.M. Santana, Specific human antibodies do not inhibit *Trypanosoma cruzi* oligopeptidase B and cathepsin B, and immunoglobulin G enhances the activity of trypomastigote-secreted oligopeptidase B. *Microbes Infect.* 7 (2005) 375–384.
- [41] J.M. Ndung’u, N.G. Wright, F.W. Jennings, M. Murray, Changes in atrial natriuretic factor and plasma renin activity in dogs infected with *Trypanosoma brucei*. *Parasitol. Res.* 78 (1992) 553–556.
- [42] S. Engel, S. Neumann, N. Kaur, V. Monga, R. Jain, J. Northup, M.C. Gershengorn, Low affinity analogs of thyrotropin-releasing hormone are super-agonists. *J. Biol. Chem.* 281 (2006) 13103–13109.
- [43] E.C. Griffiths, Peptidase inactivation of hypothalamic releasing hormones. *Horm. Res.* 7 (1976) 179–191.
- [44] R.A. Lew, T.J. Tetaz, M.J. Glucksman, J.L. Roberts, A.I. Smith, Evidence for a two-step mechanism of gonadotropin-releasing hormone metabolism by prolyl endopeptidase and metalloendopeptidase EC 3.4.24.15 in ovine hypothalamic extracts. *J. Biol. Chem.* 269 (1994) 12626–12632.
- [45] T.H. Jones, B.L. Brown, P.R. Dobson, Paracrine control of anterior pituitary hormone secretion. *J. Endocrinol.* 127 (1990) 5–13.
- [46] J.P. Bourguignon, M.L. Alvarez Gonzalez, A. Gerard, P. Franchimont, Gonadotropin releasing hormone inhibitory autofeedback by subproducts antagonist at N-methyl-D-aspartate receptors: a model of autocrine regulation of peptide secretion. *Endocrinology* 134 (1994) 1589–1592.

Table 2. Inhibition of rPOP Tb and *T. brucei* growth by specific inhibitors of trypanosome POP.

Inhibitor	IC ₅₀	
	rPOP Tb ^a	Bloodstream ^b
	nM	μM
1 	1.4	16.0 ± 3.1
2 	2.1	8.2 ± 3.2
3 	0.34	12.8 ± 3.2
4 	2	4.8 ± 0.7

^a Inhibition assays were performed directly on purified rPOP Tb. Data are the mean of two independent experiments. Less than 10% of variation was observed between both experiments.

^b Inhibition assays on cell cultures of bloodstream *T. brucei* form. Data are the mean ± SD of three experiments.

Supplementary data legends

Figure S1. Structural alignment among POP Tb, POP Tc80 and porcine (*Sus scrofa*) POP. The alignment of these proteases was performed based on the identity and secondary structure prediction. Light gray arrows indicate β -strands belonging to the seven-bladed β -propeller domain. Dark gray cylinders and black arrows represent α -helices and β -strands, respectively, that constitute the α/β hydrolase domain. The catalytic triad residues are indicated by circles. Asterisks and colons represent 100% and 50% of identity, respectively, and dots represent amino acids similarity.

Figure S2. Effect of pH on recombinant POP Tb activity. The purified His-tag-free rPOP Tb was assayed in AMT buffer (pHs 4-11 range) against N-Suc-Gly-Pro-Leu-Gly-Pro-AMC. The activity is represented by the percentage means, considering the maximum activity at pH 8.

Figure S3. Incubation of rPOP Tb with BSA. Enzyme activity was assayed by incubating 50 μ g of BSA (*lanes 2-3*) with 200 ng of rPOP Tb in 100 μ l of activity buffer for up to 16 h at 37 °C. Control (*lane 1*) consisted of substrate incubation with rPOP Tb inactivated by 200 μ M TPCK. Aliquots (20 μ l) at 1 h (*lane 2*) and 16 h (*lanes 1 and 3*) of incubation were analyzed by 8% SDS-PAGE followed by silver staining. Molecular weight markers are represented in *lane 4*.

Figure S4. Oligopeptidase B activity in the plasma of *T. brucei*-infected mice was monitored throughout the infection and measured as described in experimental procedures.

Figure S1

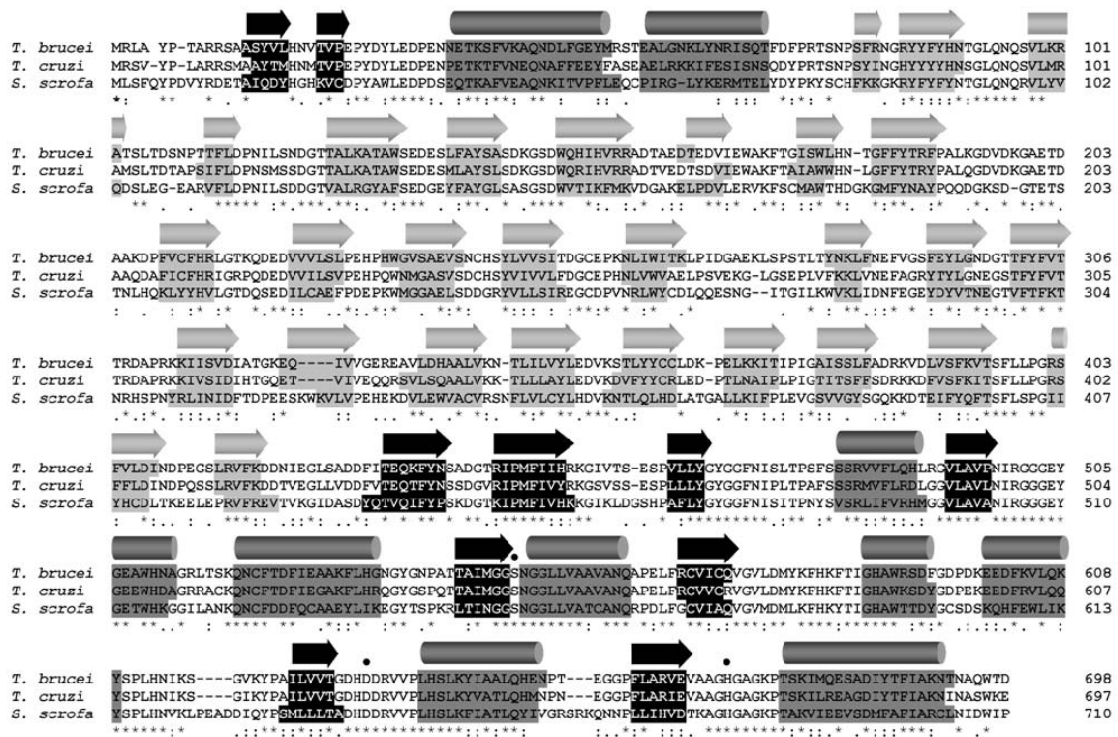


Figure S2

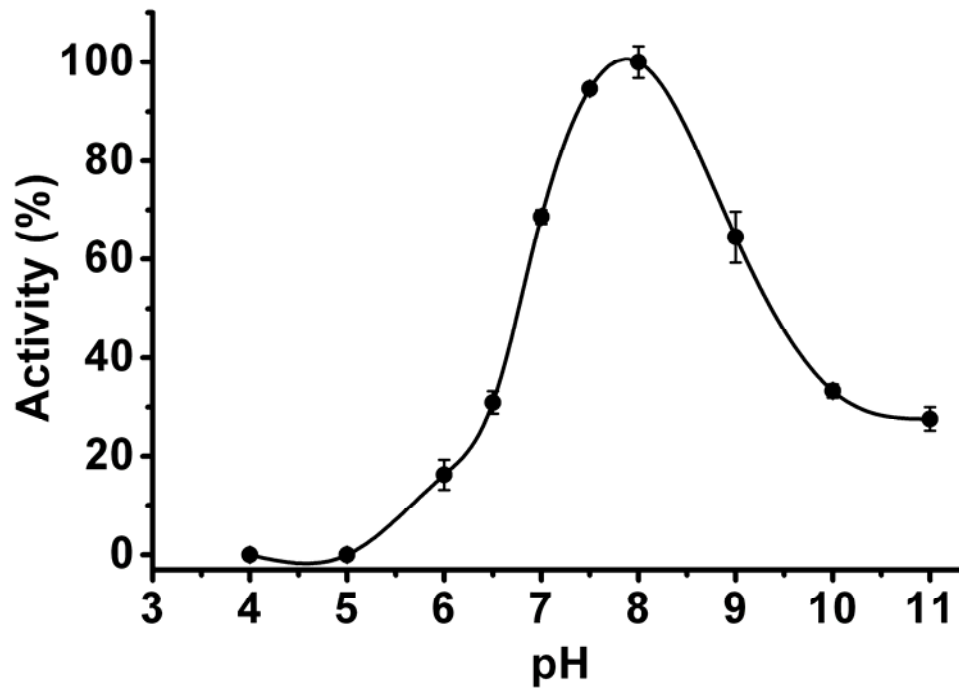


Fig S3

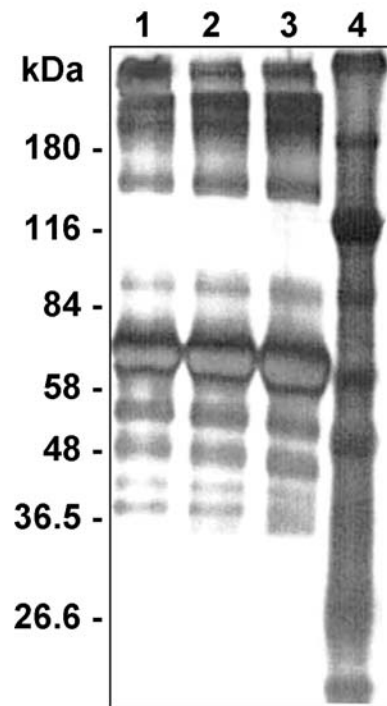
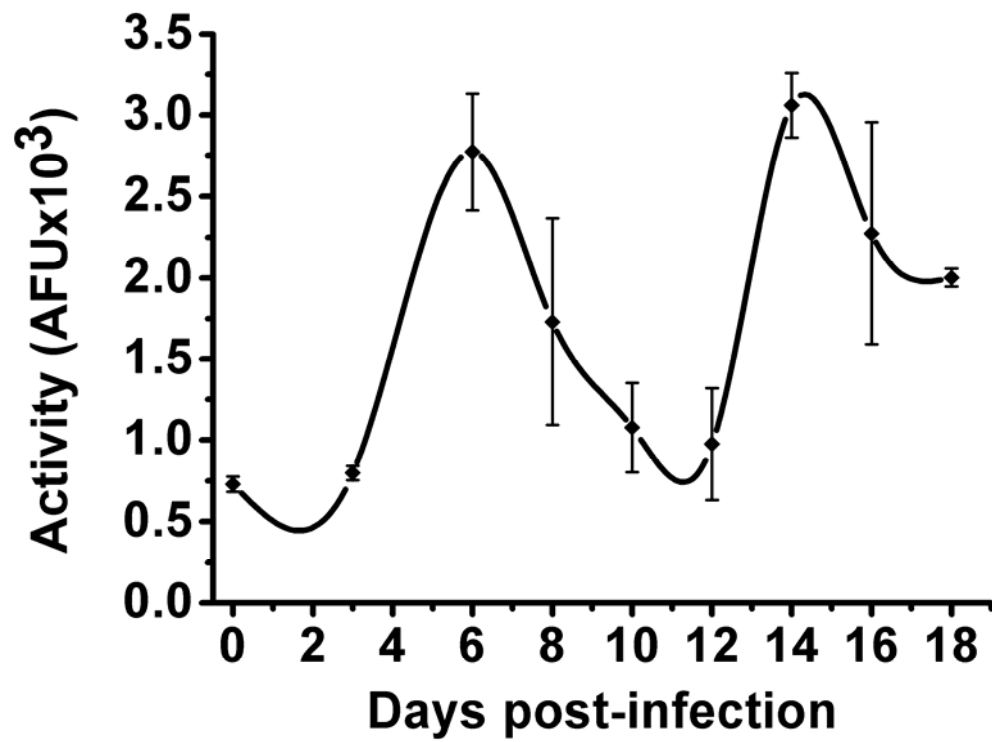


Figure S4





III. Elucidação do mecanismo catalítico da POP Tc80

Apresentado na forma de manuscrito para publicação

Combined molecular simulations and mutagenesis experiments provide evidence for a gating mechanism in POP Tc80 from *Trypanosoma cruzi*

Authors by alphabetic order:

Bernard Maigret ¹

Flávia N. Motta ²

Izabela M.D. Bastos ²

Jaime M. Santana* ²

Philippe Grellier ³

Vincent Leroux ¹

1- Nancy Université – LORIA, groupe Orpailleur – Campus scientifique, BP 239 – 54506 Vandœuvre-lès-Nancy Cedex – France

2- Laboratório de Interação Parasito-Hospedeiro – Faculdade de Medicina, Campus da UnB, Asa Norte – 70910-900 Brasília DF – Brazil

3- USM 504 Muséum National d’Histoire Naturelle, Paris, France

Keywords: Chagas' disease ; *Trypanosoma cruzi* ; Prolyl oligopeptidase ; POP Tc80 ; Homology modelling ; Protein-ligand complex ; Enzyme catalytic activation mechanism ; Mutagenesis experiments ; Binding assays ; Structure-based drug design.

Abstract

We have previously demonstrated that the secreted prolyl oligopeptidase of *Trypanosoma cruzi* (POP Tc80) could be involved in the infection process by facilitating *T. cruzi* migration through the extracellular matrix. A 3D model of POP Tc80 propose that the structure is formed by a catalytic α/β -hydrolase and a β -propeller domains. The collagen, substrate of POP Tc80, upon docking on this model, interacted in the interface between the two domains, promoting a gating access mechanism involving a "jaw opening" of POP Tc80. To validate the model, three α/β -hydrolase domain residues were identified as candidates for forming a disulfide bridge with propeller Cys255 upon Cys mutation, therefore locking POP Tc80 into its model-predicted closed state, and blocking the enzyme catalytic reactivation. Molecular dynamics simulations of the three POP Tc80 mutants were conducted and the simulation predictions were found in both qualitative and quantitative agreement with experimental results. The Ser591Cys and Asn471Cys mutants showed significantly decreased enzymatic activity correlated with the production of the disulfide bridge. Surprisingly, the Ala588Cys mutant was more active – this was shown to be related to Cys588 interacting with Arg633 of α/β -hydrolase rather than with propeller Cys255, facilitating the interdomain gating mechanism instead of obstructing it. Therefore we consider that our POP Tc80 model structure is validated, and provides a strong basis for virtual screening of chemical libraries and new binding assays. This structure-based drug design is a rational strategy in order to detect novel putative anti-Chagas compounds.

Introduction

Chagas' disease, a chronic debilitating illness, is caused by the protozoan parasite *Trypanosoma cruzi*. [1; 2] Despite extensive searches for efficient drugs started decades ago and still being carried on [3; 4; 5; 6], Chagas' disease in its chronic phase is yet incurable, with a mortality rate that constitutes a major burden imposed on millions in Latin America. [7; 8] In such a situation, the characterization of various parasitic virulence factors that could be studied as potential drug design targets is crucial.

During studies about interactions of *T. cruzi* with mammalian host, we have identified, purified and biochemically characterized the prolyl oligopeptidase of *T. cruzi*, POP Tc80, with activity on extracellular matrix compounds such as type I and IV human collagens and fibronectin. [9; 10] Specific inhibitors were subsequently designed [11; 12], and confirmed that POP Tc80 is indeed a potential target for chemotherapy against vertebrate *T. cruzi* infection. However, those inhibitors have low efficiency amongst compounds targeting mammalian POP activity [13], and while the biological role of the POP family is still under investigation it is clear that specificity might most probably be an issue in inhibitor design [14]. In such a context, rational drug design strategies are needed. Promising results on another *T. cruzi* target, cruzain, have been reported with a structure-based approach [15]. Unfortunately, unlike cruzain, the structure of POP Tc80 has not been experimentally resolved yet.

Starting from the homologous crystallized porcine POP, we have constructed a 3D model of POP Tc80 [16]. It suggests that POP Tc80, as other POPs, is composed of an α/β -hydrolase catalytic domain and a seven-bladed β -propeller non-catalytic domain [16]. POP Tc80 also features a highly conserved catalytic triad (Ser548, Asp631 and His667) whose position, near the domains' junction and visibly accessible

to ligand binding, is also common amongst POPs. Despite these structural similarities, it is known that POP Tc80 is capable of hydrolyzing much larger substrates (such as collagen) than other POPs (only able to hydrolyze oligopeptides ≤ 3 kDa). [9] Such an unique feature of POP Tc80 had to be expressed by its model. Therefore, we manually docked the triple-helical collagen [16] and found that (i) the POP Tc80 model catalytic binding site was indeed able of accommodating such a large ligand, and (ii) the collagen bound along the hydrolase-propeller interface forming a stable complex without disrupting POP Tc80 secondary structure. These observations supported the hypothesis of a cleavage mechanism upon ligand binding centered on a hinge connecting the two domains. Such an activation process by inter-domain gating was already suggested by several POP studies [17; 18].

Meanwhile, the POP Tc80 theoretical model needed to be experimentally validated. Theoretical calculations based on molecular dynamics simulations were used in order to define interesting POP Tc80 point mutations. The mutants have been both theoretically modelled/simulated and experimentally synthesized/tested; the degree of agreement between predictions and assays being used as a reliability measure of the POP Tc80 model.

Methods

Molecular dynamics (MD) simulations

The POP Tc80 protein 3D structure was solvated in a $(100 \text{ \AA})^3$ cubic box of ~26,000 TIP3P water molecules, 20 Na^+ ions added at edges for ensuring electrostatic neutrality. The NAMD program [19; 20] was employed in conjunction with the CHARMM22 forcefield [21; 22] to describe and simulate the ~90,000-atoms

investigated molecular system. Energy minimization was first performed (6,400 steps of conjugate gradients), next the system was equilibrated (500 ps of MD), and eventually a MD trajectory was produced, using the particle-mesh Ewald approach to treat long-range electrostatics. The dynamics were carried out in the NPT ensemble using Langevin dynamics and piston methods to fix temperature (300 K) and pressure (1 atm). Heavy atoms-hydrogen bonds were constrained to their equilibrium value.

A total of 4 MD simulations were performed, each with 1 fs time steps, 1 frame/ps recorded. The POP Tc80 model built as described previously [16] from the porcine muscle POP crystal structure [23] (PDB [24] code : 1QFM) was simulated during 5 ns. Three derived mutants were simulated during 500 ps. VMD [25] was used both for analyzing the MD simulations and for modelling the mutants (Mutator 1.0 plugin).

Production of POP Tc80 mutants

Site-directed mutageneses were performed using the GeneTailor™ system according to the manufactory instructions (Invitrogen). Briefly, the POP Tc80 mutageneses (S591C, N471C or A588C) were inserted by PCR using the follow primer set: S591C, sense 5' CTATTGGGCATGCGTGGAAGTGCGACTATGGTG 3' and antisense ACTTCCACGCATGCCCAATAGTAAACTTGTG; N471C, sense 5' TTTACGGCTACGGTGGCTTCTGTATTCCCTTTG 3' and antisense 5'GAAGCCACCGTAGCCGTAAAGTAACAGTGG 3'; A588C, sense 5'ACAAGTTTACTATTGGGCATTGCTGGAAGTCCG 3' and antisense 5' AATGCCCAATAGTAAACTTGTGAAATTTGTAC 3'. The whole expression plasmid pET15b/*poptc80* was amplified with these primers pairs and each respective PCR

product was methylated and used to transform *E. coli*. After confirmation of mutagenesis, plasmids were extracted and used to produce recombinant mutated protein in *E. coli* BL21(DE3). The production and purification were carried out as already described [16].

Oxidation of mutated POP Tc80

To catalyze the disulfide bond formation between mutated Cys into hydrolase domain and Cys255 into propeller domain, we incubated the pure recombinant mutated protein with 1 mM of oxidized glutathione (GSSG) or with 10 mM [26] hydrogen peroxide (H_2O_2) in alkaline pHs for 2 hours at 25 °C. To verify the effect of disulfide bond, the POP Tc80 activity was assayed as below. To reduce the disulfide bond, oxidized recombinant mutated POP Tc80 was incubated with 5 mM DTT.

POP Tc80 activity

The enzyme activity was assessed using the fluorogenic substrate N-Suc-Gly-Pro-Leu-Gly-Pro-AMC as described [16]. Briefly, the kinetic parameters were determined by incubation of 20 ng of pure recombinant mutated POP Tc80 in 25 mM Tris-HCl 5 mM DTT pH 8.0 with 6.25-150 μ M, N-Suc-Gly-Pro-Leu-Gly-Pro-AMC. AMC release was recorded up to 30 min at 460 nm upon excitation at 355 nm in a 96-well microplate fluorescence reader (FL600; Bio-Tek Instruments, Inc.) at 25 °C. Active enzyme concentration was determined by titration with a chloromethylketone irreversible inhibitor of POP Tc80 [16]. K_m and V_{max} were determined by hyperbolic regression according to Cornish-Bowden [27]. The k_{cat} was calculated by $k_{cat}=V_{max}/[E]_0$, where $[E]_0$ represents active enzyme.

Results and discussion

Target for the model validation strategy

Since it seems that inter-domain flexibility is required for the POP Tc80-specific binding of large substrates [16], a simple validation strategy was performed to determine point mutations that would prevent this flexibility according to the model and subsequently testing the mutants' activity. According to our model [16], the propeller domain of POP Tc80 has a cysteine (Cys255) which is not involved in a disulfide bond while being located at a favorable position for forming such bond with hydrolase domain residues. This event would certainly rigidify the whole protein structure, interfering with the model-predicted ligand binding induced-fit process.

Stability of the 3D model and selection of amino acids relevant for mutation

The protein backbone root mean square deviation (RMSD) fluctuations during MD show that a ~ 3 Å plateau is reached after 3 ns of simulation. Additionally, POP Tc80 secondary structure elements were all conserved during the 5 ns dynamics. Therefore, we could consider the model as stable before proceeding to further analysis regarding Cys255 neighbourhood.

During the MD trajectory, we searched for hydrolase domain residues having their side chain $C\beta$ atom located less than 10 Å away from Cys255 $S\gamma$, and identified 5 residues: Phe470, Asn471, Ala588, Trp589 and Ser591. As the two aromatic residues were featuring internally-stabilizing π - π stacking interactions, we decided not to mutate them because the hydrolase secondary structure could change as a side effect. We therefore modelled three single-residue mutated enzymes: Asn471Cys, Ala588Cys and Ser591Cys (Fig.1).

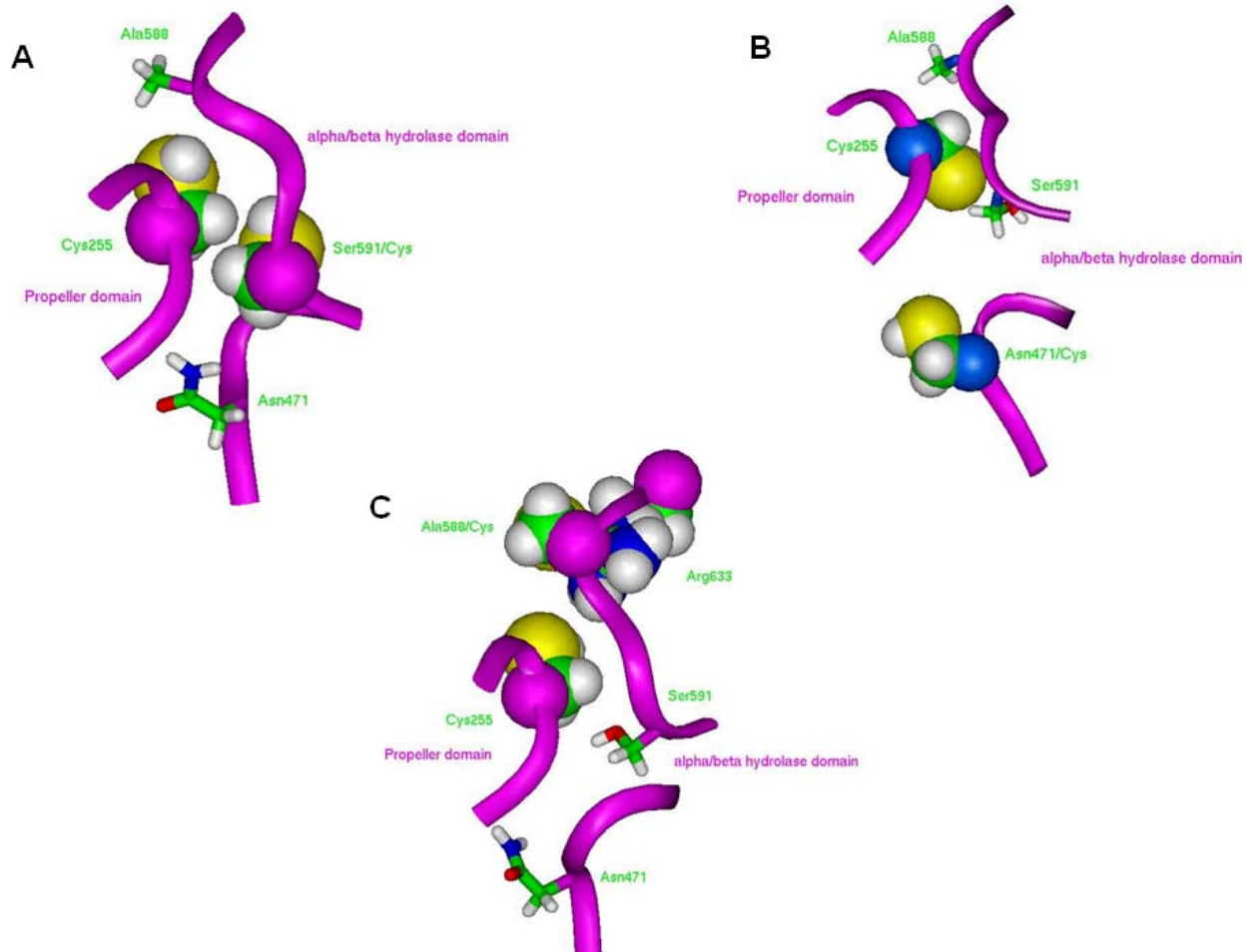


Figure 1: Molecular dynamics simulations of POP Tc80 and its mutants. The figure shows the relative position of the (A) Ser591/Cys, (B) Asn471/Cys and (C) Ala588/Cys side chains in respect with the Cys255 one.

MD revealed that both Asn471Cys and Ser591Cys featured a stable Cys*-Cys255 disulfide bridge, the Ser591Cys one being stronger (S_{γ} - S_{γ} distance ~ 5 Å vs. ~ 8 Å). Ala588Cys exhibited a different behavior as the Cys588* side chain rather moved toward hydrolase domain Arg633 guanidinium side chain, forming a ~ 5 Å salt bridge (Fig.1) This result was unexpected at the modelling stage, but is not abnormal as the statistical distribution of Cys-Arg side chain distances in proteins features a peak around 4.5-5 Å [28]. As a consequence, according to the models, the hydrolase-propeller structure is more open in the Ala588Cys mutant than with wild-type POP Tc80, possibly facilitating a gating mechanism-supported ligand binding. On the contrary and as planned, the Asn471Cys and Ser591Cys mutants are constrained in a partly-closed state by the mutation-induced disulfide bond, hindering ligand access to the catalytic site.

Activity of the mutated enzymes

To support our previously POP Tc80 structural analysis [16], which suggests an opening of the enzyme domains to substrate entrance, three site-directed mutants was generated in order to form disulfide bond between its two domain. This disulfide bond would render the enzyme into a closed state, preventing the accessibility of its substrate.

Since bacterial cytoplasm is a naturally reducing environment, recombinant proteins expressed in these organisms rarely present disulfide bridges [29]. Thus, to ensure the disulfide bridges formation between Cys255 and Cys originated from site-directed mutagenesis of Asn471, Ala588 or Ser591, the enzyme variants were treated with oxidizing agents. Other important factor to disulfide bridges formation is the milieu

pH once the ionization of thiol group occurs under pHs above of Cys pKa [17]. Thus, the oxidation of the POP Tc80 and their mutants was tested at different alkaline pHs either by GSSG or by oxygen peroxide in order to promote the Cys reactivity. However, in the presence of the oxidizing agents and at pHs higher than 8, the WT enzyme started to decrease its activity, probably due to a toxic effect of these agents on the enzyme (data not shown). Hence, all the tests to disulfide bridges formation between the domains of POP Tc80 were carried out at pH 8, enough to reactivate the Cys without affect the activity of the control enzyme

In the presence of GSSG, the enzyme activity of the Ser591Cys mutant was almost abolished showing only 10% of WT activity, while the Asn471Cys retained approximately 20%. On the opposite, the Ala588Cys mutant presented a slight activity increase of 20% compared to wild-type POP Tc80 (Fig. 2). In all cases, wild-type-like activities were restored upon DTT treatment. The inability of Ser591Cys and Asn471Cys to cleave the substrate when oxidized was due to the formation of disulfide bond between the domains and not to the reaction of other cysteines of POP Tc80. This follows from the control experiment where WT retains its ability to hydrolyze the substrate even in the presence of oxidizing reagents. Taken together, these observations correlate with the behavior comparison between models of POP Tc80 and its mutants upon MD simulations.

Similar values were obtained when the same activity assays were carried out using oxygen peroxide as oxidizing agents (Fig. 3). It shows that the effects on POP Tc80 variant activity were not due to an intrinsic feature, inhibitory or enhancer, on the enzyme, but to the formation of disulfide bridge between the domains of Ser591Cys and Asn471Cys POP Tc80 mutated forms or salt bridge of Ala588 one.

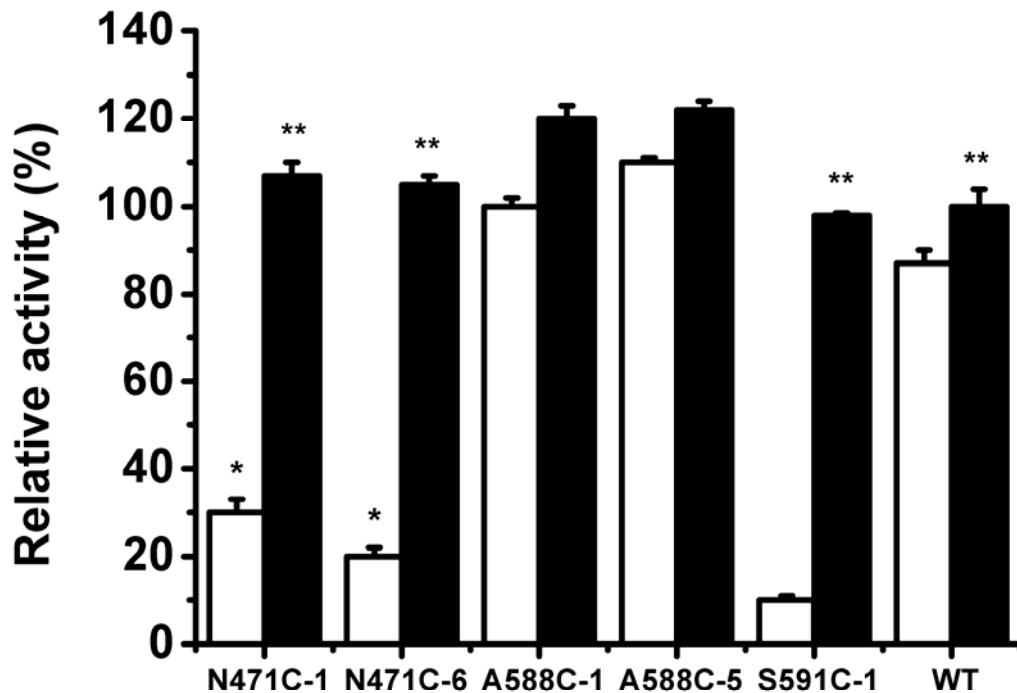


Figure 2: Disulfide bond formation with GSSG and its effect on the activity of POP Tc80 and its mutants. POP Tc80 and its mutants were oxidized with 1mM GSSG (empty bars). To reverse the effect of GSSG, the enzymes were treated with 5mM DTT (filled bars). The activities were calculated using the value of reduced WT as the maximum. * $p < 0.05$ for the S591C oxidized variant compared to N471C ones. ** $p < 0.05$ for the A588C reduced variants compared to the others reduced forms (N471C, S591C and WT).

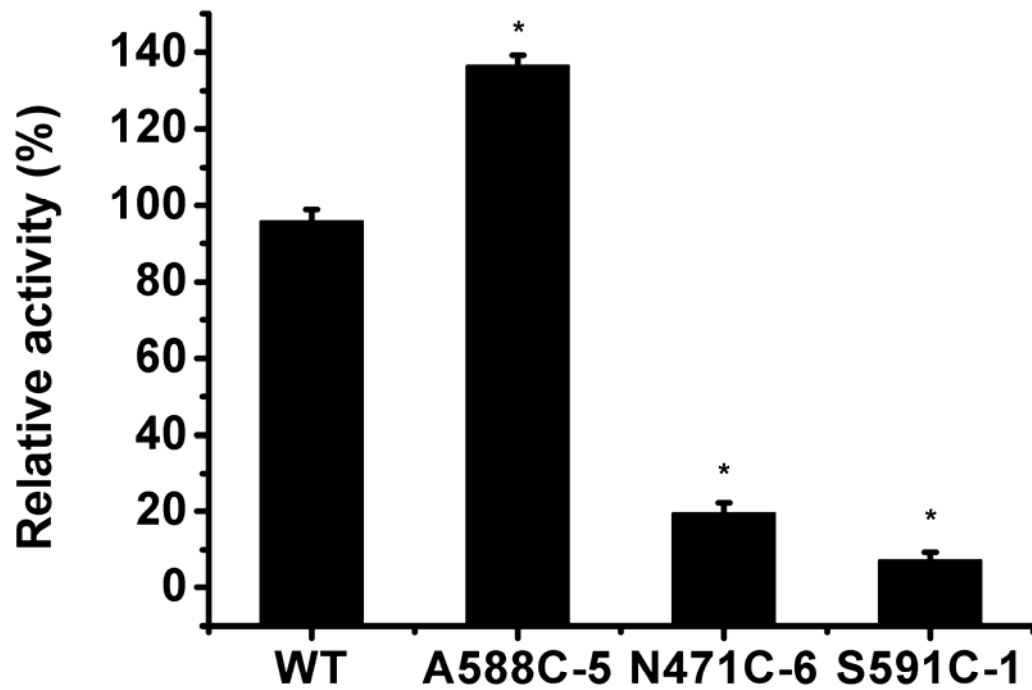


Figure 3: Disulfide bond formation with H₂O₂ and its effect on the activity of POP Tc80 and its mutants. POP Tc80 and its mutants were previously treated with 5 mM DTT and then incubated with the buffer reaction containing 10 mM H₂O₂ (empty bars) to the activity test. * p < 0.05 all variant forms compared to the control.

The kinetic profile of the active (DTT-treated) mutants (Table 1) showed no significant differences between the WT and Ser591Cys mutant parameters, although this mutant presented the highest loss of activity when oxidized. However, Ala588Cys mutation provoked a decrease of affinity (K_m 88.6) to the substrate and of its catalytic efficiency when compared to WT (K_{cat}/K_m 1.5 vs 3.5) although this mutant is the most active to cleave Suc-Gly-Pro-Leu-Gly-Pro-AMC among the POP Tc80 forms of this study. Ala588Cys MD simulation showed that its catalytic-propeller domain structure is more open, with its interface more exposed, what could be the cause of this kinetics differences. In addition, although the mutant Asn471Cys showed the same substrate affinity of the WT, it presented the lowest catalytic efficiency toward Suc-Gly-Pro-Leu-Gly-Pro-AMC.

Among the mutations carried out on POP Tc80, the Ser591Cys demonstrated be the best construction to explain the catalytic mechanism of the enzyme, since it seems to cause no changes in its structure, probed by kinetic analysis. Further experiments will be performed in order to verify the ability of these POP Tc80 mutated forms to cleave the collagen. However, the need of a movement of POP Tc80 domains to substrate entrance is better demonstrated by short substrates such as Suc-Gly-Pro-Leu-Gly-Pro-AMC than by the large ones, since short peptides could diffuse toward the catalytic pocket even in the rigid structure. Therefore, all results together showed that the enzyme with “closed” domains was not able to cleave the substrate confirming that the POP Tc80 has a flexible structure.

Table 1. Kinetic profile of POP Tc80 and its mutants

Enzyme	<i>K_m</i>	<i>K_{cat}</i>	<i>K_{cat}/K_m</i>
	(μM)	(sec^{-1})	($\text{sec}^{-1}/\mu\text{M}$)
WT	33.3 ± 3.36	108.9 ± 8.38	3.5 ± 0.3
A588C-6	88.6 ± 7.6	130.7 ± 3.07	$1.5 \pm 0,13$
N471C-5	33 ± 2.57	29.71 ± 1.57	0.9 ± 0.07
S591C-1	33.8 ± 1.83	108.9 ± 5.88	3.2 ± 0.17

Conclusions

The simulations and enzymatic results, coupled with existing POP studies, provide strong support for the hypothesis that the two domains of POP Tc80 can move relative to each other, allowing for an open state that facilitates the entry and binding of large substrates to the catalytic site. We demonstrated that mutations obstructing this mechanism might decrease POP Tc80 biological activity, and so could do tailored inhibitors. More importantly, the POP Tc80 structural model that we modeled earlier can now be considered as being validated by the mutagenesis experiments. This model is the first brick of future structure-based drug design strategies in which theoretical predictions, chemical synthesis and biological experiments will be attempted in synergy for discovering new anti-Chagas drugs.

Acknowledgements

This work was supported by CAPES, CNPq, FAPDF, FINEP and the grant N°1891.7 between CNRS and CNPq.

References

- [1] C. Chagas, Nova tripanozomíaze humana. Estudos sobre a morfologia e o ciclo evolutivo do *Schizotrypanum cruzi* n. gen., n. sp., agente etiológico de nova entidade morbida do homem. Mem. Inst. Oswaldo Cruz 1 (1909) 159-218.
- [2] N.M. El-Sayed, P.J. Myler, D.C. Bartholomeu, D. Daniel Nilsson, G. Aggarwal, A.-N. Tran, E. Ghedin, E.A. Worthey, A.L. Delcher, G. Blandin, S.J. Westenberger, E. Caler, G.C. Cerqueira, C. Branche, B. Haas, A. Anupama, E. Arner, L. Åslund, P. Attipoe, E. Bontempi, F. Bringaud, P. Burton, E. Cadag, D.A. Campbell, M. Carrington, J. Crabtree, H. Darban, J.F. da Silveira, P. de Jong, K. Edwards, P.T. Englund, G. Fazelina, T. Feldblyum, M. Ferella, A.C. Frasch, K. Gull, D. Horn, L. Hou, Y. Huang, E. Kindlund, M. Klingbeil, S. Kluge,

- H. Koo, D. Lacerda, M.J. Levin, H. Lorenzi, T. Louie, C.R. Machado, R. McCulloch, A. McKenna, Y. Mizuno, J.C. Mottram, S. Nelson, S. Ochaya, K. Osoegawa, G. Pai, M. Parsons, M. Pentony, U. Pettersson, M. Pop, J.L. Ramirez, J. Rinta, L. Robertson, S.L. Salzberg, D.O. Sanchez, A. Seyler, R. Sharma, J. Shetty, A.J. Simpson, E. Sisk, M.T. Tammi, R. Tarleton, S. Teixeira, S. van Aken, C. Vogt, P.N. Ward, B. Wickstead, J. Wortman, O. White, C.M. Fraser, K.D. Stuart, and B. Andersson, The genome sequence of *Trypanosoma cruzi*, etiologic agent of Chagas disease : Trypanosomatid genomes. *Science* 309 (2005) 409-415.
- [3] S.L. de Castro, The challenge of Chagas' disease chemotherapy : An update of drugs assayed against *Trypanosoma cruzi*. *Acta Trop.* 53 (1993) 83-98.
- [4] J.R. Coura, and S.L. de Castro, A critical review on Chagas disease chemotherapy. *Mem. Inst. Oswaldo Cruz* 97 (2002) 3-24.
- [5] J.A. Urbina, and R. Docampo, Specific chemotherapy of Chagas disease : controversies and advances. *Trends Parasitol.* 19 (2003) 495-501.
- [6] S.L. Croft, M.P. Barrett, and J.A. Urbina, Chemotherapy of trypanosomiasis and leishmaniasis. *Trends Parasitol.* 21 (2005) 508-512.
- [7] J.C.P. Dias, A.C. Silveira, and C.J. Schofield, The impact of Chagas disease control in Latin America - A review. *Mem. Inst. Oswaldo Cruz* 97 (2002) 603-612.
- [8] B. Pécoul, New drugs for neglected diseases : from pipeline to patients. *PLOS Med.* 1 (2004) 19-22.
- [9] J.M. Santana, P. Grellier, J. Schrével, and A.R.L. Teixeira, A *Trypanosoma cruzi*-secreted 80 kDa proteinase with specificity for human collagen types I and IV. *Biochem. J.* 325 (1997) 129-137.
- [10] P. Grellier, S. Vendeville, R. Joyeau, I.M. Dourado Bastos, H. Drobecq, F. Frappier, A.R.L. Teixeira, J. Schrével, E. Davioud-Charvet, C. Sergheraert, and J.M. Santana, *Trypanosoma cruzi* prolyl oligopeptidase Tc80 is involved in nonphagocytic mammalian cell invasion by trypomastigotes. *J. Biol. Chem.* 276 (2001) 47078-47086.
- [11] S. Vendeville, E. Buisine, X. Williard, J. Schrével, P. Grellier, J.M. Santana, and C. Sergheraert, Identification of inhibitors of an 80 kDa protease from *Trypanosoma cruzi* through the screening of a combinatorial peptide library. *Chem. Pharm. Bull.* 47 (1999) 194-198.
- [12] R. Joyeau, C. Maoulida, C. Guillet, F. Frappier, A.R.L. Teixeira, J. Schrével, J.M. Santana, and P. Grellier, Synthesis and activity of pyrrolidinyl- and thiazolidinyl-dipeptide derivatives as inhibitors of the Tc80 prolyl oligopeptidase from *Trypanosoma cruzi*. *Eur. J. Med. Chem.* 35 (2000) 257-266.
- [13] G. Bal, P. Van der Veken, D. Antonov, A.M. Lambeir, P. Grellier, S.L. Croft, K. Augustyns, and A. Haemers, Prolylisoxazoles: potent inhibitors of

- prolyl oligopeptidase with antitrypanosomal activity. *Bioorg Med Chem Lett* 13 (2003) 2875-8.
- [14] I. Brandt, S. Sharpé, and A.-M. Lambeir, Suggested function for prolyl oligopeptidases : A puzzling paradox. *Clin. Chim. Acta* 377 (2007) 50-61.
- [15] Y. Choe, L.S. Brinen, M.S. Price, J.C. Engel, M. Lange, C. Grisostomi, S.G. Weston, P.V. Pallai, H. Cheng, L.W. Hardy, D.S. Hartsough, M. McMakin, R.F. Tilton, C.M. Baldino, and C.S. Craik, Development of α -keto-based inhibitors of cruzain, a cysteine protease implicated in Chagas disease. *Bioorg. Med. Chem.* 13 (2005) 2141-2156.
- [16] I.M. Bastos, P. Grellier, N.F. Martins, G. Cadavid-Restrepo, M.R. de Souza-Ault, K. Augustyns, A.R. Teixeira, J. Schrevel, B. Maigret, J.F. da Silveira, and J.M. Santana, Molecular, functional and structural properties of the prolyl oligopeptidase of *Trypanosoma cruzi* (POP Tc80), which is required for parasite entry into mammalian cells. *Biochem J* 388 (2005) 29-38.
- [17] Z. Szeltner, D. Rea, T. Juhász, V. Renner, V. Fülöp, and L. Polgár, Concerted structural changes in the peptidase and the propeller domains of prolyl oligopeptidase are required for substrate binding. *J. Mol. Biol.* 340 (2004) 627-637.
- [18] M. Fuxreiter, C. Magyar, T. Juhász, Z. Szeltner, L. Polgár, and I. Simon, Flexibility of prolyl oligopeptidase : Molecular dynamics and molecular framework analysis of the potential substrate pathways. *Proteins* 60 (2005) 504-512.
- [19] L. Kalé, R. Skeel, M. Bhandarkar, R. Brunner, A. Gursoy, N. Krawetz, J. Phillips, A. Shinozaki, K. Varadarajan, and K. Schulten, NAMD2: greater scalability for parallel molecular dynamics. *J. Comp. Phys.* 151 (1999) 283-312.
- [20] J.C. Phillips, R. Braun, W. Wang, J. Gumbart, E. Tajkhorshid, E. Villa, C. Chipot, R.D. Skeel, L. Kalé, and K. Schulten, Scalable Molecular Dynamics with NAMD. *J. Comp. Chem.* 26 (2005) 1781-1802.
- [21] A.D. MacKerell Jr., D. Bashford, M. Bellott, R.L. Dunbrack, J.D. Evanseck, M.J. Field, S. Fischer, J. Gao, H. Guo, S. Ha, D. Joseph-McCarthy, L. Kuchnir, K. Kuczera, F.T.K. Lau, C. Mattos, S. Michnick, T. Ngo, D.T. Nguyen, B. Prodhom, W.E. Reiher, B. Roux, M. Schlenkrich, J.C. Smith, R. Stote, J. Straub, M. Watanabe, J. Wiórkiewicz-Kuczera, D. Yin, and M. Karplus, All-atom empirical potential for molecular modeling and dynamics studies of proteins. *J. Phys. Chem. B* 102 (1998) 3586-3616.
- [22] A.D. MacKerell Jr., M. Feig, and C.L. Brooks III, Extending the treatment of backbone energetics in protein force fields: Limitations of gas-phase quantum mechanics in reproducing protein conformational distributions in molecular dynamics simulations. *J. Comp. Chem.* 25 (2004) 1400-1415.
- [23] V. Fülöp, Z. Böcskel, and L. Polgár, Prolyl oligopeptidase : An unusual β -propeller domain regulates proteolysis. *Cell* 94 (1998) 161-170.



- [24] H.M. Berman, J. Westbrook, Z. Feng, G. Gilliland, T.N. Bhat, H. Weissig, I.N. Shindyalov, and P.E. Bourne, The Protein Data Bank. *Nucleic Acids Res.* 28 (2000) 235-242.
- [25] W. Humphrey, A. Dalke, and K. Schulten, VMD: visual molecular dynamics. *J. Mol. Graph.* 14 (1996) 33-38.
- [26] The 10 mM concentration was selected as the minimal requirement for observing significant effects on enzyme activity after a series of trials in the 1-100 mM range.
- [27] A. Cornish-Bowden, *Principles of enzyme kinetics*, Butterworths, London ; Boston, 1976.
- [28] J. Singh, and J.M. Thornton, *Atlas of protein side-chain interactions*, IRL press, Oxford, 1992.
- [29] K. Luersen, R.D. Walter, and S. Muller, *Plasmodium falciparum*-infected red blood cells depend on a functional glutathione de novo synthesis attributable to an enhanced loss of glutathione. *Biochem J* 346 Pt 2 (2000) 545-52.



IV. Nocaute do gene *poptc80* no *T. cruzi*

Estudos preliminares

IV. Nocaute do gene *poptc80* em *T. cruzi*

O genoma diplóide do *T. cruzi* contém aproximadamente 40 cromossomos codificando um conjunto predito de 22.570 proteínas, das quais pelo menos 12.570 representam pares de alelos (El-Sayed *et alli*, 2005). Cópias alélicas de genes no genoma híbrido CL-Brener podem variar na sua sequência em até 1,5%. Além disso, trissomias também foram sugeridas no caso de alguns cromossomos (Machado and Ayala, 2001; Obado *et alli*, 2005).

Funções putativas puderam ser atribuídas a 50,8% dos supostos genes codificadores de proteínas, com base em significativa similaridade com proteínas já caracterizadas ou com domínios funcionais conhecidos. Ao contrário do que é observado para os estudos *in silico* do genoma de *T. cruzi*, apenas 10 genes foram caracterizados experimentalmente por manipulação genética neste parasito (Ajioka and Swindle, 1996; Allaoui *et alli*, 1999; Annoura *et alli*, 2005; Barrio *et alli*, 2007; Caler *et alli*, 1998; Conte *et alli*, 2003; Cooper *et alli*, 1993; Gluenz *et alli*, 2007; MacRae *et alli*, 2006; Manning-Cela *et alli*, 2001; Wilkinson *et alli*, 2008).

Dado que a técnica de RNA de interferência, até o momento, falhou em *T. cruzi* (DaRocha *et alli*, 2004) - diferentemente do observado para os tripanossomos africanos (Bellofatto and Palenchar, 2008) - a estratégia de nocautear genes é mais uma ferramenta para a caracterização do grande número de genes que codificam proteínas com funções preditas ou até mesmo desconhecidas no genoma do *T. cruzi*. De uma forma geral, para a completa deleção do gene, as regiões 5' e 3' não traduzidas, do inglês UTR (Untranslated Region), representam as sequências alvos de recombinação, que permitem a substituição do alvo por um marcador de seleção como, por exemplo, uma resistência a antibiótico.

Devido à diploidia do parasito, um nocaute completo requer, em geral, dois turnos de deleção pelo uso de diferentes marcadores de seleção. Um fator decisivo para o sucesso do nocaute de um gene é o número de cópias que ele apresenta por genoma haplóide. Em geral, é praticamente inviável, em termos de resultado, nocautear um gene que apresenta mais de uma cópia por genoma. Visto que *poptc80* é um gene cópia única por genoma haplóide foi esquematizado a realização do seu nocaute e conseqüente silenciamento da POP Tc80 como forma de elucidar o papel desta enzima na patogenia da doença de Chagas. Além do mais, isto permitirá avaliar

e confirmar a especificidade e o efeito dos inibidores da POP Tc80 com eficiência em inibir a entrada de *T. cruzi* na célula hospedeira não fagocítica (Bastos *et alli*, 2005).

MATERIAIS E MÉTODOS

Parasitas e condições de cultura

Epimastigotas de *Trypanosoma cruzi* da cepa CL-Brener e Berenice foram cultivados em meio Liver Infusion Tryptone (LIT) suplementado com 5% (v/v) de soro fetal bovino inativado e 100 µg/mL de gentamicina a 28 °C. Após os testes de transfecção, os parasitos foram cultivados em meio condicionado acrescido do antibiótico de seleção G418 (100 µg/mL) nas mesmas condições descritas anteriormente. Denominou-se de meio condicionado àquele proveniente do sobrenadante de cultura de epimastigotas não transfectados suplementado com 20% de soro fetal bovino e previamente filtrado em membrana de 0,22 µm.

Extração de DNA genômico

O DNA genômico de epimastigotas das cepas CL-Brener ou Berenice foi extraído conforme procedimentos adaptados de Blin e Stafford (1976). O material foi aliquoteado e armazenado a -20 °C e, posteriormente, utilizado em reações de polimerização em cadeia (PCR). As PCRs foram realizadas para a construção do cassete contendo o gene *neo* e as UTRs 5' e 3' do gene *poptc80* e também para a confirmação da sua inserção nos parasitos transfectados, ratificando o nocaute do gene.

Preparação do cassete para nocaute de *poptc80*

A técnica utilizada para esta preparação foi baseada em (MacRae *et alli*, 2006). Os iniciadores para as UTRs de *poptc80* e para os genes contíguos foram desenhados a partir de sequências do genoma de *T. cruzi* depositadas em www.genedb.org. Os iniciadores para amplificação de *neo* foram desenhados a partir as sequência do plasmídeo *pcdna-neo*, o mesmo usado posteriormente como molde para amplificação do gene (Tabela 1). Os fragmentos das regiões 5'-UTR e

3'-UTR flanqueadoras do gene *poptc80* foram amplificadas utilizando-se os pares de iniciadores 1 e 2 ou 3 e 4 (10 pmol cada iniciador) com 80 ng de DNA genômico da cepa CL Brener, sob as seguintes condições:

95 °C por 4 min (1 ciclo)
95 °C por 1 min
60 °C por 45 s
74° C por 1 min
74°C por 10 min (1 ciclo)

} (30 ciclos)

Após amplificação de ambas as regiões, os produtos foram usados como moldes numa mesma reação de PCR para a formação de um híbrido, ou seja novo produto que contém as regiões 5' e 3'-UTRs ligadas por um pequeno fragmento com alguns sítios para enzimas de restrições de interesse. Este cassete preliminar foi clonado no vetor *pGEM-Teasy* gerando *pgem-utrpop*. O gene de resistência a neomicina, *neo*, foi amplificado com os iniciadores 5 e 6 e clonado no vetor *pgem-teasy – neo* e sua clonagem foi confirmada por sequenciamento.

Para a construção do cassete final que contém o gene *neo* flanqueado pelas regiões 5'- e 3'-UTRs de *poptc80*, o inserto de *neo* previamente digerido com *BglII* e *XhoI* foi ligado no vetor *pgem-utrpop* também digerido com as mesmas enzimas formando o vetor *pgem-poptc80-neo*. Este vetor foi digerido com *NotI* e o cassete liberado foi usado para a transfecção no *T. cruzi*.

Tabela 1. Sequência dos iniciadores usados na montagem do cassete *POPTc-NEO*.

	Iniciador	Sequência
1	5'UTR-Senso	5'gcggccgcGTGTTTCAATCTACCTGCCTGC 3' ^a
2	5'UTR-Antisenso	5' AGATCT AGTTTAAACG <u>CTCGAG</u> GGCCTTCCCCTTTTTTCCC 3' ^{b, c, d}
3	3'UTR-Senso	5' <u>CTCGAG</u> CGTTTAAACT AGATCT GTAATAAGGTGGACTGCTA 3' ^{b, c, d}
4	3'UTR-Antisenso	5'gcggccgcCGTTCGTTCCAAACACAAATATGG 3' ^a
5	NEO-Senso	5' <u>CTCGAG</u> ATGATTGAACAAGATGGATTGC 3' ^d
6	NEO-Antisenso	5' AGATCT TCAGAAGAACTCGTCAAGAAGG 3' ^b

^a As sequências em letra minúscula representam o sítio de restrição da enzima *NotI*.

^b As sequência em azul representam o sítio de restrição para enzima *BglII*.

^c As sequências em negrito representam os sítios de restrição para *DraI*.

^d As sequências sublinhadas e em itálico representam o sítio de restrição para enzima *XhoI*.

Transfecção do cassete *poptc80-neo* no *T. cruzi*

Para a transfecção, 3×10^8 parasitos foram coletados da cultura de formas epimastigotas CL-Brener, lavados três vezes com PBS e ressuspensos em 500 μ L de CITOMIX gelado (120 mM KCl; 0,15 mM CaCl_2 ; 10 mM K_2HPO_4 ; 25 mM HEPES; 2 mM EDTA; 5 mM MgCl_2 , pH 7,4). Cinquenta microgramas do cassete, previamente purificado, foram adicionados aos parasitos, seguidos de eletroporação com 3 pulsos de 400 μ F, 1,5 kV e resistência (Ω) ao infinito, em cubetas de 0,4 cm de espessura. Imediatamente após à eletroporação, as células foram colocadas em cultura e selecionadas por 6-8 semanas na presença do antibiótico G418 (neomicina; 100 μ g/mL).

Após seleção, os parasitos foram clonados em placas de 96 poços por diluição exaustiva a 5 ou 25 parasitos em 10 mL de meio de cultura (volume aproximado por placa). Neste processo foram realizadas três placas para cada diluição, utilizando meio de cultura condicionado. Desta forma, após aproximadamente dois meses em

cultura, foi possível isolar alguns clones para análise e confirmação da inserção do cassete *poptc80-neo*.

Análise por PCR dos parasitos mutantes

Para confirmar a deleção de ao menos um alelo de *poptc80* foram realizadas PCRs com diferentes pares de iniciadores (Tabela 1). Para isso, 2 μ L do extrato de formas epimastigotas de *T. cruzi* selvagem ou *poptc80*^{-/+}, ambos lisados com Tween-80 1% (v/v), foram utilizados como molde. O ciclo de amplificação foi desenvolvido de acordo com as características dos pares de iniciadores e os resultados foram analisados por eletroforese em gel de agarose, sendo o tamanho das bandas estimado com auxílio de marcadores de massa molecular.

RESULTADOS E DISCUSSÃO

Os iniciadores desenhados a partir do genoma sequenciado de CL-Brener (Figura IV.1A) foram capazes de amplificar as regiões UTRs do gene *poptc80* da própria cepa CL-Brener (Figura IV.1B) e também dos isolados Tulahuén e Berenice (não mostrado), indicando que não há polimorfismo na região dos iniciadores entre estes isolados ou, se existe, não é o suficiente para impedir a amplificação nas condições testadas.

O produto de PCR de ambas as UTRs foi submetido a uma nova PCR (Figura IV.1C) gerando um único fragmento contendo as regiões 5'-UTR e 3'-UTR do gene *poptc80* (Figura IV.1D). O próximo passo foi o de inserir o gene de resistência à neomicina entre a região 5'- e 3'- UTR, previamente clonadas, resultando na formação completa do vetor com o cassete *poptc80-neo* (Figura IV.1E) que posteriormente foi sequenciado. Com esta etapa concluída, o cassete *neo* foi excisado do seu vetor de clonagem e utilizado para a eletroporação dos parasitos.

Após a eletroporação, os parasitos foram tratados com meio LIT por 48 h, sem o antibiótico de seleção, permitindo 4 ciclos de crescimento completo. Depois disso, o antibiótico de seleção G418 foi adicionado ao meio e os parasitos transfectados foram selecionados por 8 semanas antes da clonagem. É importante ressaltar que o controle teve o mesmo tratamento que os parasitos *poptc80*^{-/+}, exceto no momento

da eletroporação, onde não havia o cassete *poptc80-neo* na solução incubada com os parasitos.

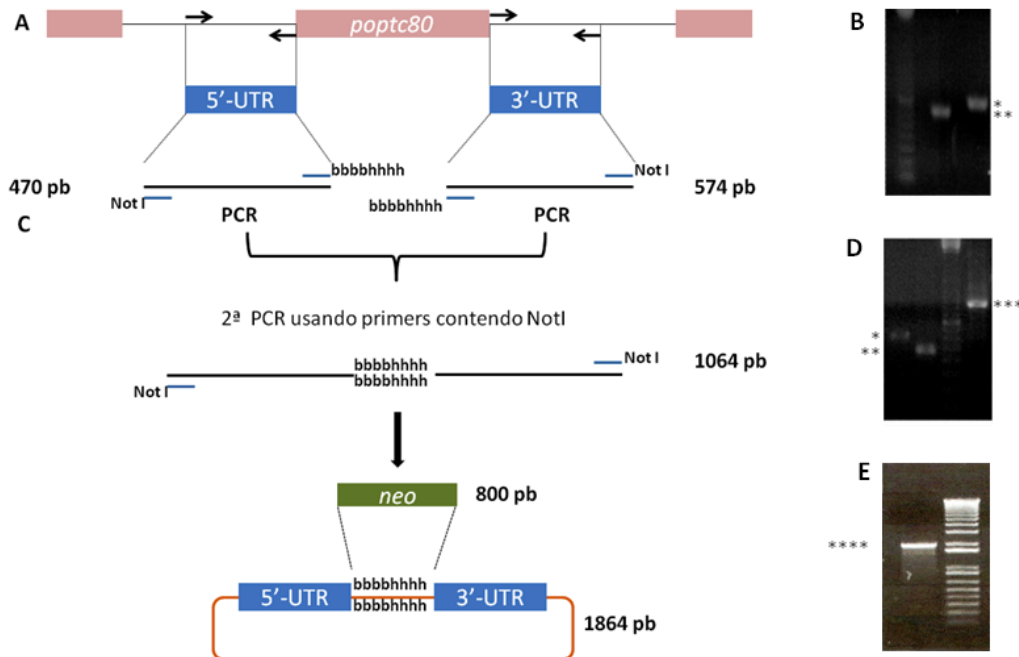


Figura IV.1. Produção do cassete para nocaute do gene da POP Tc80. A, setas indicam a posição dos iniciadores desenhados a partir das sequências das UTRs de *poptc80*. B, gel de agarose com os produtos amplificados usando os iniciadores do esquema em A com DNA genômico de epimastigotas CL-Brener. C, estratégia de clonagem. D, ampliações das UTRs do gene *poptc80* usando a estratégia em C e DNA genômico. E, amplificação do cassete *poptc-neo* usando o *pgem-poptc80-neo* como molde. M, marcador 100pb Ladder; 5', 5'UTR de *poptc80*; 3', 3'UTR de *poptc80*. (* - 470 pb; ** - 574 pb; *** - 1064 pb; **** - 1864 pb)

Os parasitos selecionados foram clonados e os clones obtidos tiveram sua cultura ampliada para assim, proceder com a análise quantitativa e qualitativa. Esta clonagem foi realizada em meio de cultura condicionado, o qual contém substâncias solúveis liberadas pelo próprio parasito que estimulam o seu crescimento e a amplificação da cultura. Evidentemente, este meio condicionado foi previamente filtrado para evitar a contaminação dos parasitos transfectados com selvagens. Durante esse cultivo, sempre sob a pressão do antibiótico G418, foram observados diferentes padrões de crescimento, como por exemplo, clones que morriam após

pouco tempo em cultura, inviabilizando sua análise. Os clones “sobreviventes” foram submetidos a PCR para confirmar a inserção do cassete *poptc80-neo* na região desejada e, conseqüentemente, o nocaute simples do gene *poptc80*.

Conforme observações prévias por meio de análise *in silico* das sequências disponíveis contidas no genoma da cepa CL-Brener, o gene *poptc80* estaria representado por somente um alelo enquanto o outro alelo contém um pseudogene da POP Tc80. Isto poderia significar que apenas um turno de nocaute seria suficiente para anular o gene *poptc80*. Para verificar isso experimentalmente, foi realizada uma PCR com DNA genômico extraído dos clones e iniciadores específicos que amplificam o gene *poptc80*. Um fragmento com tamanho do gene *poptc80* (2040 pb) foi amplificado em todos os clones testados (Figura IV.2), indicando que a deleção provavelmente ocorreu em um só alelo e que o outro ainda está presente, uma vez que os iniciadores testados não anelariam nas extremidades do pseudogene para POP Tc80.

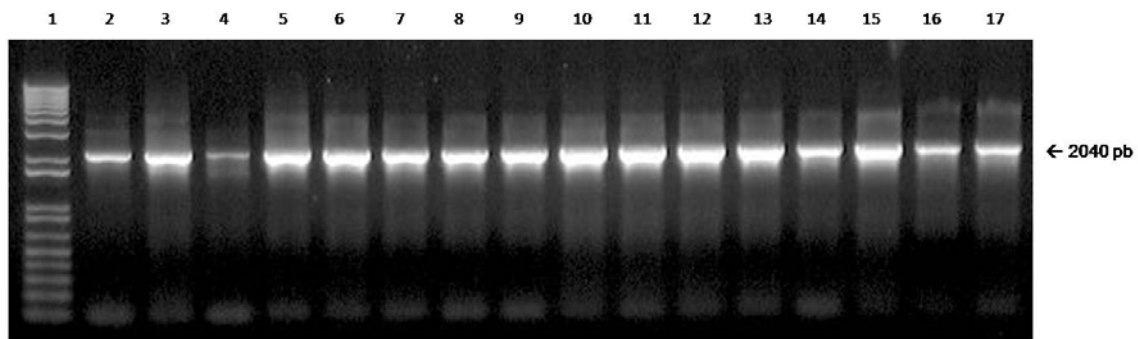


Figura IV.2. Presença do gene *poptc80* em epimastigotas clonados após primeiro turno de nocaute. A PCR foi realizada com iniciadores senso e anti-senso do gene *poptc80*. Poços: 1 – Marcador 1Kb DNA ladder; 2-Controle positivo (DNA genômico extraído previamente); 3 – Controle positivo (*poptc80* clonado em pGEM); 4 -17, clones do nocaute (*poptc80*-/+).

Para confirmar se houve a substituição do gene *poptc80* pelo *poptc80-neo* e validar o nocaute simples, foram realizadas PCRs seguindo as seguintes combinações de iniciadores:

- I. iniciador senso que anela na extremidade 5' de *neo* com iniciador antisense que anela na região 3'-UTR do gene *poptc80*
- II. iniciador senso que anela na região 5'-UTR de *poptc80* com iniciador antisense que anela na extremidade 3' do gene *neo*
- III. iniciadores senso e antisense de *neo*.

Como observado na figura 3, todos os clones testados indicam que houve recombinação homóloga entre o cassete transfectado e as regiões UTRs de *poptc80*, com conseqüente substituição deste por *poptc80-neo*.

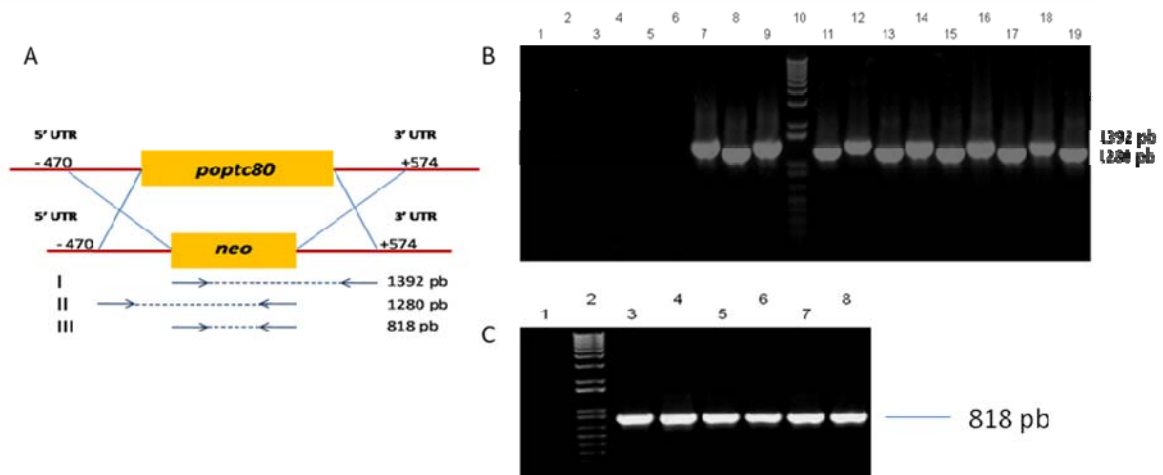


Figura IV.3. Substituição de um alelo do gene *poptc80* pelo gene *neo* no *T. cruzi* submetido a nocaute. A, esquema dos iniciadores usados para confirmação da substituição de um alelo do gene *poptc80*. B, PCR utilizando os jogos de iniciadores I e II; 1, 3, 5, 7, 9, 12, 14, 16 e 18 correspondem a amplificação I de Berenice selvagem, CL-Brener selvagem 1, CL-Brener selvagem 2 e dos clones 1, 2, 3, 4, 5 e 6, respectivamente. 2, 4, 6, 8, 10, 13, 15, 17 e 19 correspondem a amplificação II de Berenice selvagem, CL-Brener selvagem 1, CL-Brener selvagem 2 dos clones 1, 2, 3, 4, 5 e 6, respectivamente. 10, marcador 1 Kb DNA ladder. C, amplificação III; 1, controle CL-Brener selvagem; 3 a 8, clones 1 a 6, respectivamente; 2, marcador 1Kb DNA ladder.

De acordo com o genoma sequenciado de *T. cruzi*, o gene *poptc80* está localizado entre dois genes: histidina amônia-liase (*hlys*) e o gene hipotético de

código sistemático Tc00.1047053506247.240. Para corroborar a ocorrência do nocaute, foram desenhados iniciadores nas extremidades destes genes para serem utilizados em experimentos de PCR com a seguinte organização:

- I. um iniciador senso que se anela da região 5' do gene *neo* e um antisenso que se anela na região 5' do gene hipotético
- II. um iniciador senso que se anela na região 3' do gene *hlys* e um antisenso que se anela na região 3' do gene *neo*

Novamente houve amplificação dos fragmentos de tamanho esperado para os clones *poptc80*^{-/+}. Esta amplificação não ocorreu nas PCRs dos controles, onde o molde foi o DNA oriundo de epimastigotas não-tranfectados. Esses resultados confirmam que um alelo do gene *poptc80* sofreu recombinação homóloga e foi substituído por *poptc80*-*neo*, no entanto ainda resta uma cópia do referido gene.

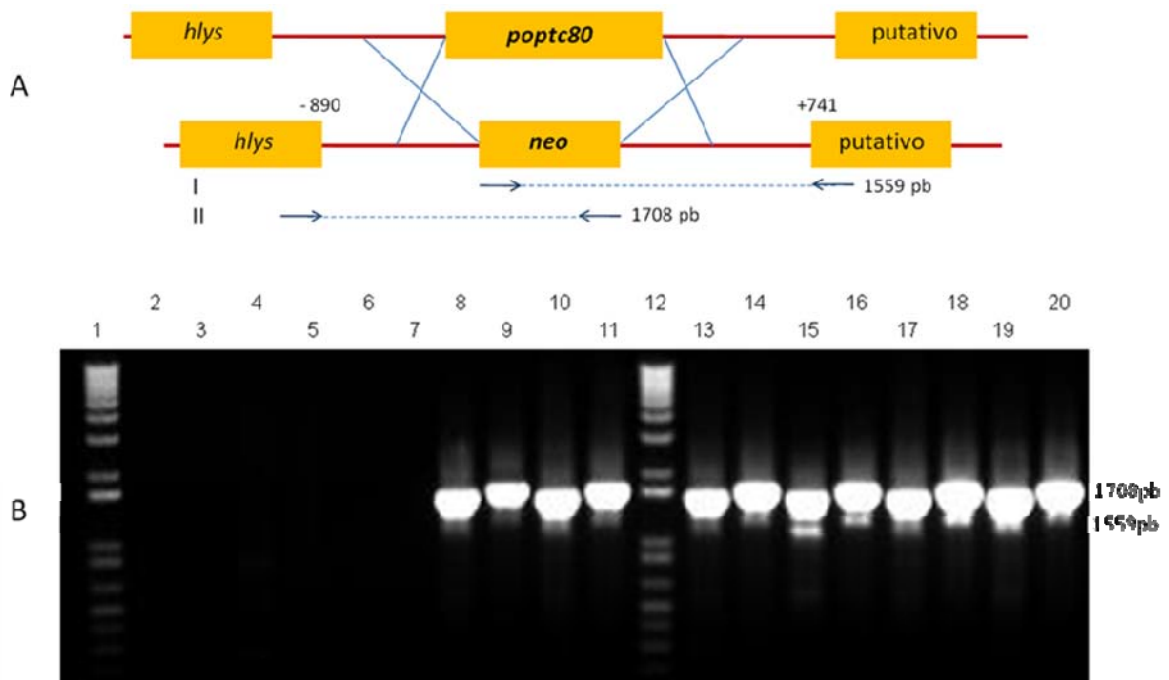


Figura IV.4. Confirmação da inserção do gene *neo* entre a região dos dois genes contíguos à *poptc80* com consequente deleção do gene *poptc80*. 2, 4, 6, 8, 10, 13, 15, 17, e 19 correspondem a amplificação I de Berenice selvagem, CL-Brener selvagem 1, CL-Brener selvagem 2 e dos clones 1, 2, 3, 4, 5 e 6, respectivamente. 3, 5, 7, 9, 11, 14, 16, 18 e 20 correspondem a amplificação II de Berenice selvagem, CL-Brener selvagem 1, CL-Brener selvagem 2 e dos clones 1, 2, 3, 4, 5 e 6, respectivamente. 12, marcador 1 Kb DNA ladder.

Durante o processo de clonagem foi observado que vários clones, selecionados das placas de 96 poços, pararam de crescer após serem repicados em frascos com volumes de 2 mL, mesmo com meio condicionado. Apesar da inviabilidade de alguns clones, foi possível notar por simples observação da cultura em microscópio invertido, que alguns parasitos apresentavam alterações em sua morfologia. Uma análise mais refinada em microscópio confocal será realizada, com a observação do número de núcleos, cinetoplastos e flagelos por parasito, além de outros aspectos de sua morfologia geral. A construção de um outro cassete contendo gene de resistência para higromicina para obtenção do duplo nocaute já está em andamento. O duplo nocaute de *poptc80* permitirá avaliar o papel deste gene na capacidade do *T. cruzi* de infectar células hospedeiras de mamíferos *in vitro* e posteriormente, animais *in vivo*.



CONCLUSÕES

Conclusões

O conjunto de experimentos realizados neste trabalho nos permite concluir que:

I. Aspectos estruturais da OPBTc:

- A OPBTc é uma enzima dimérica e sua dimerização é resistente ao tratamento com DTT e NaCl e diferentes pHs;
- No teste com substrato N-Suc-Gly-Gly-Arg, a presença de sal, no tampão de reação, diminuiu a atividade da enzima. No entanto, os espectros de dicroísmo circular na região do UV-próximo não mostraram alterações em sua estrutura terciária;
- A atividade da OPBTc é sensível a pHs mais ácidos (pH 6,0 - 4,0). Experimentos de fluorescência intrínseca e dicroísmo circular na região do UV-próximo mostraram que pHs mais ácidos afetam a estrutura da enzima, o que poderia explicar sua perda de atividade;
- A enzima mantém sua atividade até 50 °C. Acima desta temperatura, a OPBTc perde sua estrutura terciária e tende a agregar. Porém; a estrutura secundária da OPBTc é resistente a desnaturação térmica.

II. Estudo da prolil oligopeptidase de *T. brucei*:

- A POPTb é capaz de clivar colágeno nativo e semi-purificado; além de hormônios que são desregulados na doença do sono;
- Inibidores específicos para a POP Tb inibem o crescimento de formas sanguíneas;
- A POPTb é expressa em maior quantidade nas formas procíclicas do que nas formas sanguíneas do parasito;
- A POPTb está presente na sua forma ativa no plasma de camundongos infectados por *T. brucei* e esta atividade acompanha a parasitemia.

III. Elucidação do mecanismo catalítico da POP Tc80:

- Experimentos de dinâmica molecular mostraram que a cadeia lateral dos resíduos de cisteína inseridos nos mutantes Ser591Cys e o Asn491Cys está em posição favorável para formação da ponte dissulfeto com o resíduo Cys255 do domínio β -propeller;
- A mutação Ala588Cys não promoveu a formação de ponte dissulfeto com Cys255. A cadeia lateral dos resíduos Ala588Cys fica em posição favorável para formar uma ponte de sal com Arg633 o que resulta num aumento da atividade quando comparada à enzima original;
- Os mutantes Ser591Cys e o Asn491Cys quando tratados com GSSG ou H₂O₂ foram incapazes de clivar o substrato N-Suc-Gly-Pro-Leu-Gly-Pro-AMC confirmando a necessidade do movimento entre os domínios para entrada do substrato, corroborando o nosso modelo teórico.

IV. Nocaut do gene *poptc80* no *T. cruzi*:

- O cassete contendo o gene de resistência à neomicina foi corretamente inserido no genoma do *T. cruzi*;
- Após o primeiro turno do nocaut, o parasito apresentou em seu genoma; outro alelo do gene da *poptc80*, indicando que ocorreu nocaut simples de *poptc80*.



PERSPECTIVAS

Perspectivas

Nossos dados nos permitem propor algumas perspectivas no intuito de complementar e aprofundar o que foi apresentado neste trabalho.

No caso da OPBTc, realizaremos estudos comparativos de bioinformática utilizando sua sequência primária de aminoácidos na tentativa de encontrar possíveis domínios que possam ser responsáveis pela dimerização da enzima. Estes domínios serão deletados ou mutados e o comportamento da enzima será analisado pelas mesmas técnicas de estudos estruturais e enzimáticos aplicadas neste trabalho. Além disso, tentaremos cristalizar e resolver estrutura da enzima de forma a utilizá-la como uma ferramenta de auxílio na busca de inibidores específicos para a mesma.

Frente à dificuldade de cultivo de *T. brucei* em nosso laboratório, continuaremos este trabalho em colaboração com Prof. Grellier. Nossa intenção é de testar a capacidade do parasito em atravessar um modelo artificial de barreira hemato-encefálica, *in vitro* e analisar a função hormonal no plasma de ratos infectados tratados ou não com inibidores de POPTb. Finalmente, o nocaute de *poptb* será decisivo para instituir o papel da enzima na viabilidade do parasito e/ou no estabelecimento da infecção e dos sintomas da doença do sono.

A modelagem da POPTc 80 será usada como base para varredura virtual de bibliotecas de inibidores sintéticos e aqueles com melhor *score* serão testados *in vitro*, sobre a enzima e o parasito e em modelo animal da doença de Chagas, *in vivo*. Essa modelagem juntamente com a elucidação completa do mecanismo catalítico da enzima será de grande importância para o desenvolvimento de inibidores terapêuticos.

Por fim, daremos prosseguimento ao nocaute da POP Tc80 com a construção e transfecção do segundo cassete contendo o gene de resistência a higromicina flanqueado pelas 5' e 3' UTRs de *poptc80*, para a obtenção do duplo nocaute. Após a confirmação do mutante nulo para *poptc80*, partiremos para os estudos morfológicos e de viabilidade do parasito. Os mutantes serão diferenciados em tripomastigotas e sua capacidade de infecção será testada *in vitro* e *in vivo*. Durante toda a caracterização, iremos também analisar o parasito com nocaute simples de forma comparativa com o duplo nocaute. Isso ajudará a compreender como o parasito regula a expressão de *poptc80* e de outro(s) gene(s) para adaptar-se a sua nova condição.



REFERÊNCIAS BIBLIOGRÁFICAS

Referências Bibliográficas

1. Ajioka, J. and Swindle, J. (1996) The calmodulin-ubiquitin (CUB) genes of *Trypanosoma cruzi* are essential for parasite viability, *Mol Biochem Parasitol*, 78, 217-225.
2. Allaoui, A., Francois, C., Zemzoumi, K., Guilvard, E. and Ouaisi, A. (1999) Intracellular growth and metacyclogenesis defects in *Trypanosoma cruzi* carrying a targeted deletion of a Tc52 protein-encoding allele, *Mol Microbiol*, 32, 1273-1286.
3. Ammor, M.S. (2007) Recent advances in the use of intrinsic fluorescence for bacterial identification and characterization, *J Fluoresc*, 17, 455-459.
4. Andrews, N.W. and Whitlow, M.B. (1989) Secretion by *Trypanosoma cruzi* of a hemolysin active at low pH, *Mol Biochem Parasitol*, 33, 249-256.
5. Annoura, T., Nara, T., Makiuchi, T., Hashimoto, T. and Aoki, T. (2005) The origin of dihydroorotate dehydrogenase genes of kinetoplastids, with special reference to their biological significance and adaptation to anaerobic, parasitic conditions, *J Mol Evol*, 60, 113-127.
6. Ault, S.K. (2007) Pan American Health Organization's Regional Strategic Framework for addressing neglected diseases in neglected populations in Latin America and the Caribbean, *Mem Inst Oswaldo Cruz*, 102 Suppl 1, 99-107.
7. Bakker, B.M., Westerhoff, H.V. and Michels, P.A. (1995) Regulation and control of compartmentalized glycolysis in bloodstream form *Trypanosoma brucei*, *J Bioenerg Biomembr*, 27, 513-525.
8. Bal, G., Van der Veken, P., Antonov, D., Lambeir, A.M., Grellier, P., Croft, S.L., Augustyns, K. and Haemers, A. (2003) Prolylisoaxazoles: potent inhibitors of prolyl oligopeptidase with antitrypanosomal activity, *Bioorg Med Chem Lett*, 13, 2875-2878.
9. Barrett, A.J. and McDonald, J.K. (1986) Nomenclature: protease, proteinase and peptidase, *Biochem J*, 237, 935.
10. Barrett, A.J. and Rawlings, N.D. (1992) Oligopeptidases, and the emergence of the prolyl oligopeptidase family, *Biol Chem Hoppe Seyler*, 373, 353-360.
11. Barrett, A.J., Rawlings, N.D. and O'Brien, E.A. (2001) The MEROPS database as a protease information system, *J Struct Biol*, 134, 95-102.
12. Barrett, M.P., Boykin, D.W., Brun, R. and Tidwell, R.R. (2007) Human African trypanosomiasis: pharmacological re-engagement with a neglected disease, *Br J Pharmacol*, 152, 1155-1171.

13. Barrio, A.B., Van Voorhis, W.C. and Basombrio, M.A. (2007) *Trypanosoma cruzi*: attenuation of virulence and protective immunogenicity after monoallelic disruption of the cub gene, *Exp Parasitol*, 117, 382-389.
14. Barry, J.D. and McCulloch, R. (2001) Antigenic variation in trypanosomes: enhanced phenotypic variation in a eukaryotic parasite, *Adv Parasitol*, 49, 1-70.
15. Bastos, I.M., Grellier, P., Martins, N.F., Cadavid-Restrepo, G., de Souza-Ault, M.R., Augustyns, K., Teixeira, A.R., Schrevel, J., Maigret, B., da Silveira, J.F. and Santana, J.M. (2005) Molecular, functional and structural properties of the prolyl oligopeptidase of *Trypanosoma cruzi* (POP Tc80), which is required for parasite entry into mammalian cells, *Biochem J*, 388, 29-38.
16. Bastos, I.M.D. (2003) Prolil Oligopeptidases de *Trypanosoma cruzi* e *Trypanosoma brucei* compartilham propriedades genéticas, estruturais e funcionais. Pós-graduação em Patologia Molecular. Universidade de Brasília, Brasília.
17. Bellofatto, V. and Palenchar, J.B. (2008) RNA interference as a genetic tool in trypanosomes, *Methods Mol Biol*, 442, 83-94.
18. Brener, Z., Andrade, Z.A. and Barral-Neto, M. (2000) *Trypanosoma cruzi* e doença de Chagas. Ed. Guanabara, Rio de Janeiro.
19. Burleigh, B.A. and Andrews, N.W. (1995) A 120-kDa alkaline peptidase from *Trypanosoma cruzi* is involved in the generation of a novel Ca²⁺-signaling factor for mammalian cells, *J Biol Chem*, 270, 5172-5180.
20. Burleigh, B.A. and Andrews, N.W. (1998) Signaling and host cell invasion by *Trypanosoma cruzi*, *Curr Opin Microbiol*, 1, 461-465.
21. Burleigh, B.A., Caler, E.V., Webster, P. and Andrews, N.W. (1997) A cytosolic serine endopeptidase from *Trypanosoma cruzi* is required for the generation of Ca²⁺ signaling in mammalian cells, *J Cell Biol*, 136, 609-620.
22. Caler, E.V., Morty, R.E., Burleigh, B.A. and Andrews, N.W. (2000) Dual role of signaling pathways leading to Ca²⁺ and cyclic AMP elevation in host cell invasion by *Trypanosoma cruzi*, *Infect Immun*, 68, 6602-6610.
23. Caler, E.V., Vaena de Avalos, S., Haynes, P.A., Andrews, N.W. and Burleigh, B.A. (1998) Oligopeptidase B-dependent signaling mediates host cell invasion by *Trypanosoma cruzi*, *EMBO J*, 17, 4975-4986.
24. Camargo, A.C., Caldo, H. and Reis, M.L. (1979) Susceptibility of a peptide derived from bradykinin to hydrolysis by brain endo-oligopeptidases and pancreatic proteinases, *J Biol Chem*, 254, 5304-5307.

25. Cazzulo, J.J. (2002) Proteinases of *Trypanosoma cruzi*: potential targets for the chemotherapy of Chagas disease, *Curr Top Med Chem*, 2, 1261-1271.
26. Chang, K.P. and McGwire, B.S. (2002) Molecular determinants and regulation of *Leishmania* virulence, *Kinetoplastid Biol Dis*, 1, 1.
27. Clayton, C. and Hotz, H.R. (1996) Post-transcriptional control of PARP gene expression, *Mol Biochem Parasitol*, 77, 1-6.
28. Coetzer, T.H., Goldring, J.P. and Huson, L.E. (2008) Oligopeptidase B: a processing peptidase involved in pathogenesis, *Biochimie*, 90, 336-344.
29. Conte, I., Labriola, C., Cazzulo, J.J., Docampo, R. and Parodi, A.J. (2003) The interplay between folding-facilitating mechanisms in *Trypanosoma cruzi* endoplasmic reticulum, *Mol Biol Cell*, 14, 3529-3540.
30. Cooper, R., de Jesus, A.R. and Cross, G.A. (1993) Deletion of an immunodominant *Trypanosoma cruzi* surface glycoprotein disrupts flagellum-cell adhesion, *J Cell Biol*, 122, 149-156.
31. Coppens, I. and Courtoy, P.J. (2000) The adaptative mechanisms of *Trypanosoma brucei* for sterol homeostasis in its different life-cycle environments, *Annu Rev Microbiol*, 54, 129-156.
32. Cuervo, P., Domont, G.B. and De Jesus, J.B. (2010) Proteomics of trypanosomatids of human medical importance, *J Proteomics*, 73, 845-867.
33. DaRocha, W.D., Otsu, K., Teixeira, S.M. and Donelson, J.E. (2004) Tests of cytoplasmic RNA interference (RNAi) and construction of a tetracycline-inducible T7 promoter system in *Trypanosoma cruzi*, *Mol Biochem Parasitol*, 133, 175-186.
34. Davies, D.R. (1990) The structure and function of the aspartic proteinases, *Annu Rev Biophys Biophys Chem*, 19, 189-215.
35. De Matos Guedes, H.L., Duarte Carneiro, M.P., de Oliveira Gomes, D.C., Rossi-Bergmann, B. and Giovanni De-Simone, S. (2007) Oligopeptidase B from *Leishmania amazonensis*: molecular cloning, gene expression analysis and molecular model, *Parasitol Res*, 101, 865-875.
36. Docampo, R. and Moreno, S.N. (1996) The role of Ca²⁺ in the process of cell invasion by intracellular parasites, *Parasitol Today*, 12, 61-65.
37. Donelson, J.E., Hill, K.L. and El-Sayed, N.M. (1998) Multiple mechanisms of immune evasion by African trypanosomes, *Mol Biochem Parasitol*, 91, 51-66.
38. El-Sayed, N.M., Myler, P.J., Bartholomeu, D.C., Daniel Nilsson, D., Aggarwal, G., Tran, A.-N., Ghedin, E., Worthey, E.A., Delcher, A.L., Blandin, G., Westenberger, S.J., Caler, E., Cerqueira, G.C., Branche, C., Haas, B., Anupama, A., Arner, E., Åslund, L., Attipoe, P., Bontempi, E., Bringaud, F., Burton, P.,

- Cadag, E., Campbell, D.A., Carrington, M., Crabtree, J., Darban, H., da Silveira, J.F., de Jong, P., Edwards, K., Englund, P.T., Fazelina, G., Feldblyum, T., Ferella, M., Frasch, A.C., Gull, K., Horn, D., Hou, L., Huang, Y., Kindlund, E., Klingbeil, M., Kluge, S., Koo, H., Lacerda, D., Levin, M.J., Lorenzi, H., Louie, T., Machado, C.R., McCulloch, R., McKenna, A., Mizuno, Y., Mottram, J.C., Nelson, S., Ochaya, S., Osoegawa, K., Pai, G., Parsons, M., Pentony, M., Pettersson, U., Pop, M., Ramirez, J.L., Rinta, J., Robertson, L., Salzberg, S.L., Sanchez, D.O., Seyler, A., Sharma, R., Shetty, J., Simpson, A.J., Sisk, E., Tammi, M.T., Tarleton, R., Teixeira, S., van Aken, S., Vogt, C., Ward, P.N., Wickstead, B., Wortman, J., White, O., Fraser, C.M., Stuart, K.D. and Andersson, B. (2005 a) The genome sequence of *Trypanosoma cruzi*, etiologic agent of Chagas disease : Trypanosomatid genomes, *Science*, 309, 409-415.
39. El-Sayed, N.M., Myler, P.J., Blandin, G., Berriman, M., Crabtree, J., Aggarwal, G., Caler, E., Renauld, H., Worthey, E.A., Hertz-Fowler, C., Ghedin, E., Peacock, C., Bartholomeu, D.C., Haas, B.J., Tran, A.N., Wortman, J.R., Alsmark, U.C., Angiuoli, S., Anupama, A., Badger, J., Bringaud, F., Cadag, E., Carlton, J.M., Cerqueira, G.C., Creasy, T., Delcher, A.L., Djikeng, A., Embley, T.M., Hauser, C., Ivens, A.C., Kummerfeld, S.K., Pereira-Leal, J.B., Nilsson, D., Peterson, J., Salzberg, S.L., Shallom, J., Silva, J.C., Sundaram, J., Westenberger, S., White, O., Melville, S.E., Donelson, J.E., Andersson, B., Stuart, K.D. and Hall, N. (2005 b) Comparative genomics of trypanosomatid parasitic protozoa, *Science*, 309, 404-409.
40. Engel, J.C., Doyle, P.S., Hsieh, I. and McKerrow, J.H. (1998 a) Cysteine protease inhibitors cure an experimental *Trypanosoma cruzi* infection, *J Exp Med*, 188, 725-734.
41. Engel, J.C., Doyle, P.S., Palmer, J., Hsieh, I., Bainton, D.F. and McKerrow, J.H. (1998 b) Cysteine protease inhibitors alter Golgi complex ultrastructure and function in *Trypanosoma cruzi*, *J Cell Sci*, 111 (Pt 5), 597-606.
42. Fernandes, L.C., Bastos, I.M., Lauria-Pires, L., Rosa, A.C., Teixeira, A.R., Grellier, P., Schrevel, J. and Santana, J.M. (2005) Specific human antibodies do not inhibit *Trypanosoma cruzi* oligopeptidase B and cathepsin B, and immunoglobulin G enhances the activity of trypomastigote-secreted oligopeptidase B, *Microbes Infect*, 7, 375-384.
43. Friedman, T.C., Orlowski, M. and Wilk, S. (1984) Prolyl endopeptidase: inhibition in vivo by N-benzyloxycarbonyl-prolyl-prolinal, *J Neurochem*, 42, 237-241.

44. Fülöp, V., Böcskel, Z. and Polgár, L. (1998) Prolyl oligopeptidase : An unusual β -propeller domain regulates proteolysis, *Cell*, 94, 161-170.
45. Fujinaga, M., Cherney, M.M., Oyama, H., Oda, K. and James, M.N. (2004) The molecular structure and catalytic mechanism of a novel carboxyl peptidase from *Scytalidium lignicolum*, *Proc Natl Acad Sci U S A*, 101, 3364-3369.
46. Fulop, V., Szeltner, Z. and Polgar, L. (2000) Catalysis of serine oligopeptidases is controlled by a gating filter mechanism, *EMBO Rep*, 1, 277-281.
47. Fuxreiter, M., Magyar, C., Juhasz, T., Szeltner, Z., Polgar, L. and Simon, I. (2005) Flexibility of prolyl oligopeptidase: molecular dynamics and molecular framework analysis of the potential substrate pathways, *Proteins*, 60, 504-512.
48. Garcia, A., Courtin, D., Solano, P., Koffi, M. and Jamonneau, V. (2006) Human African trypanosomiasis: connecting parasite and host genetics, *Trends Parasitol*, 22, 405-409.
49. Garcia, M.P., Nobrega, O.T., Teixeira, A.R., Sousa, M.V. and Santana, J.M. (1998) Characterisation of a *Trypanosoma cruzi* acidic 30 kDa cysteine protease, *Mol Biochem Parasitol*, 91, 263-272.
50. Gerczei, T., Keseru, G.M. and Naray-Szabo, G. (2000) Construction of a 3D model of oligopeptidase B, a potential processing enzyme in prokaryotes, *J Mol Graph Model*, 18, 7-17, 57-18.
51. Giordano, R., Chammas, R., Veiga, S.S., Colli, W. and Alves, M.J. (1994) An acidic component of the heterogeneous Tc-85 protein family from the surface of *Trypanosoma cruzi* is a laminin binding glycoprotein, *Mol Biochem Parasitol*, 65, 85-94.
52. Giordano, R., Fouts, D.L., Tewari, D., Colli, W., Manning, J.E. and Alves, M.J. (1999) Cloning of a surface membrane glycoprotein specific for the infective form of *Trypanosoma cruzi* having adhesive properties to laminin, *J Biol Chem*, 274, 3461-3468.
53. Gluenz, E., Taylor, M.C. and Kelly, J.M. (2007) The *Trypanosoma cruzi* metacyclic-specific protein Met-III associates with the nucleolus and contains independent amino and carboxyl terminal targeting elements, *Int J Parasitol*, 37, 617-625.
54. Goldberg, A.L. and Rock, K.L. (1992) Proteolysis, proteasomes and antigen presentation, *Nature*, 357, 375-379.
55. Gonzalez, J., Ramalho-Pinto, F.J., Frevert, U., Ghiso, J., Tomlinson, S., Scharfstein, J., Corey, E.J. and Nussenzweig, V. (1996) Proteasome activity is

- required for the stage-specific transformation of a protozoan parasite, *J Exp Med*, 184, 1909-1918.
56. Goossens, F., De Meester, I., Vanhoof, G., Hendriks, D., Vriend, G. and Scharpe, S. (1995) The purification, characterization and analysis of primary and secondary-structure of prolyl oligopeptidase from human lymphocytes. Evidence that the enzyme belongs to the alpha/beta hydrolase fold family, *Eur J Biochem*, 233, 432-441.
57. Grab, D.J., Garcia-Garcia, J.C., Nikolskaia, O.V., Kim, Y.V., Brown, A., Pardo, C.A., Zhang, Y., Becker, K.G., Wilson, B.A., de, A.L.A.P., Scharfstein, J. and Dumler, J.S. (2009) Protease activated receptor signaling is required for African trypanosome traversal of human brain microvascular endothelial cells, *PLoS Negl Trop Dis*, 3, e479.
58. Grellier, P., Vendeville, S., Joyeau, R., Bastos, I.M., Drobecq, H., Frappier, F., Teixeira, A.R., Schrevel, J., Davioud-Charvet, E., Sergheraert, C. and Santana, J.M. (2001) *Trypanosoma cruzi* prolyl oligopeptidase Tc80 is involved in nonphagocytic mammalian cell invasion by trypomastigotes, *J Biol Chem*, 276, 47078-47086.
59. Hall, B.F., Webster, P., Ma, A.K., Joiner, K.A. and Andrews, N.W. (1992) Desialylation of lysosomal membrane glycoproteins by *Trypanosoma cruzi*: a role for the surface neuraminidase in facilitating parasite entry into the host cell cytoplasm, *J Exp Med*, 176, 313-325.
60. Humphreys, M.J., Moon, R.P., Klinder, A., Fowler, S.D., Rupp, K., Bur, D., Ridley, R.G. and Berry, C. (1999) The aspartic proteinase from the rodent parasite *Plasmodium berghei* as a potential model for plasmepsins from the human malaria parasite, *Plasmodium falciparum*, *FEBS Lett*, 463, 43-48.
61. Inouye, K., Kusano, M., Hashida, Y., Minoda, M. and Yasukawa, K. (2007) Engineering, expression, purification, and production of recombinant thermolysin, *Biotechnol Annu Rev*, 13, 43-64.
62. Johnson, A.E. (2005) Fluorescence approaches for determining protein conformations, interactions and mechanisms at membranes, *Traffic*, 6, 1078-1092.
63. Joyeau, R., Maoulida, C., Guillet, C., Frappier, F., Teixeira, A.R., Schrevel, J., Santana, J. and Grellier, P. (2000) Synthesis and activity of pyrrolidinyl- and thiazolidinyl-dipeptide derivatives as inhibitors of the Tc80 prolyl oligopeptidase from *Trypanosoma cruzi*, *Eur J Med Chem*, 35, 257-266.

64. Juhasz, T., Szeltner, Z., Fulop, V. and Polgar, L. (2005) Unclosed beta-propellers display stable structures: implications for substrate access to the active site of prolyl oligopeptidase, *J Mol Biol*, 346, 907-917.
65. Kanatani, A., Masuda, T., Shimoda, T., Misoka, F., Lin, X.S., Yoshimoto, T. and Tsuru, D. (1991) Protease II from *Escherichia coli*: sequencing and expression of the enzyme gene and characterization of the expressed enzyme, *J Biochem*, 110, 315-320.
66. Kato, A., Fukunari, A., Sakai, Y. and Nakajima, T. (1997) Prevention of amyloid-like deposition by a selective prolyl endopeptidase inhibitor, Y-29794, in senescence-accelerated mouse, *J Pharmacol Exp Ther*, 283, 328-335.
67. Kelly, S.M., Jess, T.J. and Price, N.C. (2005) How to study proteins by circular dichroism, *Biochim Biophys Acta*, 1751, 119-139.
68. Khan, A.R. and James, M.N. (1998) Molecular mechanisms for the conversion of zymogens to active proteolytic enzymes, *Protein Sci*, 7, 815-836.
69. Klemba, M. and Goldberg, D.E. (2002) Biological roles of proteases in parasitic protozoa, *Annu Rev Biochem*, 71, 275-305.
70. Koida, M. and Walter, R. (1976) Post-proline cleaving enzyme. Purification of this endopeptidase by affinity chromatography, *J Biol Chem*, 251, 7593-7599.
71. Lakowicz, J.R. (2004) Principles of Fluorescence Spectroscopy. Springer Science+Business Media, Inc, New York.
72. Lecaille, F., Kaleta, J. and Bromme, D. (2002) Human and parasitic papain-like cysteine proteases: their role in physiology and pathology and recent developments in inhibitor design, *Chem Rev*, 102, 4459-4488.
73. Legros, D., Ollivier, G., Gastellu-Etchegorry, M., Paquet, C., Burri, C., Jannin, J. and Buscher, P. (2002) Treatment of human African trypanosomiasis--present situation and needs for research and development, *Lancet Infect Dis*, 2, 437-440.
74. Ley, V., Robbins, E.S., Nussenzweig, V. and Andrews, N.W. (1990) The exit of *Trypanosoma cruzi* from the phagosome is inhibited by raising the pH of acidic compartments, *J Exp Med*, 171, 401-413.
75. Lin, L.N. and Brandts, J.F. (1983) Evidence showing that a proline-specific endopeptidase has an absolute requirement for a trans peptide bond immediately preceding the active bond, *Biochemistry*, 22, 4480-4485.
76. Lowndes, C.M., Bonaldo, M.C., Thomaz, N. and Goldenberg, S. (1996) Heterogeneity of metalloprotease expression in *Trypanosoma cruzi*, *Parasitology*, 112 (Pt 4), 393-399.

77. Macedo, V. (1980) Forma indeterminada da doença de Chagas, *Jornal Brasileiro de Medicina*, 38, 34-40.
78. Machado, C.A. and Ayala, F.J. (2001) Nucleotide sequences provide evidence of genetic exchange among distantly related lineages of *Trypanosoma cruzi*, *Proc Natl Acad Sci U S A*, 98, 7396-7401.
79. Mackey, Z.B., O'Brien, T.C., Greenbaum, D.C., Blank, R.B. and McKerrow, J.H. (2004) A cathepsin B-like protease is required for host protein degradation in *Trypanosoma brucei*, *J Biol Chem*, 279, 48426-48433.
80. MacRae, J.I., Obado, S.O., Turnock, D.C., Roper, J.R., Kierans, M., Kelly, J.M. and Ferguson, M.A. (2006) The suppression of galactose metabolism in *Trypanosoma cruzi* epimastigotes causes changes in cell surface molecular architecture and cell morphology, *Mol Biochem Parasitol*, 147, 126-136.
81. Maes, M., Goossens, F., Scharpe, S., Calabrese, J., Desnyder, R. and Meltzer, H.Y. (1995) Alterations in plasma prolyl endopeptidase activity in depression, mania, and schizophrenia: effects of antidepressants, mood stabilizers, and antipsychotic drugs, *Psychiatry Res*, 58, 217-225.
82. Maes, M., Monteleone, P., Bencivenga, R., Goossens, F., Maj, M., van West, D., Bosmans, E. and Scharpe, S. (2001) Lower serum activity of prolyl endopeptidase in anorexia and bulimia nervosa, *Psychoneuroendocrinology*, 26, 17-26.
83. Maes, M., Song, C., Lin, A., De Jongh, R., Van Gastel, A., Kenis, G., Bosmans, E., De Meester, I., Benoy, I., Neels, H., Demedts, P., Janca, A., Scharpe, S. and Smith, R.S. (1998) The effects of psychological stress on humans: increased production of pro-inflammatory cytokines and a Th1-like response in stress-induced anxiety, *Cytokine*, 10, 313-318.
84. Manning-Cela, R., Cortes, A., Gonzalez-Rey, E., Van Voorhis, W.C., Swindle, J. and Gonzalez, A. (2001) LYT1 protein is required for efficient in vitro infection by *Trypanosoma cruzi*, *Infect Immun*, 69, 3916-3923.
85. Martin, S.R. and Schilstra, M.J. (2008) Circular Dichroism and its application to the study of biomolecules. In, *Methods in Cell Biology*. Elsevier, Inc, London.
86. Matthews, D.A., Alden, R.A., Birktoft, J.J., Freer, T. and Kraut, J. (1977) Re-examination of the charge relay system in subtilisin comparison with other serine proteases, *J Biol Chem*, 252, 8875-8883.
87. Matthews, K.R. (1999) Developments in the differentiation of *Trypanosoma brucei*, *Parasitol Today*, 15, 76-80.

88. Matthews, K.R., Ellis, J.R. and Paterou, A. (2004) Molecular regulation of the life cycle of African trypanosomes, *Trends Parasitol*, 20, 40-47.
89. McCulloch, R. (2004) Antigenic variation in African trypanosomes: monitoring progress, *Trends Parasitol*, 20, 117-121.
90. McKerrow, J.H., Engel, J.C. and Caffrey, C.R. (1999) Cysteine protease inhibitors as chemotherapy for parasitic infections, *Bioorg. Med. Chem.*, 7, 639-644.
91. McKerrow, J.H., Sun, E., Rosenthal, P.J. and Bouvier, J. (1993) The proteases and pathogenicity of parasitic protozoa, *Annu Rev Microbiol*, 47, 821-853.
92. Molina, J., Urbina, J., Gref, R., Brener, Z. and Rodrigues Junior, J.M. (2001) Cure of experimental Chagas' disease by the bis-triazole DO870 incorporated into 'stealth' polyethyleneglycol-poly lactide nanospheres, *J Antimicrob Chemother*, 47, 101-104.
93. Moreno, S.N., Silva, J., Vercesi, A.E. and Docampo, R. (1994) Cytosolic-free calcium elevation in *Trypanosoma cruzi* is required for cell invasion, *J Exp Med*, 180, 1535-1540.
94. Morty, R.E., Fulop, V. and Andrews, N.W. (2002) Substrate recognition properties of oligopeptidase B from *Salmonella enterica* serovar Typhimurium, *J Bacteriol*, 184, 3329-3337.
95. Morty, R.E., Lonsdale-Eccles, J.D., Mentele, R., Auerswald, E.A. and Coetzer, T.H. (2001) Trypanosome-derived oligopeptidase B is released into the plasma of infected rodents, where it persists and retains full catalytic activity, *Infect Immun*, 69, 2757-2761.
96. Morty, R.E., Pelle, R., Vadasz, I., Uzcanga, G.L., Seeger, W. and Bubis, J. (2005) Oligopeptidase B from *Trypanosoma evansi*. A parasite peptidase that inactivates atrial natriuretic factor in the bloodstream of infected hosts, *J Biol Chem*, 280, 10925-10937.
97. Mott, F.W. (1907) Histological observations on the changes in the nervous system in trypanosome infections especially sleeping sickness and their relation to syphilitic lesions of the nervous system., *Arch. Neurol.*, 3, 581-646.
98. Myohanen, T.T., Garcia-Horsman, J.A., Tenorio-Laranga, J. and Mannisto, P.T. (2009) Issues about the physiological functions of prolyl oligopeptidase based on its discordant spatial association with substrates and inconsistencies among mRNA, protein levels, and enzymatic activity, *J Histochem Cytochem*, 57, 831-848.

99. Nikolskaia, O.V., de, A.L.A.P., Kim, Y.V., Lonsdale-Eccles, J.D., Fukuma, T., Scharfstein, J. and Grab, D.J. (2006) Blood-brain barrier traversal by African trypanosomes requires calcium signaling induced by parasite cysteine protease, *J Clin Invest*, 116, 2739-2747.
100. Nóbrega, O.T. (2001) Caracterização molecular e funcional da catepsina tipo B de *Trypanosoma cruzi*. Universidade de Brasília, Brasília.
101. Noireau, F., Diosque, P. and Jansen, A.M. (2009) *Trypanosoma cruzi*: adaptation to its vectors and its hosts, *Vet Res*, 40, 26.
102. Obado, S.O., Taylor, M.C., Wilkinson, S.R., Bromley, E.V. and Kelly, J.M. (2005) Functional mapping of a trypanosome centromere by chromosome fragmentation identifies a 16-kb GC-rich transcriptional "strand-switch" domain as a major feature, *Genome Res*, 15, 36-43.
103. Oliveira, E.C., Fujisawa, M.M., Hallal Longo, D.E., Farias, A.S., Contin Moraes, J., Guariento, M.E., de Almeida, E.A., Saad, M.J., Langone, F., Toyama, M.H., Andreollo, N.A. and Santos, L.M. (2009) Neuropathy of gastrointestinal Chagas' disease: immune response to myelin antigens, *Neuroimmunomodulation*, 16, 54-62.
104. Pacaud, M. and Richaud, C. (1975) Protease II from *Escherichia coli*. Purification and characterization, *J Biol Chem*, 250, 7771-7779.
105. Pepin, J. and Milord, F. (1994) The treatment of human African trypanosomiasis, *Adv Parasitol*, 33, 1-47.
106. Petit, A., Barelli, H., Morain, P. and Checler, F. (2000) Novel proline endopeptidase inhibitors do not modify Abeta40/42 formation and degradation by human cells expressing wild-type and swedish mutated beta-amyloid precursor protein, *Br J Pharmacol*, 130, 1613-1617.
107. Polgar, L. (2002) The prolyl oligopeptidase family, *Cell Mol Life Sci*, 59, 349-362.
108. Polgar, L. (2005) The catalytic triad of serine peptidases, *Cell Mol Life Sci*, 62, 2161-2172.
109. Prata, A. (2001) Clinical and epidemiological aspects of Chagas disease, *Lancet Infect Dis*, 1, 92-100.
110. Puente, X.S., Sanchez, L.M., Overall, C.M. and Lopez-Otin, C. (2003) Human and mouse proteases: a comparative genomic approach, *Nat Rev Genet*, 4, 544-558.
111. Rawlings, N.D. and Barrett, A.J. (1994) Families of serine peptidases, *Methods Enzymol*, 244, 19-61.

112. Rawlings, N.D. and Barrett, A.J. (1995) Families of aspartic peptidases, and those of unknown catalytic mechanism, *Methods Enzymol*, 248, 105-120.
113. Rawlings, N.D., Morton, F.R., Kok, C.Y., Kong, J. and Barrett, A.J. (2008) MEROPS: the peptidase database, *Nucleic Acids Res*, 36, D320-325.
114. Rawlings, N.D., Polgar, L. and Barrett, A.J. (1991) A new family of serine-type peptidases related to prolyl oligopeptidase, *Biochem J*, 279 (Pt 3), 907-908.
115. Rodgers, J. (2009) Human African trypanosomiasis, chemotherapy and CNS disease, *J Neuroimmunol*, 211, 16-22.
116. Rodriguez, A., Martinez, I., Chung, A., Berlot, C.H. and Andrews, N.W. (1999) cAMP regulates Ca²⁺-dependent exocytosis of lysosomes and lysosome-mediated cell invasion by trypanosomes, *J Biol Chem*, 274, 16754-16759.
117. Rodriguez, A., Rioult, M.G., Ora, A. and Andrews, N.W. (1995) A trypanosome-soluble factor induces IP₃ formation, intracellular Ca²⁺ mobilization and microfilament rearrangement in host cells, *J Cell Biol*, 129, 1263-1273.
118. Rosenthal, P.J. (1999) Proteases of protozoan parasites, *Adv Parasitol*, 43, 105-159.
119. Rosenthal, P.J. (2002) Hydrolysis of erythrocyte proteins by proteases of malaria parasites, *Curr Opin Hematol*, 9, 140-145.
120. Ruiz, R.C., Favoreto, S., Jr., Dorta, M.L., Oshiro, M.E., Ferreira, A.T., Manque, P.M. and Yoshida, N. (1998) Infectivity of *Trypanosoma cruzi* strains is associated with differential expression of surface glycoproteins with differential Ca²⁺ signalling activity, *Biochem J*, 330 (Pt 1), 505-511.
121. Ruta, S., Plasman, N., Zaffran, Y., Capo, C., Mege, J.L. and Vray, B. (1996) *Trypanosoma cruzi*-induced tyrosine phosphorylation in murine peritoneal macrophages, *Parasitol Res*, 82, 481-484.
122. Sajid, M. and McKerrow, J.H. (2002) Cysteine proteases of parasitic organisms, *Mol Biochem Parasitol*, 120, 1-21.
123. Sanchez-Sancho, F., Campillo, N.E. and Paez, J.A. (2009) Chagas Disease: Progress and New Perspectives, *Curr Med Chem*.
124. Santana, J.M., Grellier, P., Rodier, M.H., Schrevel, J. and Teixeira, A. (1992) Purification and characterization of a new 120 kDa alkaline proteinase of *Trypanosoma cruzi*, *Biochem Biophys Res Commun*, 187, 1466-1473.
125. Santana, J.M., Grellier, P., Schrevel, J. and Teixeira, A.R. (1997) A *Trypanosoma cruzi*-secreted 80 kDa proteinase with specificity for human collagen types I and IV, *Biochem J*, 325 (Pt 1), 129-137.

126. Scharfstein, J., Schmitz, V., Morandi, V., Capella, M.M., Lima, A.P., Morrot, A., Juliano, L. and Muller-Esterl, W. (2000) Host cell invasion by *Trypanosoma cruzi* is potentiated by activation of bradykinin B(2) receptors, *J Exp Med*, 192, 1289-1300.
127. Schenkman, S., Diaz, C. and Nussenzweig, V. (1991) Attachment of *Trypanosoma cruzi* trypomastigotes to receptors at restricted cell surface domains, *Exp Parasitol*, 72, 76-86.
128. Schofield, C.J., Jannin, J. and Salvatella, R. (2006) The future of Chagas disease control, *Trends Parasitol*, 22, 583-588.
129. Seemuller, E., Lupas, A., Zuhl, F., Zwickl, P. and Baumeister, W. (1995) The proteasome from *Thermoplasma acidophilum* is neither a cysteine nor a serine protease, *FEBS Lett*, 359, 173-178.
130. Shan, L., Mathews, II and Khosla, C. (2005) Structural and mechanistic analysis of two prolyl endopeptidases: role of interdomain dynamics in catalysis and specificity, *Proc Natl Acad Sci U S A*, 102, 3599-3604.
131. Simarro, P.P., Jannin, J. and Cattand, P. (2008) Eliminating human African trypanosomiasis: where do we stand and what comes next?, *PLoS Med*, 5, e55.
132. Sreerama, N. and Woody, R.W. (2004) Computation and analysis of protein circular dichroism spectra, *Methods Enzymol*, 383, 318-351.
133. Stevens, J.R., Noyes, H.A., Dover, G.A. and Gibson, W.C. (1999) The ancient and divergent origins of the human pathogenic trypanosomes, *Trypanosoma brucei* and *T. cruzi*, *Parasitology*, 118 (Pt 1), 107-116.
134. Szeltner, Z., Rea, D., Juhasz, T., Renner, V., Fulop, V. and Polgar, L. (2004) Concerted structural changes in the peptidase and the propeller domains of prolyl oligopeptidase are required for substrate binding, *J Mol Biol*, 340, 627-637.
135. Tardieux, I., Webster, P., Ravesloot, J., Boron, W., Lunn, J.A., Heuser, J.E. and Andrews, N.W. (1992) Lysosome recruitment and fusion are early events required for trypanosome invasion of mammalian cells, *Cell*, 71, 1117-1130.
136. Tarrago, T., Martin-Benito, J., Sabido, E., Claasen, B., Madurga, S., Gairi, M., Valpuesta, J.M. and Giral, E. (2009) A new side opening on prolyl oligopeptidase revealed by electron microscopy, *FEBS Lett*, 583, 3344-3348.
137. Teixeira, A.R., Nascimento, R.J. and Sturm, N.R. (2006) Evolution and pathology in chagas disease--a review, *Mem Inst Oswaldo Cruz*, 101, 463-491.
138. Todorov, A.G., Andrade, D., Pesquero, J.B., Araujo Rde, C., Bader, M., Stewart, J., Gera, L., Muller-Esterl, W., Morandi, V., Goldenberg, R.C., Neto, H.C. and Scharfstein, J. (2003) *Trypanosoma cruzi* induces edematogenic responses in

- mice and invades cardiomyocytes and endothelial cells in vitro by activating distinct kinin receptor (B1/B2) subtypes, *Faseb J*, 17, 73-75.
139. Tomlinson, S., Vandekerckhove, F., Frevert, U. and Nussenzweig, V. (1995) The induction of *Trypanosoma cruzi* trypomastigote to amastigote transformation by low pH, *Parasitology*, 110 (Pt 5), 547-554.
140. Troeberg, L., Pike, R.N., Morty, R.E., Berry, R.K., Coetzer, T.H. and Lonsdale-Eccles, J.D. (1996) Proteases from *Trypanosoma brucei brucei*. Purification, characterisation and interactions with host regulatory molecules, *Eur J Biochem*, 238, 728-736.
141. Trouiller, P., Olliaro, P., Torreele, E., Orbinski, J., Laing, R. and Ford, N. (2002) Drug development for neglected diseases: a deficient market and a public-health policy failure, *Lancet*, 359, 2188-2194.
142. Tsuji, A., Yoshimoto, T., Yuasa, K. and Matsuda, Y. (2006) Protamine: a unique and potent inhibitor of oligopeptidase B, *J Pept Sci*, 12, 65-71.
143. Urbina, J.A. and Docampo, R. (2003) Specific chemotherapy of Chagas disease : controversies and advances, *Trends Parasitol.*, 19, 495-501.
144. Usuki, H., Uesugi, Y., Iwabuchi, M. and Hatanaka, T. (2009) Activation of oligopeptidase B from *Streptomyces griseus* by thiol-reacting reagents is independent of the single reactive cysteine residue, *Biochim Biophys Acta*, 1794, 1673-1683.
145. Venalainen, J.I., Garcia-Horsman, J.A., Forsberg, M.M., Jalkanen, A., Wallen, E.A., Jarho, E.M., Christiaans, J.A., Gynther, J. and Mannisto, P.T. (2006) Binding kinetics and duration of in vivo action of novel prolyl oligopeptidase inhibitors, *Biochem Pharmacol*, 71, 683-692.
146. Venalainen, J.I., Juvonen, R.O. and Mannisto, P.T. (2004) Evolutionary relationships of the prolyl oligopeptidase family enzymes, *Eur J Biochem*, 271, 2705-2715.
147. Vendeville, S., Buisine, E., Williard, X., Schrével, J., Grellier, P., Santana, J.M. and Sergheraert, C. (1999) Identification of inhibitors of an 80 kDa protease from *Trypanosoma cruzi* through the screening of a combinatorial peptide library, *Chem. Pharm. Bull.*, 47, 194-198.
148. Vendeville, S., Goossens, F., Debreu-Fontaine, M.A., Landry, V., Davioud-Charvet, E., Grellier, P., Scharpe, S. and Sergheraert, C. (2002) Comparison of the inhibition of human and *Trypanosoma cruzi* prolyl endopeptidases, *Bioorg Med Chem*, 10, 1719-1729.

149. Walter, R., Shlank, H., Glass, J.D., Schwartz, I.L. and Kerenyi, T.D. (1971) Leucylglycinamide released from oxytocin by human uterine enzyme, *Science*, 173, 827-829.
150. Westerik, J.O. and Wolfenden, R. (1972) Aldehydes as inhibitors of papain, *J Biol Chem*, 247, 8195-8197.
151. WHO (1997) Resolution 50.36, 50th World Health Assembly, Geneva: World Health Organization.
152. WHO (2002) Control of Chagas disease, Techn. Rep. Ser. No. 905, Geneva.
153. WHO (2010) www.who.org.
154. Wilkinson, S.R., Taylor, M.C., Horn, D., Kelly, J.M. and Cheeseman, I. (2008) A mechanism for cross-resistance to nifurtimox and benznidazole in trypanosomes, *Proc Natl Acad Sci U S A*, 105, 5022-5027.
155. Wilkowsky, S.E., Barbieri, M.A., Stahl, P. and Isola, E.L. (2001) *Trypanosoma cruzi*: phosphatidylinositol 3-kinase and protein kinase B activation is associated with parasite invasion, *Exp Cell Res*, 264, 211-218.
156. Williams, R.S. and Harwood, A.J. (2000) Lithium therapy and signal transduction, *Trends Pharmacol Sci*, 21, 61-64.
157. Williams, R.S., Eames, M., Ryves, W.J., Viggars, J. and Harwood, A.J. (1999) Loss of a prolyl oligopeptidase confers resistance to lithium by elevation of inositol (1,4,5) trisphosphate, *EMBO J*, 18, 2734-2745.
158. Yoshida, N. (2006) Molecular basis of mammalian cell invasion by *Trypanosoma cruzi*, *An Acad Bras Cienc*, 78, 87-111.
159. Yoshida, N. (2008) *Trypanosoma cruzi* infection by oral route: how the interplay between parasite and host components modulates infectivity, *Parasitol Int*, 57, 105-109.
160. Yoshida, N. and Cortez, M. (2008) *Trypanosoma cruzi*: parasite and host cell signaling during the invasion process, *Subcell Biochem*, 47, 82-91.
161. Yoshimoto, T., Fischl, M., Orłowski, R.C. and Walter, R. (1978) Post-proline cleaving enzyme and post-proline dipeptidyl aminopeptidase. Comparison of two peptidases with high specificity for proline residues, *J Biol Chem*, 253, 3708-3716.
162. Yoshimoto, T., Kado, K., Matsubara, F., Koriyama, N., Kaneto, H. and Tsura, D. (1987) Specific inhibitors for prolyl endopeptidase and their anti-amnesic effect, *J Pharmacobiodyn*, 10, 730-735.
163. Zingales, B., Andrade, S.G., Briones, M.R., Campbell, D.A., Chiari, E., Fernandes, O., Guhl, F., Lages-Silva, E., Macedo, A.M., Machado, C.R., Miles, M.A., Romanha, A.J., Sturm, N.R., Tibayrenc, M. and Schijman, A.G. (2009) A



new consensus for *Trypanosoma cruzi* intraspecific nomenclature: second revision meeting recommends TcI to TcVI, *Mem Inst Oswald Cruz*, 104, 1051-1054.

164. Zhong, L., Lu, H.G., Moreno, S.N. and Docampo, R. (1998) Tyrosine phosphate hydrolysis of host proteins by *Trypanosoma cruzi* is linked to cell invasion, *FEMS Microbiol Lett*, 161, 15-20.